# Iron-N-Heterocyclic Carbene Complexes for Hydrogen Activation

BY

**Charles Kneale-Kaye**

A thesis submitted in partial fulfilment for the requirements for the degree of Master of Science by Research, at the school of School of Pharmacy and Biomedical Sciences, University of Lancashire, Preston, UK

March 2026

## RESEARCH STUDENT DECLARATION FORM

**Type of Award** Master of Science by Research M(Res)

**School** Pharmacy and Biomedical Sciences

### 1. Concurrent registration for two or more academic awards

I declare that while registered as a candidate for the research degree, I have not been a registered candidate or enrolled student for another award of the University or other academic or professional institution

### 2. Material submitted for another award

I declare that no material contained in the thesis has been used in any other submission for an academic award and is solely my own work.

### 3. Collaboration

Where a candidate's research programme is part of a collaborative project, the thesis must indicate in addition clearly the candidate's individual contribution and the extent of the collaboration. Please state below:

---

### 4. Use of a Proof-reader

No proof-reading service was used in the compilation of this thesis.

**Signature of Candidate**

**Print name:** Charles Kneale-Kaye

## Acknowledgments

First and foremost, I would like to thank my supervisor Dr Sergey Zlatogorsky for their guidance, expertise and feedback that helped me to complete this project. Sergey's guidance and feedback (which he enjoyed giving a little bit too much) was greatly appreciated, helping to further my own understanding and quality of this project. I am also thankful for the help and support from the analytical team especially when I let them know that instruments were broken and added to their workload. Thank you, Kate, Kane, Claire, Tamar and Pat.

Finally, I dedicate this work to my dad who unfortunately did not get to see me reach the end of this journey. Throughout I was always reminded of him, so this is for him. Thanks dad.

## List of Schemes

## List of Figures

## List of Tables

## Abstract

Research into alternative energy vectors is crucial for the future of our planet and society because it addresses two pressing challenges: environmental sustainability and energy security. Hydrogen economy is one of the most promising directions, however the two major problems yet to be solved are the “green” production of hydrogen and efficient hydrogen storage solutions. The problem of hydrogen storage is aimed to be addressed in this thesis.

Our approach to solving this problem is to utilize the interactions between Fe-NHC (N-Heterocyclic Carbene) complexes and $H_2$ to enable reversible capture and storage by manipulating the highly tuneable steric and electronic properties of Fe-NHC species.

The series of imidazolium pro-ligands with various combinations of two N-alkyl substituents on the imidazole ring (methyl to butyl, including straight and branched chain isomers) was prepared, and the corresponding Fe-NHC complexes were synthesised by reacting imidazolium salts with $K[HFe(CO)_4]$.

The reactivity of resultant Fe-NHC complexes towards hydrogen gas was then investigated, and the results were discussed and compared to literature.

It is anticipated that the outcomes of this work will enable and direct future developments into novel ligands for the purpose of hydrogen storage and activation.

**Table of Contents**

# Chapter 1: Introduction

## 1.0 Introduction

Fossil fuels have served as the backbone of global energy since the industrial revolution, powering modern infrastructure, transportation, and industry.[1] Their historical dominance is attributed to high energy density, abundance, and historically low cost. However, this reliance has incurred a significant environmental cost. The combustion of fossil fuels releases vast quantities of greenhouse gases, accelerating global warming and leading to severe consequences such as extreme weather, ecosystem disruption, and rising sea levels.[2] Furthermore, as a finite resource, fossil fuels are both environmentally and economically unsustainable in the long term. Despite the awareness of the threats observed much of the planet remains heavily dependent on fossil fuels underscoring the urgent need to transition to cleaner, more renewable sources of energy.

## 1.1 Current Renewable Options

There are many different more environmentally friendly and renewable solutions that are employed across the globe each with some of the mops tweel known examples being solar, wind, hydro and geothermal power.[3]

Solar power can offer versatile and relatively cheap energy with zero emissions however suffers from intermittent operation and reliance on optimal weather conditions. Wind power can produce vast amounts of energy but unfortunately can cause environmental damage and is also reliant on optimal weather conditions. Hydropower can deliver reliable and consistent power but has high startup costs and can also cause severe environmental damage. Finally geothermal power is also able to give reliable and consistent power but has high startup costs and is limited to specific locations that are tectonically active. Each of these examples have clear limitations that limit full widespread adoption therefore other options need to be investigated.[3,4]

## 1.2 Future Solutions

The key to a truly sustainable energy future is therefore not likely to be a singular solution, but would rather utilise a diversified array of renewable sources, thus overcoming the individual limitations of each solution.

Other energy sources have been investigated with hydrogen being a prime example. Therefore, it is the aim of this project to produce novel materials and investigate their ability to react/ activate hydrogen. This is to be done in the hope that these materials will become part of the backbone for a broader ecosystem of renewable energy sources.

# Chapter 2: Literature Review

## 2.0 Introduction

Various avenues have been explored for alternative energy sources to improve the resilience of the global energy grid. One such avenue is the use of hydrogen gas as an energy carrier and building/ developing the proper infrastructure to facilitate its use.

## 2.1 Hydrogen as an Energy Source

Hydrogen is a promising clean-energy alternative. It can be used in traditional internal combustion engines[5] or, more efficiently, in electrochemical fuel cells.[6] Currently, most hydrogen gas is produced *via* steam reformation of hydrocarbons, as it remains the most cost- effective method. The main drawback of this and many other production routes is their direct dependence on fossil fuels for energy or production of greenhouse gases throughout the process. Some reactions involved in the steam reformation of methane is shown in Scheme 1.[7]

$$CH_4 + H_2O \rightleftharpoons CO + 3H_2$$
$$CO + H_2O \rightleftharpoons CO_2 + H_2$$
$$CH_4 + CO_2 \rightleftharpoons 2CO + 2H_2$$

***Scheme 1: Some of the reactions that occur during the steam reformation of methane.***

While using renewable energy sources like solar or wind power can mitigate this carbon footprint,[8] it does not fully address the core issue. An attractive alternative is photocatalytic water splitting, which has no reliance on fossil fuels and produces no carbon dioxide.[9] This process could enable a truly renewable hydrogen economy,[10] but critical challenges must be overcome for its realization.

### 2.1.1 Challenges of Hydrogen Storage

Despite showing promise, hydrogen gas presents the challenge of safe and reliable storage. Current methods involve the use of compressed gas/ liquid at room or cryogenic temperatures which poses significant safety risks *e.g.* explosion due to high pressures and hydrogen's flammability.[11]

An alternative approach involves various sorption techniques. This can proceed by physisorption, where $H_2$ adsorbs to a surface *via* intermolecular forces, and/or chemisorption, where the $H_2$ reversibly reacts with the suitable substrate.[12] Due to these different interactions, there are varying approaches that have been explored.

### 2.1.2 Previous Approaches to Hydrogen Storage

Several materials have been explored to overcome the known challenges of storing hydrogen. These approaches primarily rely on either physisorption, where $H_2$ molecules adsorb by a suitable material *via* weak van der Waals forces, or chemisorption, where $H_2$ reversibly reacts with a substrate.

Carbon nanostructures, such as carbon nanotubes (CNTs), were initially promising due to their high surface area, allowing hydrogen to adsorb on surfaces and within interstitial spaces.[13,14] However, achieving significant storage capacities requires cryogenic temperatures and high pressures. While modifications such as metal doping or functionalization can enhance reactivity,[15] the combined demands of extreme operating conditions and high synthesis costs have limited their practical application.[14,16]

Metal-organic frameworks (MOFs) emerged as an attractive alternative due to their large surface area, high porosity, and tunable structures.[17,18] MOFs benefited from low-temperature hydrogen release due to the nature of gas storage (physisorption). However, a key limitation is their rapidly diminishing storage capacity at ambient temperatures, confining their high performance primarily to cryogenic conditions.[19,20]

Another alternative is the used of metal hydrides utilizing chemisorption allowing for high storage capacity at moderate pressures.[20] Magnesium hydride ($MgH_2$) is one example that offers a high weight percentage of hydrogen (7.7 wt%) and is relatively inexpensive. Unfortunately, high temperatures are required for hydrogen release and poor cyclability has been documented.[22] In the search for higher storage capacity and better cyclability, complex hydrides such as borohydrides and alanates have been investigated. One such example of lithium borohydride ($LiBH_4$) with a weight percentage of hydrogen of 18 wt%, however is

plagued by high cost, poor reversibility and decomposition at high temperatures.[23] Sodium alanate ($NaAlH_4$) operates at lower temperatures (~200°C) but still faces challenges with limited reversibility and slow kinetics.[24]

### 2.1.3 Current Challenges and Future Solutions

In summary, current hydrogen storage methods face significant challenges, including high costs, safety concerns and limited capacity under practical conditions Therefore, innovative material-based approaches are critically needed to overcome these limitations.

Potential new storage materials could potentially come because of a combination of several different disciplines and concepts such as the reactivity of N-heterocyclic carbenes (NHCs), metal-NHC complexes and their catalytic properties, the ability of Frustrated Lewis Pairs (FLPs) to activate small molecules and the reactivity of iron carbonyl derivatives.

## 2.2 Carbenes

Carbene are molecules that have a neutral divalent carbon atom and two unshared valence electrons with the general formula R-(C:)-R', where the R groups can be alkyl groups, hydrogen atoms or other substituents.[25]

Carbenes can be further classified into different types based on the electronic configuration of the carbon atom:

*Singlet Carbenes*: when the unshared electrons occupy the same $sp^2$ hybrid orbital with opposing spin as a spin pair, the carbene is a singlet (Fischer) carbene. Due to the $sp^2$ hybridization the carbene carbon atom has a bent geometry as shown in Figure 1. The free carbene is nucleophilic due to the lone pair in the $sp^2$ orbital and can also act like Lewis bases.[25,26]

*Triplet Carbenes:* when the unshared electrons occupy different orbitals, typically the p-orbital and $sp^2$ hybrid orbital with parallel spin, the carbene is a triplet (Schrock) carbene. In this state the carbene can adopt multiple geometries dependant on the geometry such as tetrahedral ($sp^3$), bent ($sp^2$) and linear (sp) with the unpaired electrons occupying different orbitals with parallel spins [25,26] as shown in Figure 1.

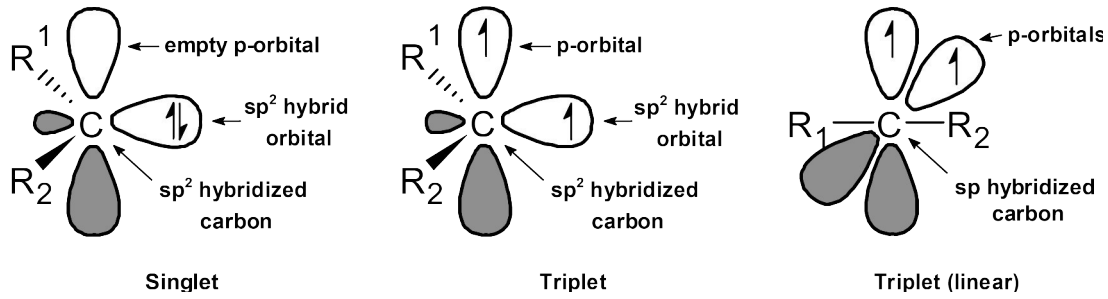


***Figure 1: Electronic and Structural configuration of Singlet (Fischer) and Triplet (Schrock) carbenes.***

### 2.2.1 Substituents and Stabilization

Carbene multiplicity and reactivity is greatly determined by the electronegativity of both substituents. Electron-withdrawing groups (EWGs) that are σ-withdrawing favour the singlet state. This is due to the EWGs ability to stabilize the sigma-orbital via inductive effects increasing the energy difference between the *σ* and *π*-orbitals.[26] Therefore, electron density leaves the *π*-orbital entering the *σ*-orbital, leaving the *π*-orbital unoccupied. Furthermore, if the substituents have lone pairs, this electron density can be shared into the unoccupied carbene *π*-orbital.[27,28]

The inverse is true for triplet carbenes if electron-donating groups (EDGs) are the substituents the triplet state is favoured. Further stabilization can be achieved by delocalization of the unpaired electrons such as with aromatic substituents.[28]

### 2.2.2 Carbene-Metal Interactions

Carbenes can be further stabilized by forming bonds with transition metals such as iron, palladium, cobalt etc. Singlet carbenes form Fischer-type complexes and triplet carbenes form Schrock-type complexes.

*Fischer Complexes:* the primary bonding in Fischer complexes is the *σ*-bond between the carbene carbon electron pair and the metal, while limited *π*-back bonding can also occur with metals in low oxidation states [29] as shown in Figure 2. Substituents on the carbene carbon atom that are *σ*-withdrawing and *π*-donating favour a singlet state due to stabilization of the unpaired electrons in the $sp^2$ hybrid orbital.[30]

*Schrock Complexes:* in comparison to Fischer complexes, double bonds between the carbene and metal are observed as shown in Figure 2. Schrock complexes mainly occur with metals that have high oxidation states.[30,31]

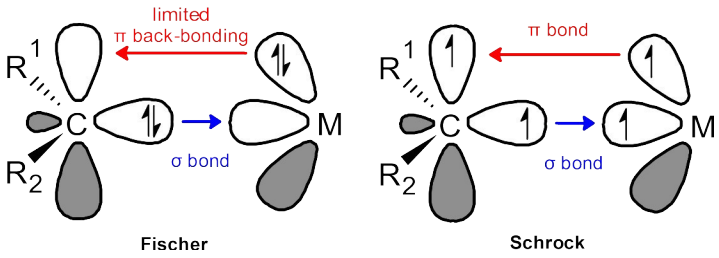


***Figure 2: Bonding of Fischer and Schrock complexes***

### 2.2.3 N-Heterocyclic Carbenes

N-Heterocyclic Carbenes (NHCs) are examples of singlet / Fischer Carbenes. They are subject to vast amounts of research regarding their properties in organocatalytic chemistry, transition metal catalysis and small molecule activation.[32]

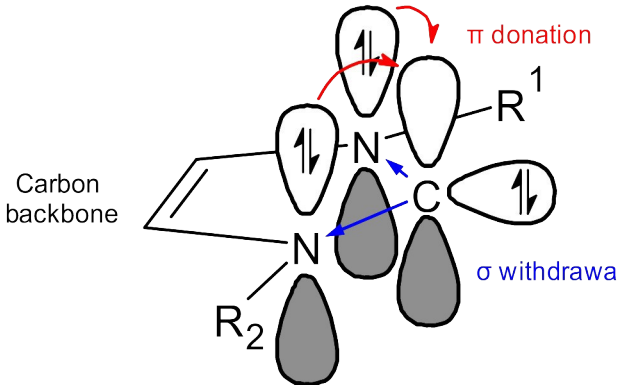


***Figure 3: General structure of imidazole based NHC (Fisher carbene) showing its electronic stabilisation***

Typical examples of NHCs are the imidazol-2-ylidienes commonly derived from imidazolium salts *via* deprotonation. They are heavily stabilized by the donation of electron density into the empty carbene *π*-orbital and *σ*-withdrawal by the nitrogen atoms [27,33] as shown in Figure 3. As a result, free NHCs are strong Lewis bases.[34,35]

Simple synthetic pathways enable many derivatives of imidazolium-based NHCs with different functional groups substituted onto the nitrogen atoms and the carbon backbone to enhance the electronic and steric properties.[36,37,38]

### 2.2.4 Metal-NHC Complexes

Transition metal complexes using NHCs were first reported approximately 60 years ago by Öfele and Kreiter using tetracarbonyl iron hydride and pentacarbonyl chromium hydride shown in Scheme 2.[39,40]

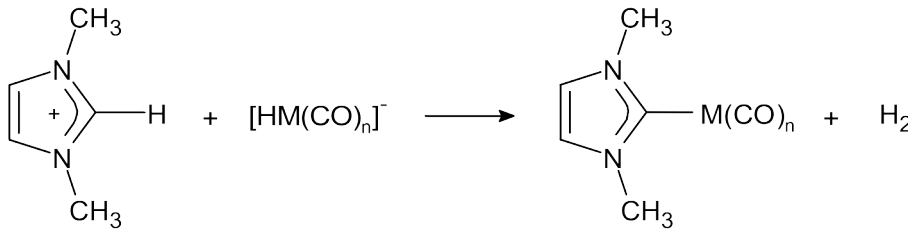


***Scheme 2: First synthesis of metal carbonyl NHC complexes. (M = Cr, n = 5; M = Fe, n = 4)***

Due to the large similarities in properties between NHCs and organophosphines, NHCs have become the ligand of choice for various catalytic processes. This is due to their ability to bond with a wide range of metals in various oxidations states, being superior σ-donors and possessing greater steric and electronic tuneability when compared to organophosphines.[41,42]

The resulting metal-NHC complexes have been observed to be active in many different coupling, polymerization and arylation reactions using metals such as palladium, ruthenium and iridium.[32,41]

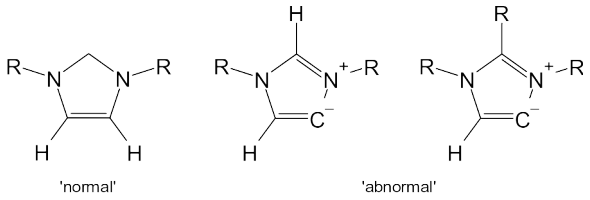


***Figure 4: Structure and electronic configuration of 'normal' and 'abnormal' NHCs. R = Aryl, tBu etc.***

Additionally, NHCs have been observed to behave differently under certain conditions. Due to potential high steric hindrance of the central carbon atom and/or protection by replacing the hydrogen atom with another group, it is possible for the carbene carbon to be present on the carbon backbone creating an 'abnormal' NHC [44] as shown in Figure 4. This is also enabled by the mesoionic effects present were both potential positive and negative charges can de delocalized. Despite binding to a different position on the NHC ligand, metal complexes using both 'normal' and 'abnormal' NHCs have been shown to have similar catalytic reactivity and properties.[44,45]

Despite these complexes showing much promise, the majority use noble metals which are expensive. Therefore, alternative metals that are of low cost, high abundance and show similar reactivity are desired.

### 2.2.5 Fe-NHC Complexes

A potential alternative to noble metals is iron due to its low cost and high abundance. Fe-NHC complexes of different oxidations states with combinations of multiple different ligands have been shown to be active in various catalytic processes.[46] Example reactions include hydrogenation, hydrosilation and C-C/ C-X/ C-N bond formation reactions, *etc*.[46,47]

The first reported synthesis used an iron carbonyl hydride and an imidazolium salt producing a $Fe^0$ complex shown in Scheme 3.[39] Similar results can be achieved by reactions of an imidazolium salt and $Fe_3(CO)_{12}$[48] or other iron sources and a free carbene/dimerized carbenes.

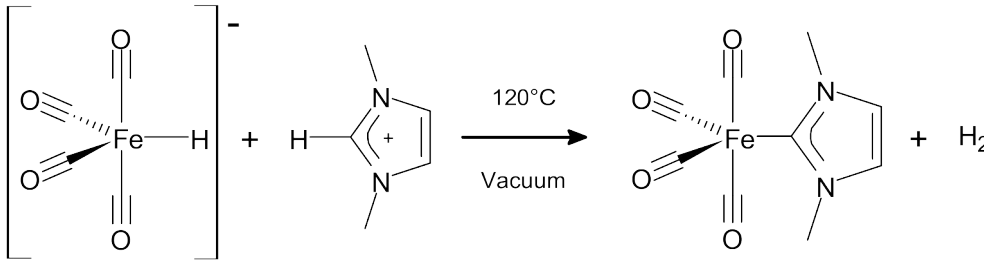


***Scheme 3: Synthesis of Fe-NHC complex using iron carbonyl hydride.***

Another method makes use of strong bases such as NaH to liberate free carbenes. These carbenes are then combined with an iron source such as $FeI_2$.[49] A derivative of this approach is using an iron precursor that has an "internal base". One such precursor that has been used is Bis[bis(trimethylsilyl)amide}iron which when combined with an imidazolium salt forms the Fe-NHC complex shown in Scheme 4.[50] Both these approaches produce $Fe^{2+}$ complexes.

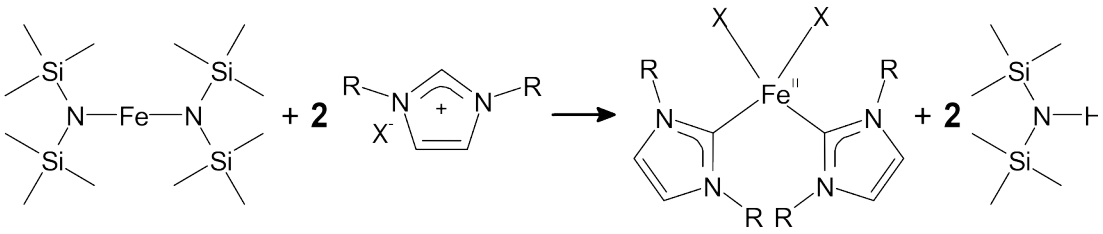

***Scheme 4: Synthesis of Fe-NHC complex using iron bis(trimethylsilyl) amide***

This approach can also enable the formation of complexes that use 'pincer ligands' where the NHCs are linked together by the N-substituents with varying functionality and lability.[49]

## 2.3 Frustrated Lewis Pairs

Frustrated Lewis Pairs (FLPs) are a novel concept that can offer a metal-free approach to activation of small molecules.[50] FLPs are comprised of a Lewis acid and base that cannot form or are disfavoured from forming a classical Lewis adduct due to steric hindrance. This 'frustration' due to high steric hinderance is what enables FLPs to activate small molecules such as hydrogen, carbonyls and amines.[53]

FLP behaviour was first demonstrated using a boron centred Lewis acid and a phosphorus centred Lewis base.[54] This Lewis acid/ base pair was observed to split the dihydrogen molecule by breaking the H-H bond with the acid accepting the hydride ($H^-$) and the base accepting the proton ($H^+$) shown in Scheme 5. Additionally, only relatively mild conditions were needed for both absorption (25°C, $H_2$ 1 bar) and release of hydrogen (80-150°C).[55]

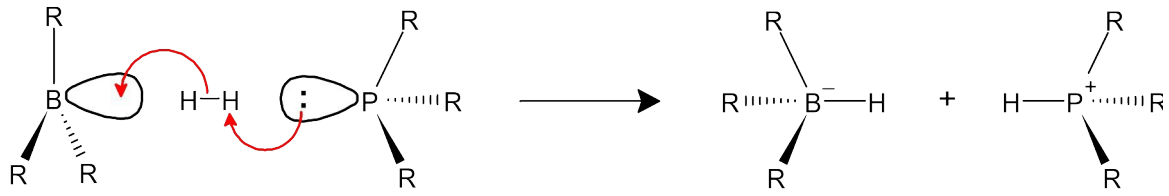


***Scheme 5: General scheme of dihydrogen activation by boron and phosphorus FLP system. R = Bulky group***

The ability of an FLP system to consistently activate small molecules can be optimized by varying the groups on both the acid and base. Use of R groups of varying size can affect the relative 'frustration' present in the FLP system.[54] Additionally, use of R groups that can enhance the electrophilicity, nucleophilicity of the Lewis acid and base respectively.

### 2.3.1 Non-Borane and non-Phosphine FLP Systems

Despite typical FLP systems usage of boron-based acids and phosphorus-based bases,[57] any element or functional group that can exhibit Lewis acidity/basicity could be used in a novel FLP system. An example is the use of N-Heterocyclic Carbenes (NHCs) as the Lewis base with a boron Lewis acid. NHC-Borane pairs have been observed to be reactive towards dihydrogen [58] and amines.[59]

NHCs are examples of singlet carbenes and are prime candidates for use due to the pair of non-bonded electrons exhibiting high nucleophilicity/ Lewis basicity[34,35] and the relative ease of structural modification to influence the electronic and steric properties.[36-38]

Despite initially being investigated for the goal of metal-free catalysis routes, the overall concept of FLPs can be applied to main-group metals.[60,61] Transition metals can show both Lewis acid (electrophilic) and Lewis base (nucleophilic)[61] properties depending on how electron rich or deficient they are. A metal compound and its corresponding counter acid/base could therefore be used as the backbone of a novel metal-based FLP system.

An example of a metal-NHC FLP system was demonstrated by Runyon et al by using $Fe(CO)_5$ as the Lewis acid and a free NHC as the base. Upon exposure to hydrogen said acid- base pair were able to heterolytically cleave hydrogen to form an iron hydride imidazolium salt shown in Scheme 6.[62]

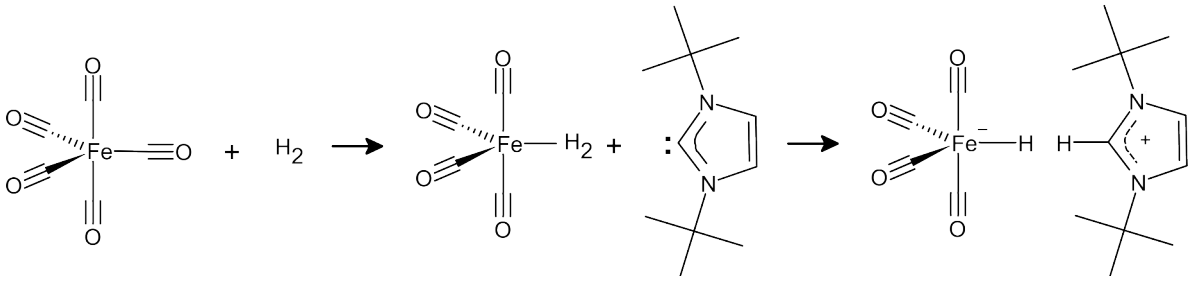

***Scheme 6: Heterolytic cleavage of hydrogen using $Fe(CO)_5$ and a free NHC.62***

## 2.4 Iron Carbonyls

Iron carbonyls are organometallic compounds featuring an iron centre with carbon monoxide (CO) ligands and are fundamental precursors in organometallic chemistry. The most common member is iron pentacarbonyl ($Fe(CO)_5$), with diiron nonacarbonyl ($Fe_2(CO)_9$) and triiron dodecacarbonyl ($Fe_3(CO)_{12}$) also being known examples. A primary application of these species is the synthesis of other iron complexes, where CO ligands are substituted with other ligands to form derivatives of $Fe(CO)_{5-x}L_x$ shown in Scheme 7.[64] Beyond its use as synthetic precursor, $Fe(CO)_5$ itself has been documented to be active in the photocatalytic hydrogenation and isomerization of olefins, [65] as well as other photoinitiated reactions.[66]

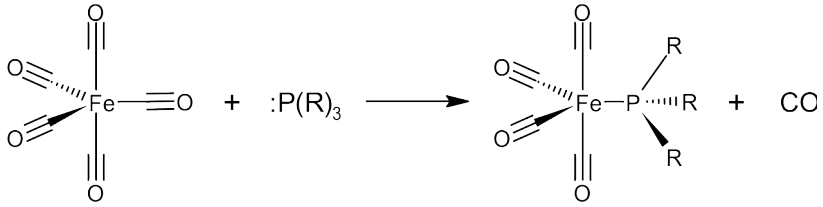


***Scheme 7: Example substitution of CO ligand of $Fe(CO)_5$ by a substituted phosphine ligand.***

Several derivatives of $Fe(CO)_5$ have been investigated and their reactivity described previously in literature. One example is disodium tetracarbonylferrate [$Na_2Fe(CO)_4$] also known as Collman's reagent which is prepared *via* reaction between $Fe(CO)_5$ and sodium metal in the presence of an electron carrier such as benzophenone.[67] Collman's reagent is extremely reactive in many different pathways and is colloquially referred to as a 'super nucleophile'. Conversions of aliphatic halides into unsymmetrical ketones, esters and carboxylic acids are only a few examples of organic conversions that have been achieved with [$Na_2Fe(CO)_4$] as shown in Scheme 8.[68,69]

Alkali metal iron carbonyl hydrides are another example of $Fe(CO)_5$ derivatives with M[$HFe(CO)_4$] (M = Na / K) being the example that is most well documented however other polynuclear hydrides are known, M[$HFe_2(CO)_8$] and M[$HFe_3(CO)_{11}$].[70,71] Tetracarbonyl iron hydride has been prepared and used *in situ* using a $Fe(CO)_5$ and a base such as NaOH / KOH.[72,73] These samples have been documented to be active reagents for the hydrogenation,[74] alkylation and arylation of carbonyl compounds[75] and reduction of carbonyl compounds[76] with many other organic conversions being possible.[77]

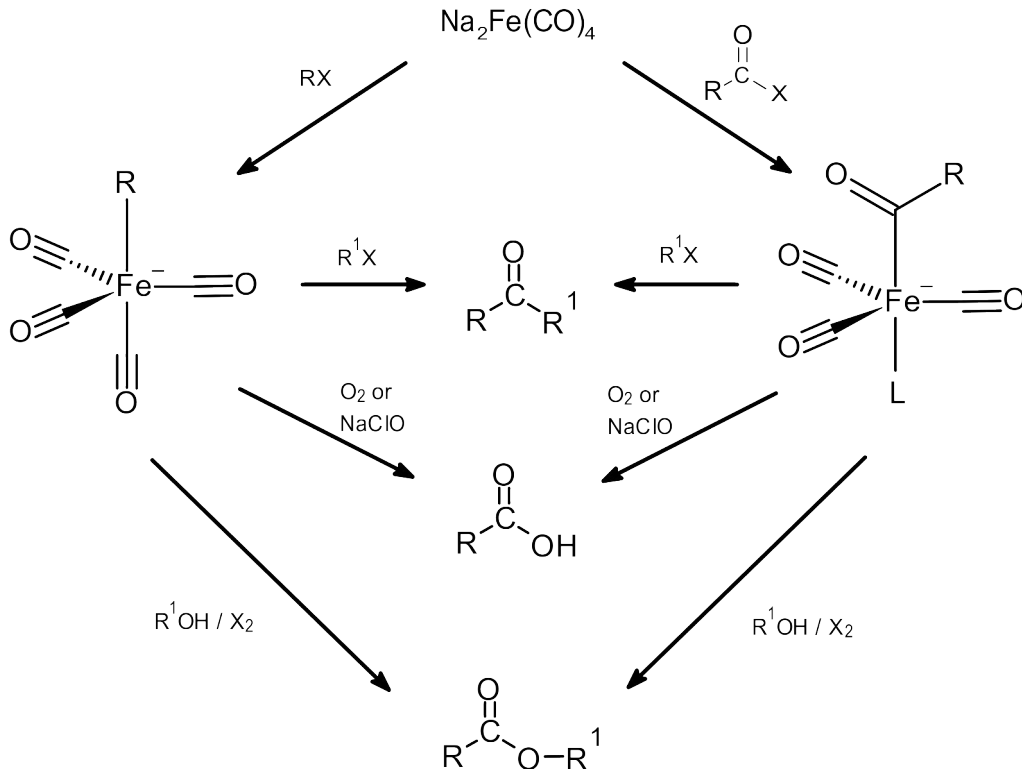


***Scheme 8: Scheme showing example organic conversions of aliphatic halides using Collman's reagent.***

# Chapter 3: Project Rationale and Methodology

## 3.1 Project Rationale

The question raised is whether the reactivity of iron carbonyl compounds can be combined with the high basicity of NHCs and their ease of steric and electronic modification to create a pseudo FLP-like system that can reversibly capture and release hydrogen under mild conditions.

Production of Fe-NHCs was first demonstrated by Ofele and Kreiter by heating a mixture of iron tetracarbonyl hydride $[HFe(CO)_4]^-$ and 1,3-dimethylimidazolium iodide to 120°C under high vacuum.[37,38]

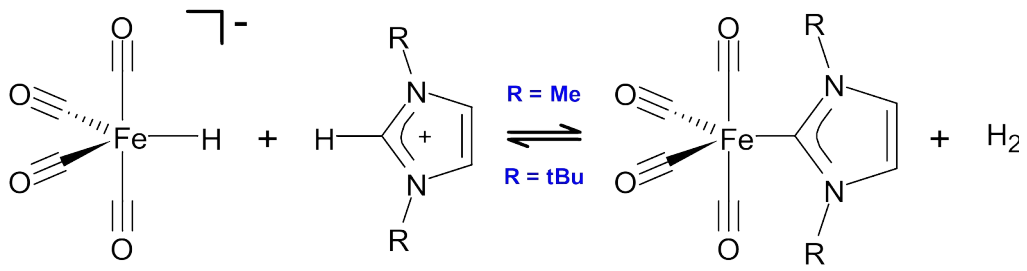


***Scheme 9: Proposed simplified reversible $H_2$ capture/ release by Fe-NHC system, R = alkyl groups etc.***

In a similar reaction to that shown in Scheme 9, N-*tert*-butyl groups have been shown to facilitate capture of hydrogen[62] however it is currently unknown if other N-substituents can influence potential reactivity towards hydrogen. Therefore, it is extremely appealing to investigate whether the use of different R groups would allow to find optimal conditions for the uptake / release of hydrogen. Possible changes in reaction conditions upon variation of the substituents on N atoms could be due to the increased stabilization of the NHC fragment *via* electronic effects thus increasing the basicity of the NHC fragment. Additionally, the bulkiness of the N-substituents may sterically hinder hydrogen from approaching / inserting into the iron- carbon bond, like the mechanism of typical FLP mode of action shown in Scheme 10.

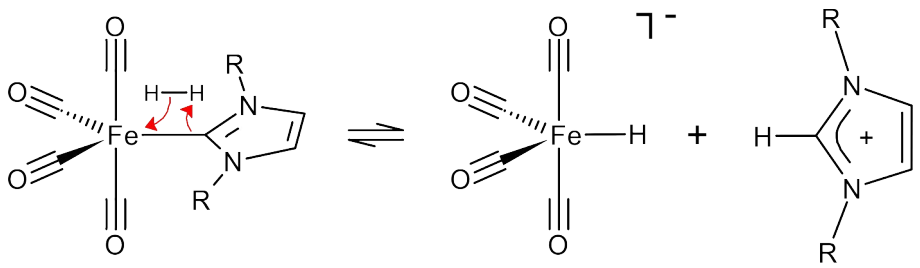

*Scheme 10: Possible 1,2-insertion of $H_2$ into the Fe-C bond.*

### 3.2 Project Methodology

*Production of NHC Ligands*

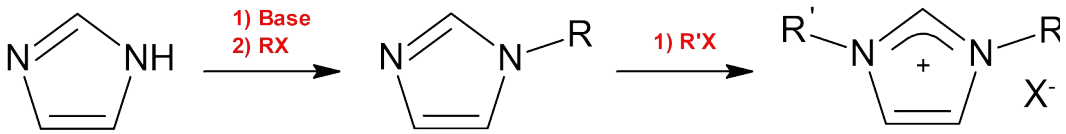


*Scheme 11: Proposed simplified synthesis route of imidazolium NHC ligands.*

Synthesis of NHC ligands would be carried out via known procedures allowing for easy production of various ligands with N-substituents of increasing size and complexity.[35,36] This also will allow the production of ligands with both symmetrical and unsymmetrical N-substituents to be tested as shown in Scheme 14.

The synthesis of these ligands follows Scheme 11 where a strong base *e.g.* KOH is used to deprotonate the imidazole molecule and addition of an iodo-alkane allows formation of desired 1-alkylimidazoles. For these syntheses propan-2-ol used as the solvent to simplify work-up due to the by-product of the reaction (KI) being largely insoluble. Iodoalkanes have been chosen for use due to all reagents being liquids at standard temperatures and pressures contrary to the corresponding chloro- and bromoalkanes. Then for the synthesis of the desired ligands the 1-alkylimidazoles previously created will be used with the corresponding iodoalkane.

Where this methodology does not give positive results a ring-closure method [35,36] will be used following the schemes shown below in Scheme 12.

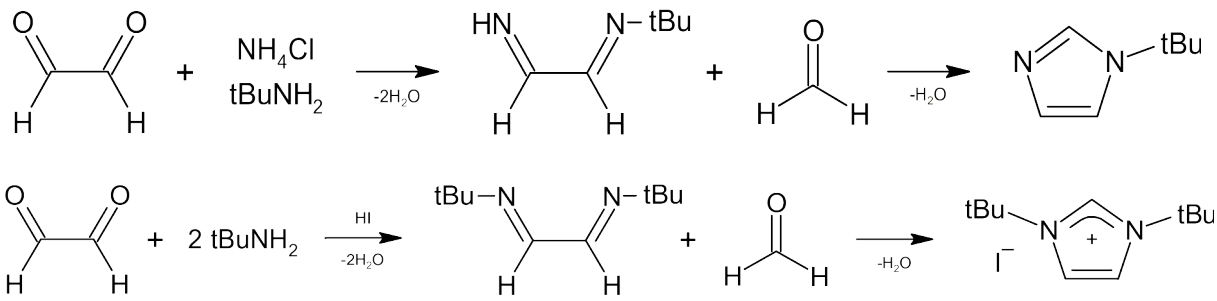


***Scheme 12: Ring-closure synthesis method for 1-tert-butylimidazole and 1,3-tert-butyl-imidazolium iodide.***

*Production of Iron Carbonyl Hydride*

Synthesis for the required potassium tetracarbonyl iron hydride follows Scheme 13 below where KOH will be used to decarboxylate $Fe(CO)_5$ using methanol as a solvent to produce the desired $K[HFe(CO)_4]$.[70,71] This synthesis will require Schlenk techniques due to the air-sensitivity of $Fe(CO)_5$ and the product $K[HFe(CO)_4]$.

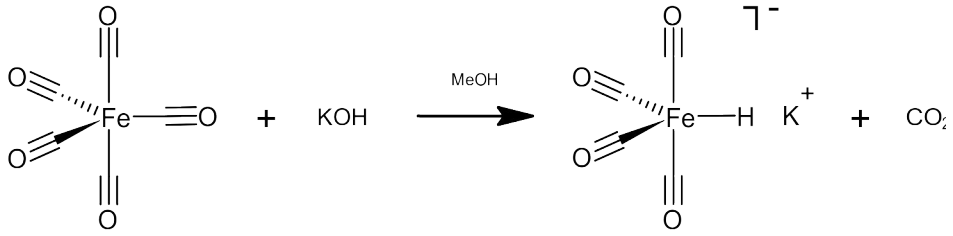


***Scheme 13: Simplified synthesis route for potassium tetracarbonyl iron hydride $K[HFe(CO)_4]$.***

Modification of this methodology may be attempted to improve yields and to successfully isolate $K[HFe(CO)_4]$.

*Production of Fe-NHC complexes*

Fe-NHC synthesized to be produced by heating $K[HFe(CO)_4]$ and the corresponding imidazolium ligand under vacuum to yield the desired $Fe(NHC)(CO)_4$ complexes by following Scheme 14 below.[37,38]

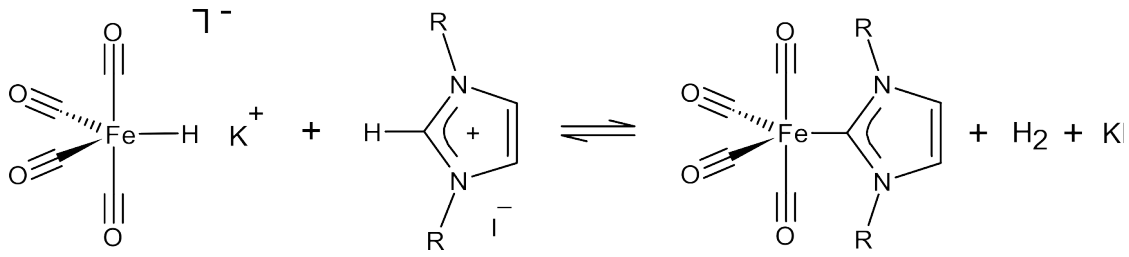

***Scheme 14: Proposed simplified synthesis route of Fe-NHC complexes using K[HFe(CO)$_4$] and 1,3-R,R'-imidazolium iodide salts***

Modification of this methodology may be attempted to improve yields and ease of isolation of the desired complexes.

*Testing of Fe-NHC complex reactivity towards $H_2$*

The resultant Fe-NHC complexes to be exposed to $H_2$ gas under approximately atmospheric pressure to confirm if any of the complexes produced can reversibly react with $H_2$. These reactions will be monitored via $^1$H NMR spectroscopy and notation of any visibly observed changes in the tested samples.

# Chapter 4: Experimental

## 4.0 General Information

All chemical reagents, solvents and starting materials were purchased from Sigma Aldrich, Tokyo Chemical Industry (TCI) or Fisher Scientific and used without further purification. All $^{1}H$, $^{13}C$ and 2D NMR spectra were collected on a Bruker Avance II HD 400 MHz NMR spectrometer; chemical shifts (δ) in parts per million (ppm) relative to $Me_4Si$, coupling constants (J) given in Hz. MS (Mass Spectrometry) data was collected using Waters Acquity QDA Detector connected to a Waters Isocratic Solvent Manager.

Elemental analysis data was collected using a Thermo Scientific Flash 2000 Organic Elemental Analyzer.

Elemental analysis data was obtained as follows: pre-weighed tin crucibles were dried overnight in an 80°C oven before being transferred to the glovebox. The required amount of sample was added to each tin cap and then quickly taken out of the glovebox in a sealed vial. The tin cap was weighed and quickly transferred to the sample tray. The weight of the sample was inputted into the software and the test run. This was then repeated twice more for each compound tested.

All synthetic procedures and practices involving volatile, air and moisture sensitive, or other hazardous substances were carried out in a controlled environment (fume hood) using appropriate PPE and Schlenk/ Glovebox techniques. Furthermore, all solvents used in air/ moisture sensitive syntheses were dried/ degassed and manipulated using Schlenk techniques.

### 4.1 1-Alkylimidazole Synthesis

#### 1-Methylimidazole [MeIm] (1)

*(Known compound, described in literature)*[83]

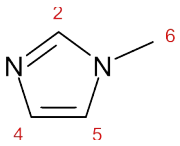


Imidazole (5g, 0.073 mol), potassium hydroxide (4.52g, 0.081 mol) and iodomethane (10.36g, 0.073 mol, 4.54 ml) in propan-2-ol (25 ml) was heated to reflux with constant stirring for 12 hours. After 12 hours, solvent was removed under vacuum and product extracted with DCM (25 ml). The DCM extract washed with water (3 x 25 ml) and dried with sodium sulphate. Solvent removed under vacuum to yield the product as pale-yellow liquid.

Yield: 5.57g, 0.068 mol (92.4%).

**$^{1}$H NMR:** (400MHz, $d_6$-DMSO, 25°C) δ 7.56 {s, *1H*, **H2**(CH)}, 7.10 {s, *1H*, **H5**(CH)}, 6.88 {s, *1H*, **H4**(CH)}, 3.63 {s, *3H*, **H6**($CH_3$)}.

**$^{13}$C NMR:** (100MHz, $d_6$-DMSO, 25°C) δ 137.92 {**C2**(CH)}, 128.44 {**C4**(CH)}, 120.50 {**C5**(CH)}, 32.74 {**C6**($CH_3$)}.

**m/z (ESI):** 83 $([C_4H_6N_2]+H)^+$

| **Elemental Analysis:** | Carbon % | Hydrogen % | Nitrogen % |
|---|---|---|---|
| Calculated | 58.51 | 7.37 | 34.12 |
| Observed | 58.55 | 7.53 | 34.06 |

Please see pages 2-12 in Supplementary Information for detailed analysis.

This method was repeated using the same molar amounts and using of appropriate iodoalkane to produce the following 1-alkylimidazoles:

**1-Ethylimidazole [Etlm] (2)**

*(Known compound, described in literature)*[38]

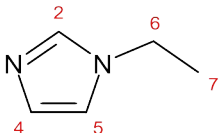


Yield: 6.32g, 0.066 mol (90.1%) as a pale-yellow liquid.

**$^{1}$H NMR:** (400MHz, $d_6$-DMSO, 25°C) δ 7.62 {app. t, $4J_{2\text{-}4} \approx 4J_{2\text{-}5} = 1.2Hz$, *1H*, **H2**(CH)}, 7.17 {app. t, $3J_{5\text{-}4} \approx 4J_{5\text{-}2} = 1.3Hz$, *1H*, **H5**(CH)}, 6.87 {app. t, $3J_{4\text{-}5} \approx 4J_{4\text{-}2} =$ *1.2Hz*, *1H*, **H4**(CH)}, 3.97 {q, $3J_{6\text{-}7} = 7.3Hz$, *2H*, **H6**($CH_2$)}, 1.32 {t, $3J_{7\text{-}6} =$ *7.3Hz*, *3H*, **H7**($CH_3$)}.

**$^{13}$C NMR:** (100MHz, $d_6$-DMSO, 25°C) δ 136.74 {**C2**(CH)}, 128.35 {**H4**(CH)}, 118.87 {**H5**(CH)}, 40.89 {**H6**($CH_2$)}, 16.39 {**C7**($CH_3$)}.

**m/z (ESI):** 97 $([C_5H_8N_2]+H)^+$

| **Elemental Analysis:** | Carbon % | Hydrogen % | Nitrogen % |
|---|---|---|---|
| Calculated | 62.47 | 8.39 | 29.14 |
| Observed | 62.37 | 8.58 | 29.06 |

Please see pages 13-23 in Supplementary Information for detailed analysis.

**1-Propylimidazole [Prlm] (3)**

*(Known compound, described in literature)*[37]

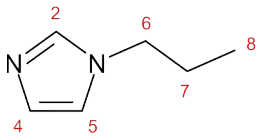


Yield: 7.04g, 0.064 mol (87.0%) as a pale-yellow liquid.

**$^{1}$H NMR:** (400MHz, $d_6$-DMSO, 25°C) δ 7.60 {app. t, $4J_{2\text{-}4} \approx 4J_{2\text{-}5} = 1.2Hz$, *1H*, **H2**(CH)}, 7.15 {app. t, $4J_{5\text{-}2} \approx 3J_{5\text{-}4} = 1.2Hz$, *1H*, **H5**(CH)}, 6.88 {app. t, $3J_{4\text{-}5} \approx 4J_{4\text{-}2} =$ *1.1Hz*, *1H*, **H4**(CH)}, 3.90 {t, $3J_{6\text{-}7} = 7.0Hz$, *2H*, **H6**($CH_2$)}, 1.70 {app. sext, $3J_{7\text{-}6} \approx 3J_{7\text{-}8} = 7.2Hz$, *2H*, **H7**($CH_2$)}, 0.80 {t, $3J_{8\text{-}7} = 7.4Hz$, *3H*, **H8**($CH_3$)}.

**$^{13}$C NMR:** (100MHz, $d_6$-DMSO, 25°C) δ 137.25 {**C2**(CH)}, 128.32 {**C4**(CH)}, 119.23 {**C5**(CH)}, 47.55 {**C6**($CH_2$)}, 23.96 {**C7**($CH_2$)}, 10.84 {**C8**($CH_3$)}

**m/z (ESI):** 111 ($[C_6H_{10}N_2]+H)^+$

| **Elemental Analysis:** | Carbon % | Hydrogen % | Nitrogen % |
|---|---|---|---|
| Calculated | 65.42 | 9.15 | 25.14 |
| Observed | 65.32 | 9.51 | 24.93 |

Please see pages 24-35 in Supplementary Information for detailed analysis.

**1-Butylimidazole [Bulm] (4)**

*(Known compound, described in literature)*[84]

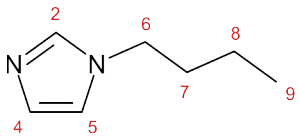


Yield: 7.50g, 0.060 mol (82.7%) as a pale-yellow liquid.

**$^{1}$H NMR:** (400MHz, $d_6$-DMSO, 25°C) δ 7.60 {app. t, $4J_{2\text{-}4} \approx {}_4J_{2\text{-}5}$ = *1.2Hz, 1H*, **H2**(CH)}, 7.15 {app. t, $3J_{5\text{-}4} \approx 4J_{5\text{-}2}$ = *1.2Hz, 1H*, **H5**(CH)}, 6.87 {app. t, $3J_{4\text{-}5} \approx 4J_{4\text{-}2}$ = *1.1Hz, 1H*, **H4**(CH)}, 3.93 {t, $3J_{6\text{-}7}$ = *7.1Hz, 2H*, **H6**($CH_2$)}, 1.65 {quin, $3J_{7\text{-}6} \approx {}^3J_{7\text{-}8}$ = *7.2Hz, 2H*, **H7**($CH_2$)}, 1.21 {app. sext, $3J_{8\text{-}7} \approx 3J_{8\text{-}9}$ = *7.3Hz, 2H*, **H8**($CH_2$)}, 0.87 {t, $3J_{9\text{-}8}$ = *7.3Hz, 3H*, **H9**($CH_3$)}.

**$^{13}$C NMR:** (100MHz, $d_6$-DMSO, 25°C) δ 137.20 {**H2**(CH)}, 128.31 {**H4**(CH)}, 119.21 {**H5**(CH)}, 45.62 {**H6**($CH_2$)}, 32.66 {**H7**($CH_2$)}, 19.16 {**H8**($CH_2$)}, 13.38 {**H9**($CH_3$)}.

**m/z (ESI):** 125 $([C_7H_{12}N_2]+H)^+$

| **Elemental Analysis:** | | Carbon % | Hydrogen % | Nitrogen % |
|---|---|---|---|---|
| | Calculated | 67.70 | 9.74 | 22.56 |
| | Observed | 67.45 | 10.01 | 22.34 |

Please see pages 36-47 in Supplementary Information for detailed analysis.

**1-Isopropylimidazole [iPrIm] (5)**

*(Known compound, described in literature)*[38]

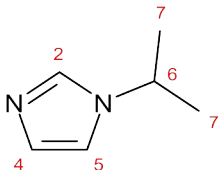


Yield: 7.04g, 0.064 mol (87.0%) as a pale-yellow liquid.

**$^{1}$H NMR:** (400MHz, $d_6$-DMSO, 25°C) δ 7.67 {app. t, $4J_{2\text{-}4} \approx {}_4J_{2\text{-}5}$ = *1.2Hz, 1H*, **H2**(CH)}, 7.22 {app. t, $3J_{5\text{-}4} \approx 4J_{5\text{-}2}$ = *1.3Hz, 1H*, **H5**(CH)}, 6.87 {app. t, $3J_{4\text{-}5} \approx 4J_{4\text{-}2}$ = *1.2Hz, 1H*, **H4**(CH)}, 4.39 {sept, $3J_{6\text{-}7}$ = *6.7Hz, 1H*, **H6**(CH)}, 1.38 {d, $3J_{7\text{-}6}$ = *6.7Hz, 6H*, **H7**($CH_3$)}.

**$^{13}$C NMR:** (100MHz, $d_6$-DMSO, 25°C) δ 135.45 {**C2**(CH)}, 128.23 {**C4**(CH)}, 117.08 {**C5**(CH)}, 48.25 {**C6**(CH)}, 23.46 {**C7**($CH_3$)}.

**m/z (ESI):** 111 ($[C_6H_{10}N_2]+H)^+$

| **Elemental Analysis:** | Carbon % | Hydrogen % | Nitrogen % |
|---|---|---|---|
| Calculated | 65.42 | 9.15 | 25.14 |
| Observed | 65.21 | 9.45 | 24.97 |

Please see pages 48-58 in Supplementary Information for detailed analysis.

**1-tert-Butylimidazole [tBuIm] (6)**

*(Known compound, described in literature)*[85]

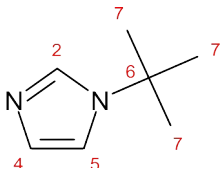


The solution of *tert*-butylamine (10.97g, 0.15 mol, 15.76 ml) and ammonium chloride (8.02g, 0.15 mol) in water (15ml) was added dropwise over 30 minutes to glyoxal 40% aq. (21.77g, 0.15 mol, 17.55 ml). To the mixture obtained, the solution of formaldehyde 37 % aq. (12.17g, 0.15 mol, 11.17 ml) in water (15ml) was then added dropwise over 30 minutes, and the reaction mixture was heated to reflux for 1 hour. After 1 hour, sodium carbonate was added until mixture was basic. The product was extracted with dichloromethane (3 x 50 ml) and the solvent was removed under vacuum. The crude oily product was purified via short-path vacuum distillation (ca 100 °C and 50 mtorr) to yield the product as pale-yellow liquid.

Yield: 6.97g, 0.056 mol (37.5%).

**$^{1}$H NMR:** (400MHz, $d_6$-DMSO, 25°C) δ 7.72 {app. t, $4J_{2\text{-}4} \approx {}_4J_{2\text{-}5}$ = *1.2Hz, 1H*, **H2**(CH)}, 7.30 {app. t, $3J_{5\text{-}4} \approx 4J_{5\text{-}2}$ = *1.3Hz, 1H*, **H5**(CH)}, 6.87 {app. t, $3J_{4\text{-}5} \approx 4J_{4\text{-}2}$ = *1.2Hz, 1H*, **H4**(CH)}, 1.49 {s, *9H*, **H7**($CH_3$)}.

**$^{13}$C NMR:** (100MHz, $d_6$-DMSO, 25°C) δ 134.55 {**C2**(CH)}, 128.15 {**C4**(CH)}, 117.00 {**C5**(CH)}, 54.44 {**C6**(C)}, 30.17 {**C7**($CH_3$)}.

**m/z (ESI):** 125 $([C_7H_{12}N_2]+H)^+$

| **Elemental Analysis:** | Carbon % | Hydrogen % | Nitrogen % |
|---|---|---|---|
| Calculated | 67.70 | 9.74 | 22.56 |
| Observed | 68.03 | 9.85 | 22.12 |

Please see pages 59-69 in Supplementary Information for detailed analysis.

### 4.2 R, R'-Imidazolium Iodide Salt Synthesis

#### 1,3-Dimethylimidazolium Iodide [Me2Iml] (7)

*(Known compound, described in literature)*[86,87,94]

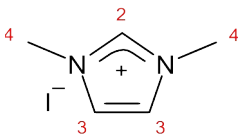


1-Methylimidazole (0.5g, 6.1 mmol, 0.49 ml), iodomethane (1.31g, 9.2 mmol, 0.57 ml) and methanol (25 ml) was heated to reflux with constant stirring for 12 hours. After 12 hours the solvent was removed under vacuum, and the crude oily product was washed with ethyl acetate (3 x 25 ml) and dried under vacuum to yield product as a white solid.

Yield: 1.31g, 5.8 mmol (95.6%).

**$^{1}$H NMR:** (400MHz, $d_6$-DMSO, 25°C) δ 9.04 {s, *1H*, **H2**(CH)}, 7.68 {s, *2H*, **H3**(CH)}, 3.84 {s, *6H*, **H4**($CH_3$)}.

**$^{13}$C NMR:** (100MHz, $d_6$-DMSO, 25°C) δ 136.99 {**C2**(CH)}, 123.43 {**C3**(CH)}, 35.74 {**C4**($CH_3$)}.

**m/z (ESI):** 97 $(C_5H_9N_2)^+$

| **Elemental Analysis:** | | Carbon % | Hydrogen % | Nitrogen % |
|---|---|---|---|---|
| | Calculated | 26.80 | 4.05 | 12.50 |
| | Observed | 26.73 | 4.18 | 12.49 |

Please see pages 70-80 in Supplementary Information for detailed analysis.

This method was repeated using the same molar amounts and using the appropriate 1-alkylimidazole and iodoalkane to produce the following R, R'-imidazolium iodide salts:

**1-Ethyl-3-methylimidazolium Iodide [MeEtIml] (8)**

*(Known compound, described in literature)*[88,94]

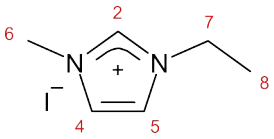


Yield: 1.41g, 5.9 mmol (97.2%) as a white solid.

**$^{1}$H NMR:** (400MHz, $d_6$-DMSO, 25°C) δ 9.13 {s, *1H*, **H2**(CH)}, 7.79 {app. t, $^{3}J_{5\text{-}4}$ ≈ $^{4}J_{5\text{-}2}$ = *1.8Hz, 1H*, **H5**(CH)}, 7.70 {app. t, $^{3}J_{4\text{-}5}$ ≈ $^{4}J_{4\text{-}2}$ = *1.8Hz, 1H*, **H4**(CH)},

4.19 {q, $^{3}J_{7\text{-}8}$ = *7.3Hz, 2H*, **H7**($CH_2$)}, 3.84 {s, *3H*, **H6**(CH)}, 1.41 {t, $^{3}J_{8\text{-}7}$ = *7.3Hz, 3H*, **H8**($CH_3$)}.

**$^{13}$C NMR:** (100MHz, $d_6$-DMSO, 25°C) δ 136.21 {**C2**(CH)}, 123.56 {**C4**(CH)}, 121.97 {**C5**(CH)}, 44.13 {**C7**($CH_2$)}, 35.76 {**C6**($CH_3$)}, 15.14 {**C8**($CH_3$)}.

**m/z (ESI):** 111 $(C_6H_{11}N_2)^+$

| **Elemental Analysis:** | | Carbon % | Hydrogen % | Nitrogen % |
|---|---|---|---|---|
| | Calculated | 30.27 | 4.66 | 11.77 |
| | Observed | 30.22 | 4.66 | 11.98 |

Please see pages 81-91 in Supplementary Information for detailed analysis.

**1-Methyl-3-propylimidazolium Iodide [MePrIml] (9)**

*(Known compound, described in literature)*[88,90]

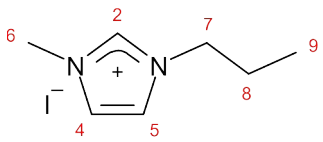


Yield: 1.42g, 5.6 mmol (92.2%) as a pale-yellow oil.

**$^{1}$H NMR:** (400MHz, $d_6$-DMSO, 25°C) δ 9.14 {app. t, $4J_{2\text{-}4} \approx 4J_{2\text{-}5} = 2.0Hz$, *1H*, **H2**(CH)}, 7.79 {app. t, $3J_{5\text{-}4} \approx 4J_{5\text{-}2} = 1.8Hz$, *1H*, **H5**(CH)}, 7.72 {app. t, $3J_{4\text{-}5} \approx 4J_{4\text{-}2} = 1.8Hz$, 1H, **H4**(CH)}, 4.13 {t, $3J_{7\text{-}8} = 7.2Hz$, *2H*, **H7**($CH_2$)}, 3.86 {s, *3H*, **H6**($CH_3$)}, 1.80 {app. sext, $3J_{8\text{-}7} \approx 3J_{8\text{-}9} = 7.4Hz$, *2H*, **H8**($CH_2$)}, 0.84 {t, $^{3}J_{9\text{-}8} = 7.4Hz$, *3H*, **H9**($CH_3$)}.

**$^{13}$C NMR:** (100MHz, $d_6$-DMSO, 25°C) δ 136.46 {**C2**(CH)}, 123.58 {**C4**(CH)}, 122.23 {**C5**(CH)}, 50.23 {**C7**($CH_2$)}, 35.83 {**C6**($CH_3$)}, 22.83 {**C8**($CH_2$)}, 10.42 {**C9**($CH_3$)}.

**m/z (ESI):** 125 $(C_7H_{13}N_2)^+$

| **Elemental Analysis:** | Carbon % | Hydrogen % | Nitrogen % |
|---|---|---|---|
| Calculated | 33.35 | 5.20 | 11.11 |
| Observed | 33.38 | 5.21 | 11.24 |

Please see pages 92-103 in Supplementary Information for detailed analysis.

**1-Butyl-3-methylimidazolium Iodide [MeBuIm] (10)**

*(Known compound, described in literature)*[87,88,91,94]

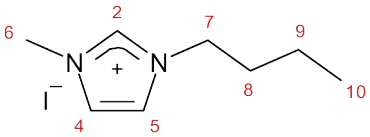


Yield: 1.47g, 5.5 mmol (90.7%) as a pale-yellow oil.

**$^{1}$H NMR:** (400MHz, $d_6$-DMSO, 25°C) δ 9.16 {app. t, $4J_{2\text{-}4} \approx 4J_{2\text{-}5} = 1.8Hz$, *1H*, **H2**(CH)}, 7.80 {app. t, $3J_{5\text{-}4} \approx 4J_{5\text{-}2} = 1.8Hz$, *1H*, **H5**(CH)}, 7.72 {app. t, $3J_{4\text{-}5} \approx 4J_{4\text{-}2} = 1.8Hz$, *1H*, **H4**(CH)}, 4.17 {t, $3J_{7\text{-}8} = 7.2Hz$, *2H*, **H7**($CH_2$)}, 3.85 {s, *3H*, **H6**($CH_3$)}, 1.76 {quin, $3J_{8\text{-}7} \approx 3J_{8\text{-}9} = 7.3Hz$, *2H*, **H8**($CH_2$)}, 1.25 {app. sext, $3J_{9\text{-}8} \approx 3J_{9\text{-}10} = 7.3Hz$, *2H*, **H9**($CH_2$)}, 0.88 {t, $3J_{10\text{-}9} = 7.4Hz$, *3H*, **H10**($CH_3$)}.

**$^{13}$C NMR:** (100MHz, $d_6$-DMSO, 25°C) δ 136.42 {**C2**(CH)}, 123.53 {**C4**(CH)}, 122.21 {**C5**(CH)}, 48.45 {**C7**($CH_2$)}, 35.84 {**C6**($CH_3$)}, 31.30 {**C8**($CH_2$)}, 18.71 {**C9**($CH_2$)}, 13.26 {**C10**($CH_3$)}.

**m/z (ESI):** 139 $(C_8H_{15}N_2)^+$

| **Elemental Analysis:** | Carbon % | Hydrogen % | Nitrogen % |
|---|---|---|---|
| Calculated | 36.11 | 5.68 | 10.53 |
| Observed | 36.27 | 5.83 | 10.21 |

Please see pages 104-115 in Supplementary Information for detailed analysis.

**1-Isopropyl-3-methylimidazolium Iodide [iPrMeIml] (11)**

*(Known compound, described in literature)*[87]

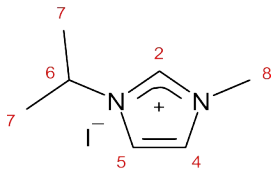


Yield: 1.36g, 5.4 mmol (88.3%) as a white solid.

**$^{1}$H NMR:** (400MHz, $d_6$-DMSO, 25°C) δ 9.19 {app. t, $4J_{2\text{-}4} \approx 4J_{2\text{-}5} = 1.8Hz$, *1H*, **H2**(CH)}, 7.88 {app. t, $3J_{5\text{-}4} \approx 4J_{5\text{-}2} = 1.8Hz$, *1H*, **H5**(CH)}, 7.72 {app. t, $3J_{4\text{-}5} \approx 4J_{4\text{-}2} = 1.8Hz$, *1H*, **H4**(CH)}, 4.62 {sept, $3J_{6\text{-}7} = 6.7Hz$, *1H*, **H6**(CH)}, 3.84 {s, *3H*, **H8**($CH_3$)}, 1.46 {d, $3J_{7\text{-}6} = 6.6Hz$, *6H*, **H7**($CH_3$)}.

**$^{13}$C NMR:** (100MHz, $d_6$-DMSO, 25°C) δ 135.33 {**C2**(CH)}, 123.68 {**C4**(CH)}, 120.46 {**C5**(CH)}, 52.12 {**C8**($CH_3$)}, 35.77 {**C6**(CH)}, 22.36 {**C7**($CH_3$)].

**m/z (ESI):** 125 $(C_7H_{13}N_2)^+$

| **Elemental Analysis:** | Carbon % | Hydrogen % | Nitrogen % |
|---|---|---|---|
| Calculated | 33.35 | 5.20 | 11.11 |
| Observed | 32.89 | 5.24 | 11.05 |

Please see pages 116-126 in Supplementary Information for detailed analysis.

**1-Methyl-3-*tert*-butylimidazolium iodide [tBuMeIml] (12)**

*(Known compound, described in literature)*[86]

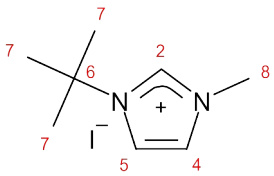


Yield: 1.24g, 4.7 mmol (76.5%) as a white solid.

**$^{1}$H NMR:** (400MHz, $d_6$-DMSO, 25°C) δ 9.23 {app. t, $4J_{2\text{-}4} \approx 4J_{2\text{-}5} = 2.0Hz$, *1H*, **H2**(CH)}, 7.99 {app. t, $3J_{5\text{-}4} \approx 4J_{5\text{-}2} = 2.0Hz$, *1H*, **H5**(CH)}, 7.75 {app. t, $3J_{4\text{-}5} \approx 4J_{4\text{-}2} = 1.8Hz$, *1H*, **H4**(CH)}, 3.84 {s, *3H*, **H8**($CH_3$)}, 1.57 {s, *3H*, **H7**($CH_3$)}.

**$^{13}$C NMR:** (100MHz, $d_6$-DMSO, 25°C) δ 135.01 {**C2**(CH)}, 123.76 {**C4**(CH)}, 120.07 {**C5**(CH)}, 59.32 {**C6**(C)}, 35.75 {**C8**($CH_3$)}, 29.02 {**C7**($CH_3$)}.

**m/z (ESI):** 139 $(C_8H_{15}N_2)^+$

| **Elemental Analysis:** | | Carbon % | Hydrogen % | Nitrogen % |
|---|---|---|---|---|
| | Calculated | 36.11 | 5.68 | 10.53 |
| | Observed | 36.28 | 5.76 | 10.21 |

Please see pages 127-137 in Supplementary Information for detailed analysis.

**1,3-Diethylimidazolium iodide [Et2Iml] (13)**

*(Known compound, described in literature)*[89]

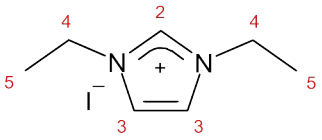


Yield: 1.23g, 4.9 mmol (79.9%) as a white solid.

**$^{1}$H NMR:** (400MHz, $d_6$-DMSO, 25°C) δ 9.20 {s, *1H*, **H2**(CH)}, 7.81 {app. d, $4J_{3\text{-}2}$ = *1.6Hz*, *2H*, **H3**(CH)}, 4.19 {q, $3J_{4\text{-}5}$ = *7.1Hz*, *4H*, **H4**($CH_2$)}, 1.42 {t, $3J_{5\text{-}4}$ = *7.3Hz*, *6H*, **H5**($CH_3$)}.

**$^{13}$C NMR:** (100MHz, $d_6$-DMSO, 25°C) δ 135.39 {**C2**(CH)}, 122.11 {**C3**(CH)}, 44.19 {**C4**($CH_2$)}, 15.06 {**C5**($CH_3$)}.

**m/z (ESI):** 125 $(C_7H_{13}N_2)^+$

| **Elemental Analysis:** | Carbon % | Hydrogen % | Nitrogen % |
|---|---|---|---|
| Calculated | 33.35 | 5.20 | 11.11 |
| Observed | 33.42 | 5.20 | 11.22 |

Please see pages 138-148 in Supplementary Information for detailed analysis.

**1-Ethyl-3-propylimidazolium iodide [EtPrIml] (14)**

*(Known compound, described in literature)*[90,94]

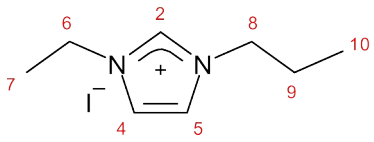


Yield: 1.47g, 5.5 mmol (90.7%) as a pale-yellow oil.

**$^{1}$H NMR:** (400MHz, $d_6$-DMSO, 25°C) δ 9.24 {s, *1H*, **H2**(CH)}, 7.83 {s, *1H*, **H5**(CH)}, 7.81 {s, *1H*, **H4**(CH)}, 4.20 {q, $^{3}J_{6\text{-}7}$ = *7.3Hz*, *2H*, **H6**($CH_2$)}, 4.13 {t, $^{3}J_{8\text{-}9}$ = *7.1Hz*, *2H*, **H8**($CH_2$)}, 1.81 {app. sext, $^{3}J_{9\text{-}8} \approx {}^{3}J_{9\text{-}10}$ = *7.3Hz*, *2H*, **H9**($CH_2$)}, 1.42 {t, $^{3}J_{6\text{-}5}$ = *7.3Hz*, *3H*, **H7**($CH_3$)}, 0.85 {t, $^{3}J_{10\text{-}9}$ = *7.3Hz*, *3H*, **H10**($CH_3$)}.

**$^{13}$C NMR:** (100MHz, $d_6$-DMSO, 25°C) δ 135.63 {**C2**(CH)}, 122.37 {**C4**(CH)}, 122.12 {**C5**(CH)}, 50.29 {**C8**($CH_2$)}, 44.21 {**C6**($CH_2$)}, 22.78 (**C9**($CH_2$)}, 15.03 {**C7**($CH_3$)}, 10.44 {**C10**($CH_3$)}.

**m/z (ESI):** 139 $(C_8H_{15}N_2)^+$

| **Elemental Analysis:** | Carbon % | Hydrogen % | Nitrogen % |
|---|---|---|---|
| Calculated | 36.11 | 5.68 | 10.53 |
| Observed | 36.28 | 5.80 | 10.21 |

Please see pages 149-160 in Supplementary Information for detailed analysis.

**1-Butyl-3-ethylimidazolium iodide [EtBuIm] (15)**

*(Known compound, described in literature)*[91,94]

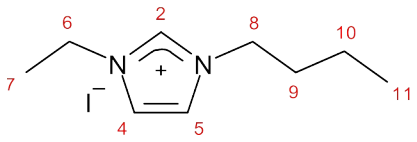


Yield: 1.65g, 5.9 mmol (96.6%) as a pale-yellow oil.

**$^{1}$H NMR:** (400MHz, $d_6$-DMSO, 25°C) δ 9.22 {s, *1H*, **H2**(CH)}, 7.82 {s, *1H*, **H5**(CH)}, 7.80 {s, *1H*, **H4**(CH)}; 4.18 {m, *4H*, **H6/8**($CH_2$)}, 1.77 {quin, $^{3}J_{9\text{-}8} \approx {}^{3}J_{9\text{-}10}$ = *7.3Hz*, *2H*, **H9**($CH_2$)}, 1.42 {t, $^{3}J_{7\text{-}6}$ = *7.3Hz*, *3H*, **H7**($CH_3$)}, 1.26 {app. sext, $^{3}J_{10\text{-}9} \approx {}^{3}J_{10\text{-}11}$ = *7.4Hz*, *2H*, **H10**($CH_2$)}, 0.90 {t, $^{3}J_{11\text{-}10}$ = *7.4Hz*, *3H*, **H11**($CH_3$)}.

**$^{13}$C NMR:** (100MHz, $d_6$-DMSO, 25°C) δ 135.64 {**C2**(CH)}, 122.40 {**C4**(CH)}, 122.13 {**C5**(CH)}, 48.56 {**C6**($CH_2$)}, 44.22 {**C8**($CH_2$)}, 31.29 {**C9**($CH_2$)}, 18.80 {**C10**($CH_2$)}, 15.03 {**C7**($CH_3$)}, 13.29 {**C11**($CH_3$)}.

**m/z (ESI):** 153 $(C_9H_{17}N_2)^+$

| **Elemental Analysis:** | Carbon % | Hydrogen % | Nitrogen % |
|---|---|---|---|
| Calculated | 38.59 | 6.12 | 10.00 |
| Observed | 38.58 | 6.11 | 9.74 |

Please see pages 161-172 in Supplementary Information for detailed analysis.

**1-Ethyl-3-*iso*propylimidazolium iodide [iPrEtIml] (16)**

*(Known compound, described in literature)*[92]

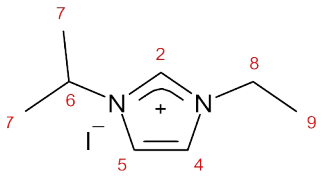


Yield: 1.31g, 4.9 mmol (80.9%) as a white solid.

**$^{1}$H NMR:** (400MHz, $d_6$-DMSO, 25°C) δ 9.25 {s, *1H*, **H2**(CH)}, 7.91 {app. t, $4J_{5\text{-}2} \approx {}^{3}J_{5\text{-}4}$ = *1.9Hz*, *1H*, **H5**(CH)}, 7.83 {app. t, $4J_{4\text{-}2} \approx 3J_{4\text{-}5}$ = *1.9Hz*, *1H*, **H4**(CH)},

4.62 {sept, $3J_{6\text{-}7}$ = *6.7Hz*, *1H*, **H6**(CH)}, 4.18 {q, $3J_{8\text{-}9}$ = *7.3Hz*, *2H*, **H8**($CH_2$)},

1.47 {d, $3J_{7\text{-}6}$ = *6.7Hz*, *6H*, **H7**($CH_3$)}, 1.43 {t, $3J_{9\text{-}8}$ = *7.3Hz*, *3H*, **H9**($CH_3$)}.

**$^{13}$C NMR:** (100MHz, $d_6$-DMSO, 25°C) δ 134.48 {**C2**(CH)}, 122.20 {**C4**(CH)}, 120.59 {**C5**(CH)}, 52.19 {**C6**(CH)}, 44.23 {**C8**($CH_2$)}, 22.34 {**C7**($CH_3$)}, 15.00 {**C9**($CH_3$)}.

**m/z (ESI):** 139 $(C_8H_{15}N_2)^+$

| **Elemental Analysis:** | | Carbon % | Hydrogen % | Nitrogen % |
|---|---|---|---|---|
| | Calculated | 36.11 | 5.68 | 10.53 |
| | Observed | 36.52 | 5.65 | 10.27 |

Please see pages 173-184 in Supplementary Information for detailed analysis.

**1-Ethyl-3-*tert*-butylimidazolium iodide [tBuEtIml] (17)**

*(Novel compound)*

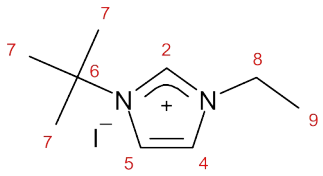


Yield: 1.29g, 4.6 mmol (75.4%) as a white solid.

**$^{1}$H NMR:** (400MHz, $d_6$-DMSO, 25°C) δ 9.25 {app. t, $4J_{2\text{-}4} \approx 4J_{2\text{-}5} = 1.7Hz$, *1H*, **H2**(CH)}, 8.02 {app. t, $4J_{5\text{-}2} \approx 3J_{5\text{-}4} = 2.0Hz$, *1H*, **H5**(CH)}, 7.87 {app. t, $4J_{4\text{-}2} \approx 3J_{4\text{-}5} = 1.9Hz$, *1H*, **H4**(CH)}, 4.18 {q, $3J_{8\text{-}9} = 7.3Hz$, *2H*, **H8**($CH_2$)}, 1.58 {s, *9H*, **H7**($CH_3$)}, 1.44 {t, $3J_{9\text{-}8} = 7.3Hz$, *3H*, **H9**($CH_3$)}.

**$^{13}$C NMR:** (100MHz, $d_6$-DMSO, 25°C) δ 134.14 {**C2**(CH)}, 122.24 {**C4**(CH)}, {120.27 {**C5**(CH)}, 59.37 {**C6**(C)}, 44.24 {**C8**($CH_2$)}, 29.02 {**C7**($CH_3$)}, 15.09 {**C9**($CH_3$)}.

**m/z (ESI):** 153 $(C_9H_{17}N_2)^+$

| **Elemental Analysis:** | Carbon % | Hydrogen % | Nitrogen % |
|---|---|---|---|
| Calculated | 38.59 | 6.12 | 10.00 |
| Observed | 38.58 | 6.14 | 9.73 |

Please see pages 185-195 in Supplementary Information for detailed analysis.

**1,3-Dipropylimidazolium iodide [Pr2Iml] (18)**

*(Known compound, described in literature)*[93,94]

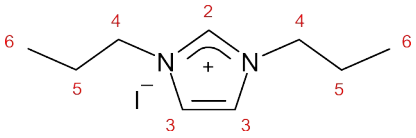


Yield: 1.26g, 4.5 mmol (73.7%) as a yellow oil.

**$^{1}$H NMR:** (400MHz, $d_6$-DMSO, 25°C) δ 9.22 {s, *1H*, **H2**(CH)}, 7.82 {app. d, $^{4}J_{3\text{-}2}$ = *1.7Hz*, *2H*, **H3**(CH)}, 4.14 {t, $^{3}J_{4\text{-}5}$ = *7.1Hz*, *4H*, **H4**($CH_2$)}, 1.81 {app. sext, $^{3}J_{5\text{-}4} \approx {}^{3}J_{5\text{-}6}$ = *7.3Hz*, *4H*, **H5**($CH_2$)}, 0.84 {t, $^{3}J_{6\text{-}5}$ = *7.3Hz*, *6H*, **H6**($CH_3$)}.

**$^{13}$C NMR:** (100MHz, $d_6$-DMSO, 25°C) δ 135.95 {**C2**(CH)}, 122.47 {**C3**(CH)}, 50.33 {**C4**($CH_2$)}, 22.76 {**C5**($CH_2$)}, 10.41 {**C6**($CH_3$)}.

**m/z (ESI):** 153 $(C_9H_{17}N_2)^+$

| **Elemental Analysis:** | Carbon % | Hydrogen % | Nitrogen % |
|---|---|---|---|
| Calculated | 38.59 | 6.12 | 10.00 |
| Observed | 38.54 | 6.13 | 9.71 |

Please see pages 196-206 in Supplementary Information for detailed analysis.

**1-Butyl-3-propylimidazolium iodide [PrBuIml] (19)**

*(Known compound, described in literature)*[94]

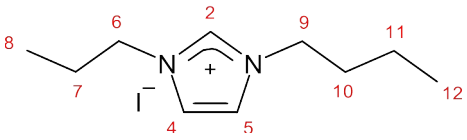


Yield: 1.65g, 5.6 mmol (92.2%) as an orange oil.

**$^{1}$H NMR:** (400MHz, $d_6$-DMSO, 25°C) δ 9.23 {s, *1H*, **H2**(CH)}, 7.82 {m, *2H*, **H4/5**(CH)}, 4.18 {t, $^{3}J_{7\text{-}8}$ = *7.2Hz*, *2H*, **H9**($CH_2$)}, 4.14 {t, $^{3}J_{4\text{-}5}$ = *7.1Hz*, *2H*, **H6**($CH_2$)}, 1.80 {m, *4H*, **H7/10**($CH_2$)}, 1.25 {app. sext, $^{3}J_{9\text{-}8}$ ≈ $^{3}J_{9\text{-}10}$ = *7.4Hz*, *2H*, **H11**($CH_2$)}, 0.89 {t, $^{3}J_{10\text{-}9}$ = *7.4Hz*, *3H*, **H12**($CH_3$)}, 0.84 {t, $^{3}J_{6\text{-}5}$ = *7.3Hz*, *3H*, **H8**($CH_3$)}.

**$^{13}$C NMR:** (100MHz, $d_6$-DMSO, 25°C) δ 135.93 {**C2**(CH)}, 122.46 {**C4/C5**(CH)}, 122.45 {**C5/C4**(CH)}, 50.33 (**C6**($CH_2$)}, 48.57 {**C9**($CH_2$)}, 31.26 {**C10**($CH_2$)}, 22.76 {**C7**($CH_2$)}, 18.77 {**C11**($CH_2$)}, 13.28 {**C12**($CH_3$)}, 10.41 {**C8**($CH_3$)}.

**m/z (ESI):** 167 $(C_{10}H_{19}N_2)^+$

| **Elemental Analysis:** | Carbon % | Hydrogen % | Nitrogen % |
|---|---|---|---|
| Calculated | 40.83 | 6.51 | 9.52 |
| Observed | 40.41 | 6.46 | 9.17 |

Please see pages 207-218 in Supplementary Information for detailed analysis.

**1-Isopropyl-3-propylimidazolium iodide [iPrPrIml] (20)**

*(Known compound, described in literature)*[90,94]

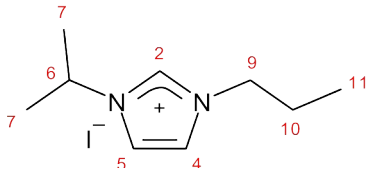


Yield: 1.31g, 4.7 mmol (76.6%) as a pale-yellow oil.

**$^{1}$H NMR:** (400MHz, $d_6$-DMSO, 25°C) δ 9.29 {app. t, $4J_{2\text{-}4} \approx 4J_{2\text{-}5} = 1.7Hz$, *1H*, **H2**(CH)}, 7.93 {app. t, $4J_{5\text{-}2} \approx 3J_{5\text{-}4} = 1.9Hz$, *1H*, **H5**(CH)}, 7.83 {app. t, $4J_{4\text{-}2} \approx 3J_{4\text{-}5} = 1.8Hz$, *1H*, **H4**(CH)}, 4.63 {sept, $3J_{6\text{-}7} = 6.7Hz$, *1H*, **H6**(CH)}, 4.12 {t, $3J_{9\text{-}10} = 7.2Hz$, *2H*, **H9**($CH_2$)}, 1.82 {app. sext, $3J_{10\text{-}9} \approx 3J_{10\text{-}11} = 7.4Hz$, *2H*, **H10**($CH_2$)}, 1.48 {d, $3J_{7\text{-}6} = 6.7Hz$, *6H*, **H7**($CH_3$)}, 0.85 {t, $3J_{11\text{-}10} = 7.4Hz$, *3H*, **H11**($CH_3$)}.

**$^{13}$C NMR:** (100MHz, $d_6$-DMSO, 25°C) δ 134.75 {**C2**(CH)}, 122.51 {**C4**(CH)}, 120.63 {**C5**(CH)}, 52.19 {**C6**(CH)}, 50.35 {**C9**($CH_2$)}, 22.75 {**C10**($CH_2$)}, 22.33 {**C7**($CH_3$)}, 10.46 {**C11**($CH_3$)}.

**m/z (ESI):** 153 $(C_9H_{17}N_2)^+$

| **Elemental Analysis:** | Carbon % | Hydrogen % | Nitrogen % |
|---|---|---|---|
| Calculated | 38.59 | 6.12 | 10.00 |
| Observed | 38.61 | 6.29 | 9.69 |

Please see pages 219-230 in Supplementary Information for detailed analysis.

**1-Propyl-3-*tert*-butylimidazolium iodide [tBuPrIml] (21)**

*(Novel compound)*

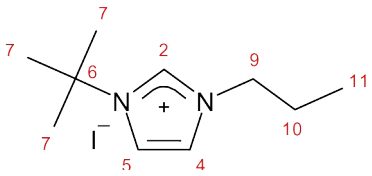


Yield: 1.28g, 4.4 mmol (71.5%) as a cream solid.

**$^{1}$H NMR:** (400MHz, $d_6$-DMSO, 25°C) δ 9.28 {app. t, $4J_{2\text{-}4} \approx 4J_{2\text{-}5} = 1.7Hz$, *1H*, **H2**(CH)}, 8.03 {app. t, $4J_{5\text{-}2} \approx 3J_{5\text{-}4} = 2.0Hz$, *1H*, **H5**(CH)}, 7.86 = {app. t, $4J_{4\text{-}2} \approx 3J_{4\text{-}5} = 1.9Hz$, *1H*, **H4**(CH)}, 4.11 {t, $3J_{9\text{-}10} = 7.2Hz$, *2H*, **H9**($CH_2$)}, 1.83 {app. sext, $3J_{10\text{-}9} \approx 3J_{10\text{-}11} = 7.4Hz$, *2H*, **H10**($CH_2$)}, 1.58 {s, *9H*, **H7**($CH_3$)}, 0.86 {t, $3J_{11\text{-}10} = 7.4Hz$, *3H*, **H11**($CH_3$)}.

**$^{13}$C NMR:** (100MHz, $d_6$-DMSO, 25°C) δ 134.40 {**C2**(CH)}, 122.59 {**C4**(CH)}, 120.30 {**C5**(CH)}, 59.42 {**C6**(C)}, 50.38 {**C9**($CH_2$)}, 29.02 {**C7**($CH_3$)}, 22.81 {**C10**($CH_2$)}, 10.51 {**C11**($CH_3$)}.

**m/z (ESI):** 167 $(C_{10}H_{19}N_2)^+$

| **Elemental Analysis:** | Carbon % | Hydrogen % | Nitrogen % |
|---|---|---|---|
| Calculated | 40.83 | 6.51 | 9.52 |
| Observed | 40.35 | 6.46 | 9.07 |

Please see pages 231-242 in Supplementary Information for detailed analysis.

**1,3-Dibutylimidazolium iodide [Bu2Iml] (22)**

*(Known compound, described in literature)*[86]

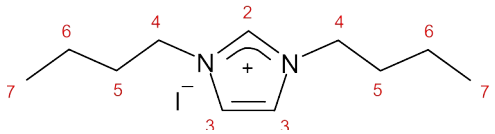


Yield: 1.51g, 4.9 mmol (80.3%) as a white solid.

**$^{1}$H NMR:** (400MHz, $d_6$-DMSO, 25°C) δ 9.26 {s, *1H*, **H2**(CH)}, 7.82 {app. d, $4J_{3\text{-}2}$ = *1.6Hz*, *2H*, **H3**(CH)}, 4.17 {t, $3J_{4\text{-}5}$ = *7.2Hz*, *2H*, **H4**($CH_2$)}, 1.77 {quin, $3J_{5\text{-}4}$ ≈ $^{3}J_{5\text{-}6}$ = *7.3Hz*, *4H*, **H5**($CH_2$)}, 1.24 {app. sext, $3J_{6\text{-}5}$ ≈ $3J_{6\text{-}7}$ = *7.4Hz*, *4H*, **H6**($CH_2$)}, 0.89 {t, $3J_{7\text{-}6}$ = *7.4Hz*, *6H*, **H7**($CH_3$)}.

**$^{13}$C NMR:** (100MHz, $d_6$-DMSO, 25°C) δ 135.90 {**C2**(CH)}, 122.43 {**C3**(CH)}, 48.56 {**C4**($CH_2$)}, 31.24 {**C5**($CH_2$)}, 18.76 {**C6**($CH_2$)}, 13.26 {**C7**($CH_3$)}.

**m/z (ESI):** 181 $(C_{11}H_{21}N_2)^+$

| **Elemental Analysis:** | Carbon % | Hydrogen % | Nitrogen % |
|---|---|---|---|
| Calculated | 42.87 | 6.87 | 9.09 |
| Observed | 42.96 | 6.87 | 9.07 |

Please see pages 243-254 in Supplementary Information for detailed analysis.

**1-Butyl-3-isopropylimidazolium iodide [iPrBuIml] (23)**

*(Known compound, described in literature)*[94]

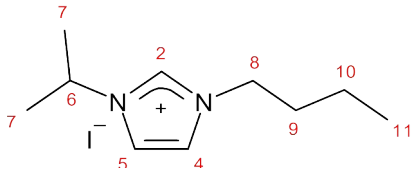


Yield: 1.56g, 5.3 mmol (87.2%) as a white solid.

**$^{1}$H NMR:** (400MHz, $d_6$-DMSO, 25°C) δ 9.28 {s, *1H*, **H2**(CH)}, 7.92 {app. t, $4J_{5\text{-}2}$ ≈ $^{3}J_{5\text{-}4}$ = *1.8Hz*, *1H*, **H5**(CH)}, 7.83 {app. t, $4J_{4\text{-}2}$ ≈ $3J_{4\text{-}5}$ = *1.8Hz*, *1H*, **H4**(CH)},

4.62 {sept, $3J_{6\text{-}7}$ = *6.7Hz*, *1H*, **H6**(CH)}, 4.15 {t, $3J_{8\text{-}9}$ = *7.3Hz*, *2H*, **H8**($CH_2$)},

1.78 {quin, $3J_{9\text{-}8}$ ≈ $3J_{9\text{-}10}$ = *7.3Hz*, *2H*, **H9**($CH_2$)}, 1.48 {d, $3J_{7\text{-}6}$ = *6.7Hz*, *6H*,

**H7**($CH_3$)}, 1.26 {app. sext, $3J_{10\text{-}9}$ ≈ $3J_{10\text{-}11}$ = *7.4Hz*, *2H*, **H10**($CH_2$)}, 0.90 {t, $^{3}J_{11\text{-}10}$ = *7.3Hz*, *3H*, **H11**($CH_3$)}.

**$^{13}$C NMR:** (100MHz, $d_6$-DMSO, 25°C) δ 134.73 {**C2**(CH)}, 122.52 {**C4**(CH)}, 120.63 {**C5**(CH)}, 52.20 {**C6**(CH)}, 48.62 {**C8**($CH_2$)}, 31.27 {**C9**($CH_2$)}, 22.33 {**C7**($CH_3$)}, 18.85 {**C10**($CH_2$)}, 13.31 {**C11**($CH_3$)}.

**m/z (ESI):** 167 $(C_{10}H_{19}N_2)^+$

| **Elemental Analysis:** | Carbon % | Hydrogen % | Nitrogen % |
|---|---|---|---|
| Calculated | 40.83 | 6.51 | 9.52 |
| Observed | 40.38 | 6.49 | 9.72 |

Please see pages 255-266 in Supplementary Information for detailed analysis.

**1-Butyl-*tert*-butylimidazolium iodide [tBuBuIml] (24)**

*(Novel Compound)*

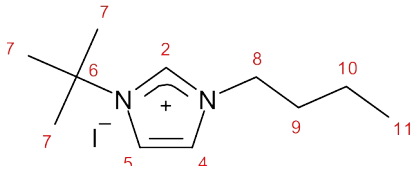


Yield: 1.29g, 4.2 mmol (68.8%) as a cream solid.

**$^{1}$H NMR:** (400MHz, $d_6$-DMSO, 25°C) δ 9.29 {app. t, $4J_{2\text{-}4} \approx 4J_{2\text{-}5} = 1.8Hz$, *1H*, **H2**(CH)}, 8.03 {app. t, $4J_{5\text{-}2} \approx 3J_{5\text{-}4} = 2.0Hz$, *1H*, **H5**(CH)}, 7.87 {app. t, $4J_{4\text{-}2} \approx 3J_{4\text{-}5} = 1.8Hz$, *1H*, **H4**(CH)}, 4.15 t, $3J_{8\text{-}9} = 7.3Hz$, *2H*, **H8**($CH_2$)}, 1.80 {quin, $3J_{9\text{-}8} \approx 3J_{9\text{-}10} = 7.5Hz$, *2H*, **H9**($CH_2$)}, 1.58 {s, *9H*, **H7**($CH_3$)}, 1.27 {app. sext, $3J_{10\text{-}9} \approx 3J_{10\text{-}11} = 7.3Hz$, *2H*, **H10**($CH_2$)}, 0.90 {t, $3J_{11\text{-}10} = 7.4Hz$, *3H*, **H11**($CH_2$)}.

**$^{13}$C NMR:** (100MHz, $d_6$-DMSO, 25°C) δ 134.37 {**C2**(CH)}, 122.57 {**C4**(CH)}, 120.29 {**C5**(CH)}, 59.42 {**C6**(C)}, 48.65 {**C8**($CH_2$)}, 31.33 {**C9**($CH_2$)}, 29.02 {**C7**($CH_3$)}, 18.90 {**C10**($CH_2$)}, 13.34 {**C11**($CH_3$)}.

**m/z (ESI):** 181 $(C_{11}H_{21}N_2)^+$

| **Elemental Analysis:** | Carbon % | Hydrogen % | Nitrogen % |
|---|---|---|---|
| Calculated | 42.87 | 6.87 | 9.09 |
| Observed | 43.07 | 6.89 | 9.03 |

Please see pages 267-278 in Supplementary Information for detailed analysis.

**1,3-Di-Isopropylimidazolium iodide [iPr2Iml] (25)**

*(Known compound, described in literature)*[87]

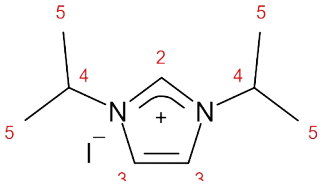


Yield: 1.59g, 5.7 mmol (93.0%) as a white solid.

**$^{1}$H NMR:** (400MHz, $d_6$-DMSO, 25°C) δ 9.29 {app. t, $4J_{2\text{-}3} \approx 4J_{2\text{-}3'}$ = *1.7Hz*, *1H*, **H2**(CH)}, 7.94 {app. d, $3J_{3\text{-}2}$ = *1.7Hz*, *2H*, **H3**(CH)}, 4.62 {sept, $3J_{4\text{-}5}$ = *6.7Hz*, *2H*, **H4**(CH)}, 1.48 {d, $3J_{5\text{-}4}$ = *6.7Hz*, *12H*, **H5**($CH_3$)}.

**$^{13}$C NMR:** (100MHz, $d_6$-DMSO, 25°C)δ 133.55 {**C2**(CH)}, 120.66 {**C3**(CH)}, 52.25 {**C4**(CH)}, 22.35 {**C5**($CH_3$)}.

**m/z (ESI):** 153 $(C_9H_{17}N_2)^+$

| **Elemental Analysis:** | Carbon % | Hydrogen % | Nitrogen % |
|---|---|---|---|
| Calculated | 38.59 | 6.12 | 10.00 |
| Observed | 38.71 | 6.21 | 9.67 |

Please see pages 279-289 in Supplementary Information for detailed analysis.

**1-Isopropyl-3-*tert*-butylimidazolium iodide [iPrtBuIm] (26)**

*(Novel Compound)*

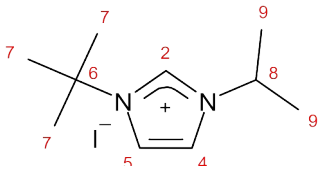


Yield: 1.37g, 4.7 mmol (76.5%) as a cream solid.

**$^{1}$H NMR:** (400MHz, $d_6$-DMSO, 25°C) δ 9.23 {app. t, $4J_{2\text{-}4} \approx 4J_{2\text{-}5} = 1.7Hz$, *1H*, **H2**(CH)}, 8.05 {app. t, $4J_{5\text{-}2} \approx 3J_{5\text{-}4} = 2.0Hz$, *1H*, **H5**(CH)}, 7.98 {app. t, $4J_{4\text{-}2} \approx 3J_{4\text{-}5} = 1.9Hz$, *1H*, **H4**(CH)}, 4.63 {sept, $3J_{8\text{-}9} = 6.7Hz$, *1H*, **H8**(CH)}, 1.59 {s, *9H*, **H7**($CH_3$)}, 1.48 {d, $3J_{9\text{-}8} = 6.7Hz$, *6H*, **H9**($CH_3$)}

**$^{13}$C NMR:** (100MHz, $d_6$-DMSO, 25°C) δ 133.13 {**C2**(CH)}, 120.51 {**C4**(CH)}, 120.46 {**C5**(CH)}, 59.44 {**C6**(C)}, 52.32 {**C8**(CH)}, 29.05 {**C7**($CH_3$)}, 22.37 {**C9**($CH_3$)}.

**m/z (ESI):** 167 $(C_{10}H_{19}N_2)^+$

| **Elemental Analysis:** | Carbon % | Hydrogen % | Nitrogen % |
|---|---|---|---|
| Calculated | 40.83 | 6.51 | 9.52 |
| Observed | 40.67 | 6.45 | 9.22 |

Please see pages 290-300 in Supplementary Information for detailed analysis.

**1,3-Di-*tert*-butylimidazolium iodide [tBu2Iml] (27)**

*(Novel Compound)*

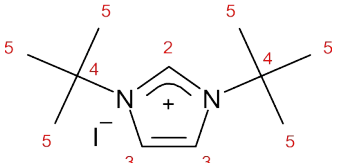


Tert-butylamine (0.29g, 4 mmol, 0.42 ml) and hydriodic acid (0.46, 2 mmol, 0.27 mL) in methanol (10ml) was added dropwise over 30 minutes to 40% aq. glyoxal (0.29g, 2 mmol, 0.23 ml). Formaldehyde 37 % aq. (0.16g, 2 mmol, 0.15 ml) in methanol (10 ml) was added dropwise over 30 minutes then heated to reflux for 12 hours. After 12 hours the solvent was removed under vacuum, and the crude product was washed with ethyl acetate (25 ml) which was then decanted. Washing repeated an additional 2 times then product then dried under vacuum to yield product as a cream solid.

Yield: 0.34g, 1.1 mmol (54.8%).

**$^{1}$H NMR:** (400MHz, $d_6$-DMSO, 25°C) δ 9.01 {app. t, $4J_{2\text{-}3} \approx 4J_{2\text{-}3'} = 1.8Hz$, *1H*, **H2**(CH)}, 8.06 {app. d, $4J_{3\text{-}2} = 1.8Hz$, *2H*, **H3**(CH)}, 1.60 {s, *18H*, **H5**($CH_3$)}.

**$^{13}$C NMR:** (100MHz, $d_6$-DMSO, 25°C) δ 132.23 {**C2**(CH)}, 120.53 {**C3**(CH)}, 59.69 {**C4**(C)}, 29.14 {**C5**($CH_3$)}.

**m/z (ESI):** 181 $(C_{11}H_{21}N_2)^+$

| **Elemental Analysis:** | Carbon % | Hydrogen % | Nitrogen % |
|---|---|---|---|
| Calculated | 42.87 | 6.87 | 9.09 |
| Observed | 42.94 | 6.90 | 9.29 |

Please see pages 301-311 in Supplementary Information for detailed analysis.

### 4.3 Potassium Tetracarbonyl Iron Hydride Synthesis [$KHFe(CO)_4$]

*(Known compound, described in literature)*[71,72,73]

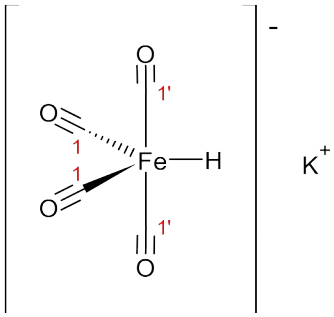


***Method 1:***

Freshly distilled iron pentacarbonyl (2g, 10 mmol, 1.34 mL) and commercial (90% purity, Sigma-Aldrich) potassium hydroxide (0.56g, 10 mmol) in methanol (5 mL) were stirred constantly for 12 hours under argon atmosphere at room temperature. After 24 hours the solvent was removed under vacuum. Acetonitrile (10 mL) was added, and the reaction mixture was stirred for 1 hour. The solution was filtered via cannula, and the solvent was removed under vacuum to yield product as a red/ maroon solid.

Yield: 1.07g, 5.1 mmol (51.4%).

***Method 2:***

In a glovebox, re-melted potassium metal (0.1025g, 2.621 mmol) was pressed against the side of a round bottom Schlenk flask, which was then taken out of the glovebox, attached to the Schlenk line and cooled in an ice bath. Dry, degassed methanol was then added dropwise *via* cannula with constant stirring whilst avoiding direct contact between the solvent and metal. The potassium was then allowed to react with the methanol vapours. Slow addition of methanol was repeated until all the potassium had reacted. Degassed water (47.2mg, 47.2 µL, 2.621 mmol) was then added. Assuming the reaction was quantitative freshly distilled $Fe(CO)_5$ (0.354 mL, 0.514g, 2.621 mmol) was added and left to stir for 24 hours. After 24 hours a dark red/ purple with a small amount of solid was observed upon which solvent was removed under vacuum. Acetonitrile (10 mL) was added, and the reaction mixture was stirred for 1 hour. The solution was filtered via cannula, and the solvent was removed under vacuum to yield product as a red solid.

Yield: 0.35g, 1.7 mmol (64.4%).

**$^{1}$H NMR:** (400MHz, $d_6$-DMSO capillary for lock, 25°C)

δ 8.98 {s, *1H*, Fe-H} (MeOH solution).

δ 8.70 {s, *1H*, Fe-H} (MeCN solution).

**$^{13}$C NMR:** (100MHz, $d_6$-DMSO capillary for lock, 25°C)

δ 219.95 {**C1/C1'**(CO)}, 210.51 {**C1/C1'**(CO)} (MeOH solution),

δ 221.28 {**C1/C1'**(CO)} (MeCN solution)

**m/z (ESI):** 169 $(HFe[CO]_4)^-$

| **Elemental Analysis:** | | Carbon % | Hydrogen % | Nitrogen % |
|---|---|---|---|---|
| | Calculated | 23.08 | 0.48 | 0 |
| | Calculated + 0.5 MeCN | 26.28 | 1.10 | 3.06 |
| | Observed | 26.41 | 0.96 | 3.48 |

Please see pages 312-317 in Supplementary Information for detailed analysis.

### 4.4 Fe-NHC Complex Synthesis

**Tetracarbonyl (1,3-Dimethylimidazol-2-ylidene) Iron [FeMe2]**

*(Known compound, described in literature)*[39,40,48]

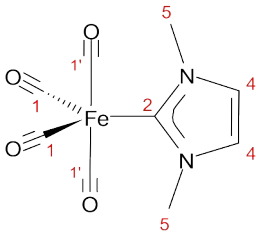


In a Schlenk tube, the mixture of solid potassium tetracarbonyl iron hydride (40 mg, 0.19 mmol) and 1,3-dimethylimidazolium iodide (85 mg, 0.38 mmol) was heated to 120°C, at which point the reaction mixture turned into a deep red viscous liquid, which was further heated under dynamic vacuum for 4 hours, resulting in the formation of brown-black viscous liquid. Upon cooling, toluene (3 mL) was added to the reaction mixture, and the yellow solution was filtered off, leaving brown-black solid behind. The solvent was then removed from the yellow solution under vacuum, and the crude product was purified via vacuum sublimation onto a liquid nitrogen cooled cold finger.

Yield: 27.2 mg, 0.1 mmol (54.2%) as a pale-yellow solid.

**$^{1}$H NMR:** (400MHz, $C_6D_6$, 25°C) δ 5.72 {s, *2H*, **H4**(CH)}, 3.03 {s, *6H*, **H5**($CH_3$)}.

**$^{13}$C NMR:** (100MHz, $C_6D_6$, 25°C) δ 216.96 {**C1/C1'**(CO)}, 181.31 {**C2**(Carbene)}, 123.20 {**C4**(CH)}, 39.13 {**C5**($CH_3$)}.

**m/z (ESI):** 97 $([C_5H_8N_2]+H)^+$, 169 $([Fe(CO)_4]+H)^-$

| **Elemental Analysis:** | | Carbon % | Hydrogen % | Nitrogen % |
|---|---|---|---|---|
| | Calculated | 40.94 | 3.05 | 10.61 |
| | Observed | 40.48 | 3.16 | 10.65 |

Please see pages 318-327 in Supplementary Information for detailed analysis.

**Hydrogen testing:**

In an NMR tube a clear yellow solution of FeMe2 in $C_6D_6$ was degassed using the following method. The NMR tube was placed into cool water (5-10°C) for 1 minute and then exposed to vacuum for 1-2 seconds. This was then repeated two more times, gently shaking the NMR tube in between exposure to vacuum. The sample was then exposed to atmospheric pressure of hydrogen gas for 1 hour, the NMR tube was sealed and $^1$H NMR spectrum was recorded. The sample was then heated to 80°C in the sand bath overnight. The sample was left to cool to room temperature and 1H NMR spectrum obtained. Other than the $H_2$ gas peak at 4.47 ppm in the NMR spectra, no other physical or analytical changes observed.

These methods were repeated using the same molar amounts, usage of appropriate R, R'-imidazolium iodide salt for synthesis of the following complexes and Hydrogen testing of those complexes:

**Tetracarbonyl (1-ethyl-3-methylimidazol-2-ylidene) Iron [FeMeEt]**

*(Novel Compound)*

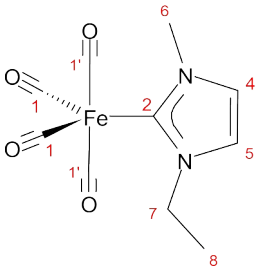


Yield: 25.9 mg, 0.1 mmol (49.0%) as a pale-yellow solid.

**$^{1}$H NMR:** (400MHz, $C_6D_6$, 25°C) δ 5.90 {s, *1H*, **H5**(CH)}, 5.82 {s, *1H*, **H4**(CH)}, 3.71 {q, $^{3}J_{7\text{-}8}$ = *7.5Hz*, *2H*, **H7**($CH_2$)}, 3.07 {s, *3H*, **H6**($CH_3$)}, 0.88 {t, $^{3}J_{8\text{-}7}$ = *6.8Hz*, *3H*, **H8**($CH_3$)}.

**$^{13}$C NMR:** (100MHz, $C_6D_6$, 25°C) δ 217.34 {**C1/C1'**(CO)}, 180.14 {**C2**(Carbene)}, 123.90 {**C4**(CH)}, 121.19 {**C5**(CH)}, 46.34 {**C7**($CH_2$)}, 39.13 {**C6**($CH_3$)}, 15.58 {**C8**($CH_3$)}.

**m/z (ESI):** 111 $([C_6H_{10}N_2]+H)^+$, 169 $([Fe(CO)_4]+H)^-$

| **Elemental Analysis:** | | Carbon % | Hydrogen % | Nitrogen % |
|---|---|---|---|---|
| | Calculated | 43.20 | 3.63 | 10.08 |
| | Observed | 43.31 | 3.71 | 9.81 |

Please see pages 328-337 in Supplementary Information for detailed analysis.

**Hydrogen testing:**

Other than the $H_2$ gas peak at 4.47 ppm in the NMR spectra, no other changes were observed.

**Tetracarbonyl (1-*I*sopropyl-3-methylimidazol-2-ylidene) Iron [FeiPrMe]**

*(Novel Compound)*

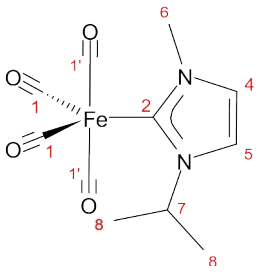


Yield: 21.9 mg, 0.075 mmol (39.0%) as a yellow solid.

**$^{1}$H NMR:** (400MHz, $C_6D_6$, 25°C) δ 6.11 {d, $3J_{5\text{-}4}$ = *2.1Hz*, *1H*, **H5**(CH)}, 5.86 {d, $3J_{4\text{-}5}$ = *2.1Hz*, *1H*, **H4**(CH)}, 5.19 {sept, $3J_{7\text{-}8}$ = *6.7Hz*, *1H*, **H7**(CH)}, 3.07 {s, *3H*, **H6**($CH_3$)}, 0.94 {d, $3J_{7\text{-}6}$ = *6.7Hz*, *6H*, **H8**($CH_3$)}.

**$^{13}$C NMR:** (100MHz, $C_6D_6$, 25°C) δ 217.45 {**C1/C1'**(CO)}, 179.39 {**C2**(Carbene)}, 124.61 {**C4**(CH)}, 117.81 {**C5**(CH)}, 52.70 {**C7**(CH)}, 39.23 {**C6**($CH_3$)}, 22.68 {**C8**($CH_3$)}.

**m/z (ESI):** 125 ($[C_7H_{12}N_2]+H)^+$, 169 ($[Fe(CO)_4]+H)^-$, 291 ([Complex]-H)$^-$, 291 ([Complex]+H)$^+$.

| **Elemental Analysis:** | | Carbon % | Hydrogen % | Nitrogen % |
|---|---|---|---|---|
| | Calculated | 45.24 | 4.14 | 9.59 |
| | Observed | 45.57 | 4.23 | 9.41 |

Please see pages 358-367 in Supplementary Information for detailed analysis.

**Hydrogen testing:**

Other than the $H_2$ gas peak at 4.47 ppm in the NMR spectra, no other changes were observed.

**Tetracarbonyl (1,3-Di*iso*propylimidazol-2-ylidene) Iron [FeiPr2]**

*(Known compound, described in literature)*[48]

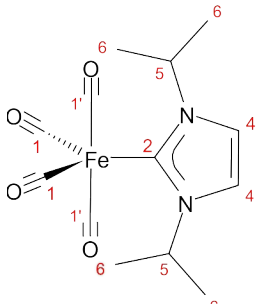


Yield: 28.1 mg, 0.088 mmol (45.6%) as a yellow solid.

**$^{1}$H NMR:** (400MHz, $C_6D_6$, 25°C) δ 6.32 {s, *2H*, **H4**(CH)}, 5.25 {sept, $3J_{5\text{-}6}$ = *6.7Hz*, *2H*, **H5**(CH)}, 0.93 {d, $3J_{6\text{-}5}$ = *6.7Hz*, *12H*, **H6**($CH_3$)}.

**$^{13}$C NMR:** (100MHz, $C_6D_6$, 25°C) δ 218.42 {**C1/C1'**(CO)}, 178.37 {**C2**(Carbene)}, 119.03 {**C4**(CH)}, 52.46 {**C5**(CH)}, 22.74 {**C6**($CH_3$)}.

**m/z (ESI):** 153 $([C_9H_{14}N_2]+H)^+$, 319 $([Complex]-H)^-$

| **Elemental Analysis:** | | Carbon % | Hydrogen % | Nitrogen % |
|---|---|---|---|---|
| | Calculated | 48.77 | 5.04 | 8.75 |
| | Observed | 48.85 | 5.09 | 8.70 |

Please see pages 459-468 in Supplementary Information for detailed analysis.

**Hydrogen testing:**

Other than the $H_2$ gas peak at 4.47 ppm in the NMR spectra, no other changes were observed.

**Tetracarbonyl (1-methyl-3-propylimidazol-2-ylidene) Iron [FeMePr]**

*(Novel Compound)*

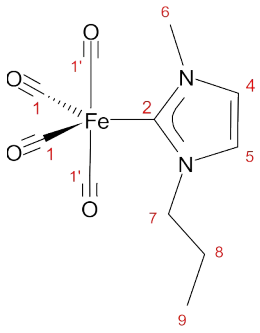


In a Schlenk tube, the mixture of potassium tetracarbonyl iron hydride (40 mg, 0.19 mmol) and 1-methyl-3-propylimidazolium iodide (96 mg, 0.38 mmol) was heated to 120°C, at which point the reaction mixture turned into a deep red viscous liquid, which was further heated under dynamic vacuum for 4 hours, resulting in the formation of brown viscous liquid. Upon cooling, toluene (3 mL) was added to the reaction mixture, and the yellow solution was filtered off, leaving brown residue behind. The solvent was then removed from the yellow solution under vacuum to yield the product as a yellow/ brown oil.

Yield: 24.2 mg, 0.083 mmol (43.1%) a yellow oil.

**$^{1}$H NMR:** (400MHz, $C_6D_6$, 25°C) δ 5.92 {d, $3J_{5\text{-}4}$ = *1.8Hz*, *1H*, **H5**(CH)}, 5.83 {d, $3J_{4\text{-}5}$ = *2.1Hz*, *1H*, **H4**(CH)}, 3.67 {t, $3J_{7\text{-}8}$ = *7.4Hz*, *2H*, **H7**($CH_2$)}, 3.09 {s, *3H*, **H6**($CH_3$)}, 1.40 {app. sext, $3J_{8\text{-}7} \approx 3J_{8\text{-}9}$ = *7.3Hz*, *2H*, **H8**($CH_2$)}, 0.62 {t, $3J_{9\text{-}8}$ = *7.4Hz*, *3H*, **H9**($CH_3$)}.

**$^{13}$C NMR:** (100MHz, $C_6D_6$, 25°C) δ 217.40 {**C1/C1'**(CO)}, 180.51 {**C2**(Carbene)}, 123.52 {**C4**(CH)}, 121.87 {**C5**(CH)}, 52.94 {**C7**($CH_2$)}, 39.11 {**C6**($CH_3$)}, 23.89 {**C8**($CH_2$)}, 10.70 {**C9**($CH_3$)}.

**m/z (ESI):** 125 $([C_7H_{12}N_2]+H)^+$, 169 $([Fe(CO)_4]+H)^-$, 181 $(Fe+[C_7H_{12}N_2])^+$

| **Elemental Analysis:** | | Carbon % | Hydrogen % | Nitrogen % |
|---|---|---|---|---|
| | Calculated | 45.24 | 4.14 | 9.59 |
| | Observed | 45.56 | 4.09 | 9.36 |

Please see pages 338-347 in Supplementary Information for detailed analysis.

**Hydrogen testing:**

Other than the $H_2$ gas peak at 4.47 ppm in the NMR spectra, no other changes were observed. These methods were repeated using the same molar amounts, usage of appropriate R, R'- imidazolium iodide salt for synthesis of the following complexes and Hydrogen testing of those complexes:

**Tetracarbonyl (1-butyl-3-methylimidazol-2-ylidene) Iron [FeMeBu]**

*(Novel Compound)*

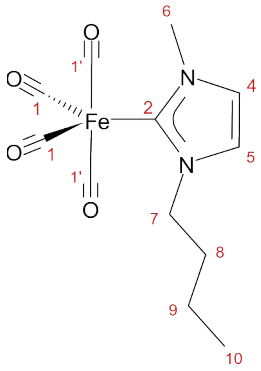


Yield: 22.3 mg, 0.104 mmol (37.9%) as a yellow/ brown oil.

**$^{1}$H NMR:** (400MHz, $C_6D_6$, 25°C) δ 5.95 {d, $^{3}J_{5\text{-}4}$ = *2.1Hz*,*1H*, **H5**(CH)}, 5.84 {d, $^{3}J_{4\text{-}5}$ = *1.8Hz*,*1H*, **H4**(CH)}, 3.75 {t, $^{3}J_{7\text{-}8}$ = *7.4Hz, 2H*, **H7**($CH_2$)}, 3.09 {s, *3H*, **H6**($CH_3$)}, 1.39 {quin, $^{3}J_{8\text{-}7} \approx {}^{3}J_{8\text{-}9}$ = *7.7Hz*, *2H*, **H8**($CH_2$)}, 1.04 {app. sext, $^{3}J_{9\text{-}8} \approx {}^{3}J_{9\text{-}10}$ = *7.4Hz, 2H*, **H9**($CH_2$)}, 0.74 {t, $^{3}J_{10\text{-}9}$ = *7.3Hz, 3H*, **H10**($CH_3$)}.

**$^{13}$C NMR:** (100MHz, $C_6D_6$, 25°C) δ 217.44 {**C1/C1'**(CO)}, 180.59 {**C2**(Carbene)}, 123.54 {**C4**(CH)}, 121.85 {**C5**(CH)}, 51.38 {**C7**($CH_2$)}, 39.14 {**C6**($CH_3$)}, 32.64 {**C8**($CH_2$)}, 19.84 {**C9**($CH_2$)}, 13.76 {**C10**($CH_3$)}.

**m/z (ESI):** 139 ($[C_8H_{14}N_2]+H)^+$, 169 ($[Fe(CO)_4]+H)^-$, 195 ($Fe+[C_8H_{14}N_2])^-$, 277 ([Complex]-CO)$^-$, 291 ([Complex]-$CH_3$)$^-$, 305 ([Complex]-H)$^-$.

| **Elemental Analysis:** | Carbon % | Hydrogen % | Nitrogen % |
|---|---|---|---|
| Calculated | 47.09 | 4.61 | 9.15 |
| Observed | 47.14 | 4.57 | 9.19 |

Please see pages 348-357 in Supplementary Information for detailed analysis.

**Hydrogen testing:**

Other than the $H_2$ gas peak at 4.47 ppm in the NMR spectra, no other changes were observed.

**Tetracarbonyl (1,3-Diethylimidazol-2-ylidene) Iron [FeEt2]**

*(Novel Compound)*

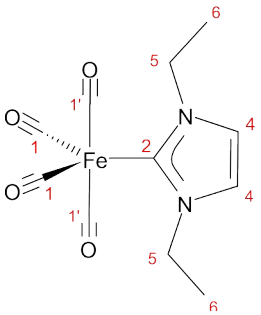


Yield: 24.7 mg, 0.085 mmol (44.0%) as a yellow oil.

**$^{1}$H NMR:** (400MHz, $C_6D_6$, 25°C) δ 6.06 {s, *2H*, **H4**(CH)}, 3.77 {q, $3J_{5\text{-}6}$ = *7.4Hz*, *4H*, **H5**($CH_2$)}, 0.91 {t, $3J_{6\text{-}5}$ = *7.3Hz*, *6H*, **H6**($CH_3$)}.

**$^{13}$C NMR:** (100MHz, $C_6D_6$, 25°C) δ 217.99 {**C1/C1'**(CO)}, 178.89 {**C2**(Carbene)}, 121.92 {**C4**(CH)}, 46.29 {**C5**($CH_2$)}, 15.57 {**C6**($CH_3$)}.

**m/z (ESI):** 125 ($[C_7H_{12}N_2]+H)^+$, 293 ($[Complex]+H)^+$, 180 ($Fe+[C_7H_{12}N_2])^-$, 291 ($[Complex]-H)^-$.

| **Elemental Analysis:** | | Carbon % | Hydrogen % | Nitrogen % |
|---|---|---|---|---|
| | Calculated | 45.24 | 4.14 | 9.59 |
| | Observed | - | - | - |

Please see pages 368-377 in Supplementary Information for detailed analysis.

**Hydrogen testing:**

Other than the $H_2$ gas peak at 4.47 ppm in the NMR spectra, no other changes were observed.

**Tetracarbonyl (1-Ethyl-3-propylimidazol-2-ylidene) Iron [FeEtPr]**

*(Novel Compound)*

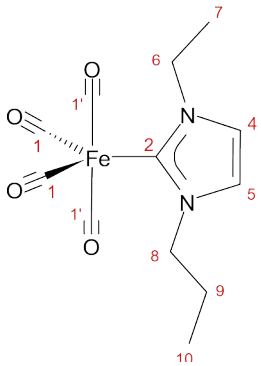


Yield: 20.9 mg, 0.068 mmol (35.6%) as a yellow/ brown oil.

**$^{1}$H NMR:** (400MHz, $C_6D_6$, 25°C) δ 6.00 {s, *2H*, **H4/5**(CH)}, 3.77 {q, $^{3}J_{6\text{-}7}$ = *7.3Hz*, *2H*, **H6**($CH_2$)}, 3.70 {t, $^{3}J_{8\text{-}9}$ = *7.3Hz*, *2H*, **H8**($CH_2$)}, 1.41 {app. sext, $^{3}J_{9\text{-}8} \approx {}^{3}J_{9\text{-}10}$ = *7.6Hz, 2H*, **H9**($CH_2$)}, 0.88 {t, $^{3}J_{7\text{-}6}$ = *7.4Hz*, *3H*, **H7**($CH_3$)}, 0.63 {t, $^{3}J_{10\text{-}9}$ = *7.4Hz*, *3H*, **H10**($CH_3$)}.

**$^{13}$C NMR:** (100MHz, $C_6D_6$, 25°C) δ 218.10 {**C1/C1'**(CO)}, 179.65 {**C2**(Carbene)}, 122.52 {**C4**(CH)}, 121.40 {**C5**(CH)}, 52.88 {**C8**($CH_2$)}, 46.31 {**C6**($CH_2$)}, 23.94 {**C9**($CH_2$)}, 15.51 {**C7**($CH_3$)}, 10.74 {**C10**($CH_3$)}.

**m/z (ESI):** 139 ($[C_8H_{14}N_2]+H)^+$, 169 ($[Fe(CO)_4]+H)^-$, 277 ($[Complex]-CO)^-$ or ($[Complex]-CH_2CH_3)^-$.

**Elemental Analysis:**

| | Carbon % | Hydrogen % | Nitrogen % |
|---|---|---|---|
| Calculated | 47.09 | 4.61 | 9.15 |
| Observed | - | - | - |

Please see pages 378-387 in Supplementary Information for detailed analysis.

**Hydrogen testing:**

Other than the $H_2$ gas peak at 4.47 ppm in the NMR spectra, no other changes were observed.

**Tetracarbonyl (1-Butyl-3-ethylimidazol-2-ylidene) Iron [FeEtBu]**

*(Novel Compound)*

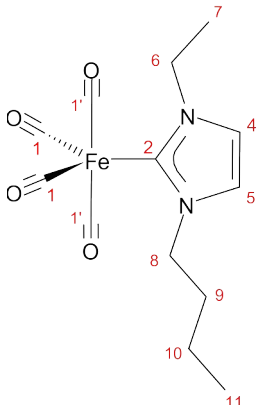


Yield: 17.8 mg, 0.056 mmol (29.0%) as a yellow/ brown oil.

| | |
|---|---|
| **$^{1}$H NMR:** *(400Mhz, $C_6D_6$)* | (400MHz, $C_6D_6$, 25°C) δ 6.06 {d, $^{3}J_{4\text{-}5}$ = *2.1Hz*, *1H*, **H4/5**(CH)}, 6.03 {d, $^{3}J_{4\text{-}5}$ = *2.1Hz*, *1H*, **H4/5**(CH)}, 3.77 {multi, *4H*, **H6/8**($CH_2$)}, 1.40 {quin, $^{3}J_{9\text{-}8}$ ≈ $^{3}J_{9\text{-}10}$ = *7.7Hz*, *2H*, **H9**($CH_2$)}, 1.06 {sext, $^{3}J_{10\text{-}9}$ ≈ $^{3}J_{10\text{-}11}$ = *7.4Hz*, *2H*, **H10**($CH_2$)}, 0.89 {t, $^{3}J_{7\text{-}6}$ = *7.3Hz*, *3H*, **H7**($CH_3$)}, 0.75 (t, $^{3}J_{11\text{-}10}$ = *7.3Hz*, *3H*, **H11**($CH_3$)}. |
| **$^{13}$C NMR:** *(100Mhz, $C_6D_6$)* | (100MHz, $C_6D_6$, 25°C) δ 218.16 {**C1/C1'**(CO)}, 179.60 {**C2**(Carbene)}, 122.50 {**C4/5**(CH)}, 121.47 {**C4/5**(CH)}, 51.31 {**C8**($CH_2$)}, 46.33 {**C6**($CH_2$)}, 32.69 {**C9**($CH_2$)}, 19.85 {**C10**($CH_2$)}, 15.54 {**C7**($CH_3$)}, 13.76 {**C11**($CH_3$)}. |
| **m/z (ESI):** | 139 ($[C_9H_{16}N_2]+H)^+$, 168 ($[Fe(CO)_4]?)^-$. |

| **Elemental Analysis:** | Carbon % | Hydrogen % | Nitrogen % |
|---|---|---|---|
| Calculated | 48.77 | 5.04 | 8.75 |
| Observed | - | - | - |

Please see pages 388-397 in Supplementary Information for detailed analysis.

**Hydrogen testing:**

Other than the $H_2$ gas peak at 4.47 ppm in the NMR spectra, no other changes were observed.

**Tetracarbonyl (1-*Iso*propyl-3-methylimidazol-2-ylidene) Iron [FeiPrEt]**

*(Novel Compound)*

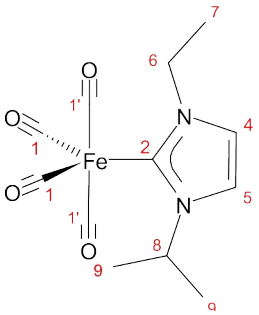


Yield: 20.7 mg, 0.068 mmol (35.1%) as a yellow/ brown oil.

**$^{1}$H NMR:** (400MHz, $C_6D_6$, 25°C) δ 6.17 {d, $^{3}J_{5\text{-}4}$ = *2.1Hz*, *1H*, **H5**(CH)}, 6.00 {d, $^{3}J_{4\text{-}5}$ = *2.1Hz*, *1H*, **H4**(CH)}, 5.26 {sept, $^{3}J_{8\text{-}9}$ = *6.7Hz*, *1H*, **H8**(CH)}, 3.70 {q, $^{3}J_{6\text{-}7}$ = *7.3Hz*, *2H*, **H6**($CH_2$)}, 0.91 {m, *9H*, **H7/H9**($CH_3$)}.

**$^{13}$C NMR:** (100MHz, $C_6D_6$, 25°C) δ 218.04 {**C1/C1'**(CO)}, 178.56 {**C2**(Carbene)}, 122.60 {**C4**(CH)}, 118.40 {**C5**(CH)}, 52.65 {**C8**(CH)}, 46.24 {**C6**($CH_2$)}, 22.69 {**C7**($CH_3$)}, 15.75 {**C9**($CH_3$)}.

**m/z (ESI):** 139 $([C_8H_{14}N_2]+H)^+$, 169 $([Fe(CO)_4]+H)^-$, 277 $([Complex]-CH_2CH_3)^-$.

| **Elemental Analysis:** | | Carbon % | Hydrogen % | Nitrogen % |
|---|---|---|---|---|
| | Calculated | 47.09 | 4.61 | 9.15 |
| | Observed | - | - | - |

Please see pages 398-407 in Supplementary Information for detailed analysis.

**Hydrogen testing:**

Other than the $H_2$ gas peak at 4.47 ppm in the NMR spectra, no other changes were observed.

**Tetracarbonyl (1,3-Dipropylimidazol-2-ylidene) Iron [FePr2]**

*(Novel Compound)*

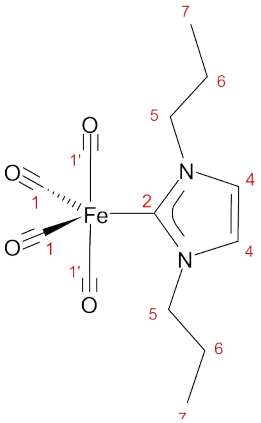


Yield: 19.2 mg, 0.060 mmol (31.2%) as a yellow/ brown oil.

**$^{1}$H NMR:** (400MHz, $C_6D_6$, 25°C) δ 6.06 {s, *2H*, **H4**(CH)}, 3.74 {t, $^{3}J_{5\text{-}6}$ = *7.4Hz*, *4H*, **H5**($CH_2$)}, 1.41 {app, sext, $^{3}J_{6\text{-}5} \approx {}^{3}J_{6\text{-}7}$ = *7.3Hz*, *4H*, **H6**($CH_2$)}, 0.63 (t, $^{3}J_{7\text{-}6}$ = *7.4Hz*, *6H*, **H7**($CH_3$)}.

**$^{13}$C NMR:** (100MHz, $C_6D_6$, 25°C) δ 218.31 {**C1/C1'**(CO)}, 179.92 {**C2**(Carbene)}, 122.18 {**C4**(CH)}, 52.92 {**C5**($CH_2$)}, 23.87 {**C6**($CH_2$)}, 10.77 {**C7**($CH_3$)}

**m/z (ESI):** 153 ($[C_9H_{16}N_2]+H)^+$, 319 ([Complex]-H)$^-$.

| **Elemental Analysis:** | Carbon % | Hydrogen % | Nitrogen % |
|---|---|---|---|
| Calculated | 48.77 | 5.04 | 8.75 |
| Observed | - | - | - |

Please see pages 408-417 in Supplementary Information for detailed analysis.

**Hydrogen testing:**

Other than the $H_2$ gas peak at 4.47 ppm in the NMR spectra, no other changes were observed.

**Tetracarbonyl (1-Butyl-3-propylimidazol-2-ylidene) Iron [FePrBu]**

*(Novel Compound)*

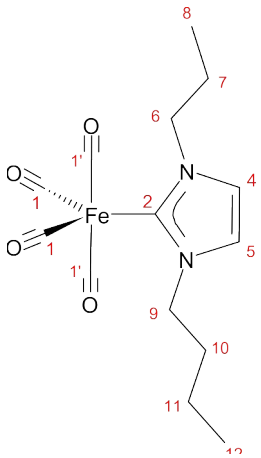


Yield: 11.3 mg, 0.042 mmol (17.6%) as a yellow/ brown oil.

**$^{1}$H NMR:** (400MHz, $C_6D_6$, 25°C) δ 6.08 {d, $^{3}J_{4\text{-}5}$ = *1.8Hz*, *1H*, **H4/5**(CH)}, 6.05 {d, $^{3}J_{4\text{-}5}$ = *1.8Hz*, *1H*, **H4/5**(CH)}, 3.82 {t, $^{3}J_{9\text{-}10}$ = *7.3Hz*, *2H*, **H9** ($CH_2$)}, 3.74 {t, $^{3}J_{6\text{-}7}$ = *7.4Hz*, *2H*, **H6**($CH_2$)}, 1.40 {multi, *4H*, **H7/10**($CH_2$)}, 1.06 {app. sext, $^{3}J_{11\text{-}10} \approx {}^{3}J_{11\text{-}12}$ = *7.4Hz*, *2H*, **H11**($CH_2$)}, 0.75 {t, $^{3}J_{12\text{-}11}$ = *7.4Hz*, *3H*, **H12**($CH_3$)}, 0.64 {t, $^{3}J_{8\text{-}7}$ = *7.4Hz*, *3H*, **H8**($CH_3$)}.

**$^{13}$C NMR:** (100MHz, $C_6D_6$, 25°C) δ 218.35 {**C1/C1'**(CO)}, 180.01 {**C2**(Carbene)}, 122.19 {**C4/5**(CH)}, 122.12 {**C4/5**(CH)}, 52.93 {**C6**($CH_2$)}, 51.34 {**C9**($CH_2$)}, 32.64 {**C10**($CH_2$)}, 23.91 {**C7**($CH_2$)}, 19.87 {**C11**($CH_2$)}, 13.77 {**C12**($CH_3$)}, 10.77 {**C8**($CH_3$)}.

**m/z (ESI):** 167 ($[C_{10}H_{18}N_2]+H)^+$, 169 ($[Fe(CO)_4]+H)^-$,

**Elemental Analysis:**

| | Carbon % | Hydrogen % | Nitrogen % |
|---|---|---|---|
| Calculated | 50.32 | 5.43 | 8.38 |
| Observed | - | - | - |

Please see pages 418-428 in Supplementary Information for detailed analysis.

**Hydrogen testing:**

Other than the $H_2$ gas peak at 4.47 ppm in the NMR spectra, no other changes were observed.

**Tetracarbonyl (1-*iso*propyl-3-propylimidazol-2-ylidene) Iron [FeiPrPr]**

*(Novel Compound)*

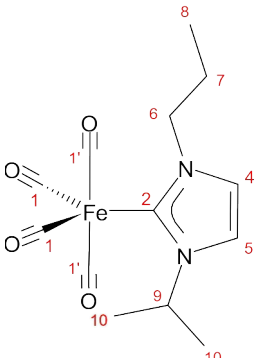


Yield: 17.3 mg, 0.054 mmol (28.1%) as a yellow/ brown oil.

**$^{1}$H NMR:** (400MHz, $C_6D_6$, 25°C) δ 6.19 {d, $3J_{5\text{-}4}$ = *2.1Hz*, *1H*, **H5**(CH)}, 6.04 {d, $3J_{4\text{-}5}$ = *2.1Hz*, *1H*, **H4**(CH)}, 5.30 {sept, $3J_{9\text{-}10}$ = *6.8Hz*, *1H*, **H9**(CH)}, 3.66 {t, $3J_{6\text{-}7}$ = *7.3Hz*, *2H*, **H6**($CH_2$)}, 1.44 {app. sext, $3J_{7\text{-}6} \approx 3J_{7\text{-}8}$= *7.3Hz*, *2H*, **H7**($CH_2$)}, 0.94 {d, $3J_{10\text{-}9}$ = *6.7Hz*, *6H*, **H10**($CH_3$)}, 0.64 {t, $3J_{8\text{-}7}$ = *7.4 Hz*, *3H*, **H8**($CH_3$)}.

**$^{13}$C NMR:** (100MHz, $C_6D_6$, 25°C) δ 218.12 {**C1/C1'**(CO)}, 178.82 {**C2**(Carbene)}, 123.39 {**C4**(CH)}, 118.18 {**C5**(CH)}, 52.81 {**C6**($CH_2$)}, 52.73 {**C9**(CH)}, 24.11 {**C7**($CH_2$)}, 22.67 {**C10**($CH_3$)}, 10.69 {**C8**($CH_3$)}.

**m/z (ESI):** 153 $([C_9H_{16}N_2]+H)^+$, 277 $([Complex]\text{-}CH_2CH_2CH_3)^-$, 319 $([Complex]\text{-}H)^-$.

| **Elemental Analysis:** | | Carbon % | Hydrogen % | Nitrogen % |
|---|---|---|---|---|
| | Calculated | 48.77 | 5.04 | 8.75 |
| | Observed | - | - | - |

Please see pages 429-438 in Supplementary Information for detailed analysis.

**Hydrogen testing:**

Other than the $H_2$ gas peak at 4.47 ppm in the NMR spectra, no other changes were observed.

**Tetracarbonyl (1,3-Dibutylimidazol-2-ylidene) Iron [FeBu2]**

*(Novel Compound)*

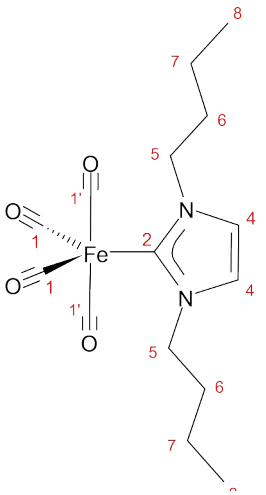


Yield: 17.1 mg, 0.049 mmol (25.5%) as a yellow/ brown oil.

**$^{1}$H NMR:** (400MHz, $C_6D_6$, 25°C) δ 6.10 {s, *2H*, **H4**(CH)}, 3.82 {t, $^{3}J_{5\text{-}6}$ = *7.4Hz*, *4H*, **H5**($CH_2$)}, 1.41 {quin, $^{3}J_{6\text{-}5} \approx {}^{3}J_{6\text{-}7}$ = *7.7Hz*, *4H*, **H6**($CH_2$)}, 1.07 {app. sext, $^{3}J_{7\text{-}6} \approx {}^{3}J_{7\text{-}8}$ = *7.4Hz, 4H*, **H7**($CH_2$)}, 0.76 {t, $^{3}J_{8\text{-}7}$ = *7.3Hz*, *6H*, **H8**($CH_3$)}.

**$^{13}$C NMR:** (100MHz, $C_6D_6$, 25°C) δ 218.42 {**C1/C1'**(CO)}, 179.93 {**C2**(Carbene)}, 122.19 {**C4**(CH)}, 51.36 {**C5**($CH_2$), 32.67 {**C6**($CH_2$)}, 19.87 {**C7**($CH_2$)}, 13.78 {**C8**($CH_3$)}.

**m/z (ESI):** 181 ($[C_{11}H_{20}N_2]+H)^+$, 169 ($[Fe(CO)_4]+H)^-$,

| **Elemental Analysis:** | Carbon % | Hydrogen % | Nitrogen % |
|---|---|---|---|
| Calculated | 51.74 | 5.79 | 8.05 |
| Observed | - | - | - |

Please see pages 439-448 in Supplementary Information for detailed analysis.

**Hydrogen testing:**

Other than the $H_2$ gas peak at 4.47 ppm in the NMR spectra, no other changes were observed.

**Tetracarbonyl (1-Butyl-3-Isopropylimidazol-2-ylidene) Iron [FeiPrBu]**

*(Novel Compound)*

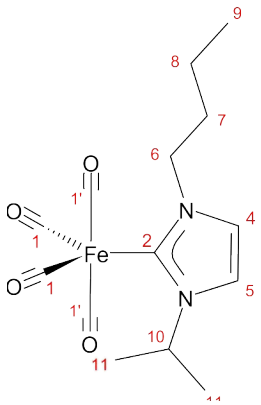


Yield: 13.4mg, 0.04 mmol (20.8%) as a yellow/ brown oil.

**$^{1}$H NMR:** (400MHz, $C_6D_6$, 25°C) δ 6.21 {d, $3J_{5\text{-}4}$ = *2.1Hz*, *1H*, **H5**(CH)}, 6.08 {d, $3J_{4\text{-}5}$ = *2.1Hz*, *1H*, **H4**(CH)}, 5.30 {sept, $3J_{10\text{-}11}$ = *6.8Hz*, *1H*, **H10**(CH)}, 3.74 {t, $^{3}J_{6\text{-}7}$ = *7.3Hz*, *2H*, **H8**($CH_2$)}, 1.43 {quin, $3J_{7\text{-}6} \approx 3J_{7\text{-}8}$ = *7.9Hz*, *2H*, **H7**($CH_2$)}, 1.07 {app. sext, $3J_{8\text{-}7} \approx 3J_{8\text{-}9}$ = *7.4Hz*, *2H*, **H8**($CH_2$)}, 0.94 {d, $3J_{11\text{-}10}$ = *7.0Hz*, *6H*, **H11**($CH_3$)}, 0.74 {t, $3J_{9\text{-}8}$ = *7.4Hz*, *3H*, **H9**($CH_3$)}.

**$^{13}$C NMR:** (100MHz, $C_6D_6$, 25°C) δ 218.18 {**C1/C1'**(CO)}, 178.90 {**C2**(Carbene)}, 123.32 {**C4**(CH)}, 118.19 {**C5**(CH)}, 52.73 {**C10**(CH)}, 51.26 {**C6**($CH_2$)}, 32.84 {**C7**($CH_2$)}, 22.69 {**C11**($CH_3$)}, 19.82 {**C8**($CH_2$)}, 13.77 {**C9**($CH_3$)}.

**m/z (ESI):** 167 ($[C_{10}H_{18}N_2]$+H)$^{+}$, 170 ($[Fe(CO)_4]$+H?)$^{-}$, 277 ([Complex]-$CH_2CH_2CH_2CH_3$)$^{-}$ or ([Complex]-2{CO})$^{-}$.

| **Elemental Analysis:** | | Carbon % | Hydrogen % | Nitrogen % |
|---|---|---|---|---|
| | Calculated | 50.32 | 5.43 | 8.38 |
| | Observed | - | - | - |

Please see pages 449-458 in Supplementary Information for detailed analysis.

**Hydrogen testing:**

Other than the $H_2$ gas peak at 4.47 ppm in the NMR spectra, no other changes were observed.

### 5.1.1 1-Alkylimidazole Synthesis

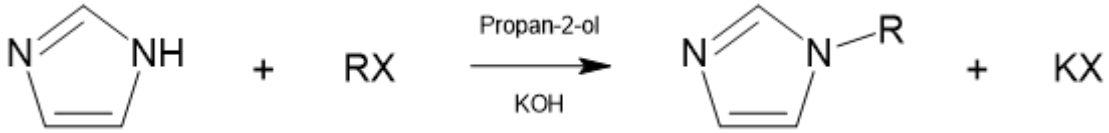


***Scheme 15: General synthesis of alkylimidazoles (R = methyl ethyl, propyl, butyl, isopropyl).***

As shown above in Scheme 15, all the desired 1-alkylimidazoles except 1-*tert*-butylimidazole (as it could not be synthesised by this method, see below in Section 4.1.2) were successfully produced. Imidazole and potassium hydroxide were reacted with the corresponding iodoalkane (in a 1 : 1.1 : 1 molar ratio respectively) in propan-2-ol under reflux for 12 hours. Following the removal of solvent and extraction of the crude product with DCM, the latter was washed with water and the organic phase dried with anhydrous sodium sulphate. The solvent was then removed to give desired products as pale-yellow liquids in good to excellent yields (82.7% – 92.4%).

1-Alkylimidazoles synthesised were hygroscopic. Additionally, upon being left to stand in the open laboratory, the liquids slowly deepened in colour to yellow and then to yellow / pale orange. This possibly suggests that the 1-alkyimidazoles formed may be mildly sensitive to either prolonged oxygen, moisture or UV exposure. Short-path vacuum distillation was able to remove this yellow / orange colouration. However, the NMR spectra of both distilled and non- distilled samples were identical and either could be used for further reactions.

**Table 1: Summary of MS fragments and their m/z values for compounds 1-6**

| **Fragment (m/z)** | **Compound** | | | | | |
|---|---|---|---|---|---|---|
| | **MeIm (1)**  | **EtIm (2)** 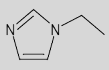 | **PrIm (3)** 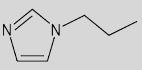 | **BuIm (4)** 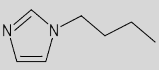 | ***i*PrIm (5)** 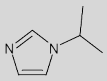 | ***t*BuIm (6)** 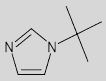 |
| **$[M+H]^+$** | 83 | 97 | 111 | 125 | 111 | 125 |
| **$[Im + H]^+$** | 69 | 69 | 69 | 69 | 69 | 69 |
| **$Alkyl^+$** | - | - | 43 | 57 | 43 | 57 |

Mass spectra of compounds **1**-**5** showed expected peak values corresponding to the respective molecular ions. Additionally, fragmentation was seen resulting in m/z = 69 ([imidazole + H]$^+$) and the corresponding alkyl fragments. Alkyl fragmentation was not observed in the spectra of compounds **1** and **2** due to the limitations of the instrumentation used showing a minimum of m/z = 30.

See Table 1 for a summary of MS data obtained for compounds **1**-**6**.

$^1$H NMR spectra of compounds **1**-**5** show three peaks in the region of 6.8-7.8 ppm with an integration of 1H each that correspond to the imidazole ring protons. The peaks assigned to **H2** (here and later refer to Table 2 for atom numbering scheme) appear between 7.56 – 7.72 ppm, peaks assigned to **H5** appear between 7.10 – 7.30 ppm and peaks assigned to **H4** appear at 6.87 – 6.88 ppm. Other than in compound **1** all the imidazole proton peaks appear as apparent triplets (apparent singlets in compound **1**). Any remaining peaks observed are assigned to alkyl groups.

See Table 2 for a summary of $^1$H and $^{13}$C NMR data obtained for compounds **1**-**6**.

**Table 2: Summary of $^{1}H$ and $^{13}C$ NMR data for compounds 1-6**

| Compound | $C_{\{2\}}$-H 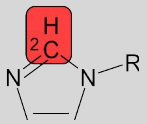 | Backbone $C_{\{4\}}H{=}C_{\{5\}}H$ 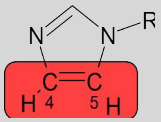 | R Group 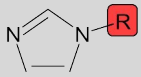 |
|---|---|---|---|
| 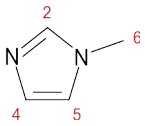 MeIm (**1**) | $^{1}H$: 7.56 {s, **H2**}<br>$^{13}C$: 137.92 {**C2**} | $^{1}H$: 7.10 {s, **H5**},<br>6.88 (s, **H4**}<br>$^{13}C$: 128.44 {s, **C4**}, 120.50 {**C5**} | $^{1}H$: 3.63 {s, **H6**}<br>$^{13}C$: 32.74 {**C6**} |
| 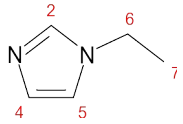 EtIm (**2**) | $^{1}H$: 7.62 {app.t, *J* = *1.2Hz*, **H2**}<br>$^{13}C$: 136.74 {**C2**} | $^{1}H$: 7.17 {app. t, *J* = *1.3Hz*, **H5**},<br>6.87 (app. t, *J* = *1.2Hz*, **H4**}<br>$^{13}C$: 128.35 {**C4**}, 118.87 {**C5**} | $^{1}H$: 3.97 {q, $^{3}J$ = *7.3Hz*, **H6**}, 1.32 {t, $^{3}J$ = *7.3Hz*, **H7**}<br>$^{13}C$: 40.89 {**C6**}, 16.39 {**C7**} |
| 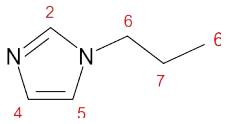 PrIm (**3**) | $^{1}H$: 7.60 {app.t, *J* = *1.2Hz*, **H2**}<br>$^{13}C$: 137.25 {**C2**} | $^{1}H$: 7.15 {app.t, *J* = *1.2Hz*, **H5**},<br>6.88 (app.t, *J* = *1.1Hz*, **H4**}<br>$^{13}C$: 128.32 {**C4**}, 119.23 {**C5**} | $^{1}H$: 3.90 {t, $^{3}J$ = *7.0Hz*, **H6**}, 1.70 {app. sext, $^{3}J$ = *7.3Hz*, **H7**}, 0.80 {t, $^{3}J$ = *7.4Hz*, **H8**}<br>$^{13}C$: 47.55 {**C6**}, 23.96 {**C7**}, 10.84 {**C8**} |
| 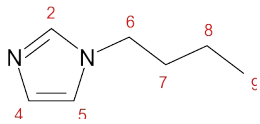 BuIm (**4**) | $^{1}H$: 7.60 {app.t, *J* = *1.2Hz*, **H2**}<br>$^{13}C$: 137.20 {**C2**} | $^{1}H$: 7.15 {app.t, *J* = *1.2Hz*, **H5**},<br>6.87 (app.t, *J* = *1.1Hz*, **H4**}<br>$^{13}C$: 128.31 {**C4**}, 119.21 {**C5**} | $^{1}H$: 3.93 {t, $^{3}J$ = *7.1Hz*, **H6**}, 1.65 {quin, $^{3}J$ = *7.2Hz*, **H7**}, 1.21 {app sext, $^{3}J$ = *14.5/ 7.3Hz*, **H8**}, 0.87 {t, $^{3}J$ = *7.3Hz*, **H9**}<br>$^{13}C$: 45.62 {**C6**}, 32.66 {**C7**}, 19.16 {**C8**}, 13.38 {**C9**} |
| 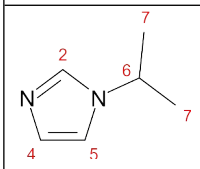 iPrIm (**5**) | $^{1}H$: 7.67 {app.t, *J* = *1.2Hz*, **H2**}<br>$^{13}C$: 135.45 {**C2**} | $^{1}H$: 7.22 {app.t, *J* = *1.3Hz*, **H5**},<br>6.87 (app.t, *J* = *1.2Hz*, **H4**}<br>$^{13}C$: 128.23 {**C4**}, 117.08{**C5**} | $^{1}H$: 4.39 {sept, $^{3}J$ = *6.7Hz*, **H6**}, 1.38 {d, $^{3}J$ = *6.7Hz*, **H7**}<br>$^{13}C$: 48.25 {**C6**}, 23.46 {**C7**} |
| 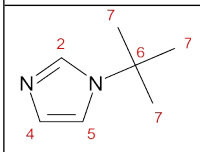 tBuIm (**6**) | $^{1}H$: 7.72 {app.t, *J* = *1.2Hz*, **H2**}<br>$^{13}C$: 134.55 {**C2**} | $^{1}H$: 7.30 {app.t, *J* = *1.2Hz*, **H5**},<br>6.87 (app.t, *J* = *1.2Hz*, **H4**}<br>$^{13}C$: 128.15 {**C4**}, 117.00 {**C5**} | $^{1}H$: 1.49 {s, **H7**}<br>$^{13}C$: 54.44 {**C6**}, 30.17 {**C7**} |

### 5.1.2 1-*tert*-Butylimidazole Synthesis

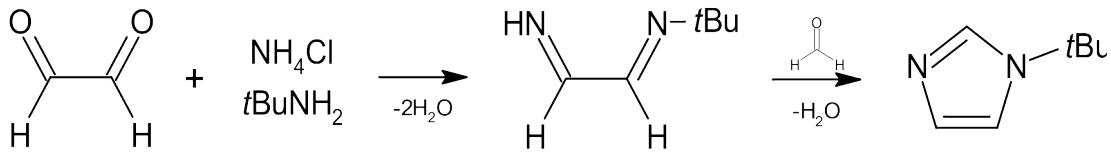


***Scheme 16: Ring-closure synthesis of 1-tert-butyl-imidazole.***

Scheme 16 shows preparation of 1-*tert*-butylimidazole. A mixture of *tert*-butylamine and ammonium chloride was gradually added to 40% aq. glyoxal followed by slow addition of 37% aq. formaldehyde in a 1:1:1:1 molar ratio. The reaction mixture was then heated to reflux for 1 hour. The reaction mixture was then cooled down to room temperature, sodium carbonate was added until the mixture was basic (pH10) and the crude product was extracted with DCM. The solvent was then removed, and the crude oil was purified by short-path vacuum distillation to give the product as a pale-yellow liquid in moderate yield (37.5%).

Similar to other 1-alkylimidazoles, upon being left to stand in the open laboratory the liquid gradually changed colour to yellow / pale orange and distillation of the sample removed this colouration. Additionally, NMR spectra confirmed that both distilled and non-distilled samples of compound **6** were identical and hence could be used for further reactions.

Mass spectrum of compound **6** revealed the expected peak corresponding with the molecular ion ($[M+H]^+$), m/z = 125. Fragmentation was also observed, peaks at m/z = 69 and 57 correspond to imidazole (Im+H) and the *tert*-butyl fragment respectively.

See Table 1 (page 84) for a summary of MS data obtained for compound **6**.

The $^1$H NMR spectrum of compound **6** shows 3 apparent triplets, all with an integration of 1H between 7.72-6.87 ppm, which correspond with the imidazole ring protons. Similar to the spectra of other 1-akylimidazoles produced, the peak at 7.72 ppm was assigned to **H2** (N-$C_{(2)}$**H**-N), the peak at 7.30 ppm was assigned to **H5** and the peak at 6.87 ppm was assigned to **H4**.

The $^{13}$C NMR spectrum of compound **6** matches the trend seen in compounds **1**-**5**, where three peaks at 134.55, 128.15 and 117.00 correspond to **C2**, **C4** and **C5** respectively. The remaining peaks at 54.44 ppm and 30.17 ppm correspond to the quaternary carbon and the methyl carbon atoms of the *tert*-butyl group respectively.

See Table 2 (page 86) for a summary of $^1$H and $^{13}$C NMR data obtained for compound **6**.

### 5.1.3 Overview of 1-Alkylimidazoles Syntheses

Compounds **1-6** all previously described and characterised in literature.[37,38,83,84,85]

The synthesis of compounds **1-5** was performed without significant complications, confirming the general applicability and efficacy of the developed method.

Synthesis of 1-*tert*-butylimidazole was originally attempted using the same methodology used to produce compounds **1-5**, however very limited success was achieved. After addition of 2- iodo-2-methylpropane and heating to reflux, white vapours were released from the reaction mixture. Following the work-up only trace amounts of a yellow oil were isolated.

Analysis of the trace oil by $^{1}$H NMR and LC-MS seemingly confirmed the presence of 1-*tert*-butylimidazole, however possible imidazole impurity peaks were also seen.

Multiple repeat reactions were attempted with various modifications of conditions to improve yields. The modifications made to the original methodology included dropwise addition of 2-iodo-2-methylpropane to the reaction mixture, dropwise addition of imidazole / base mixture to a solution of 2-iodo-2-methylpropane, usage of different solvents, i.e. methanol / ethanol and water, conduction of the reaction at reflux / room temperature and at 0°C.

Unfortunately, no modifications made gave any quantifiable improvement to the yield of compound **6**. This suggests the occurrence of an alternative, more favourable reaction pathway(s). The side reaction is likely to follow the elimination mechanism leading to the alkene formation as shown in Scheme 17 below. If so, this would reform the imidazole and eliminate iodide therefore producing isobutylene gas as the white vapours which were observed in the reaction.

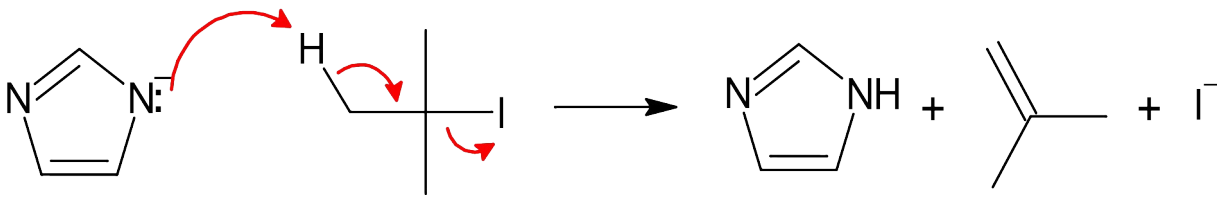


***Scheme 17: Possible mechanism for elimination side-reaction.***

This may be due to significant steric hindrance around the quaternary carbon atom, therefore impeding nucleophilic attack at the quaternary carbon atom.

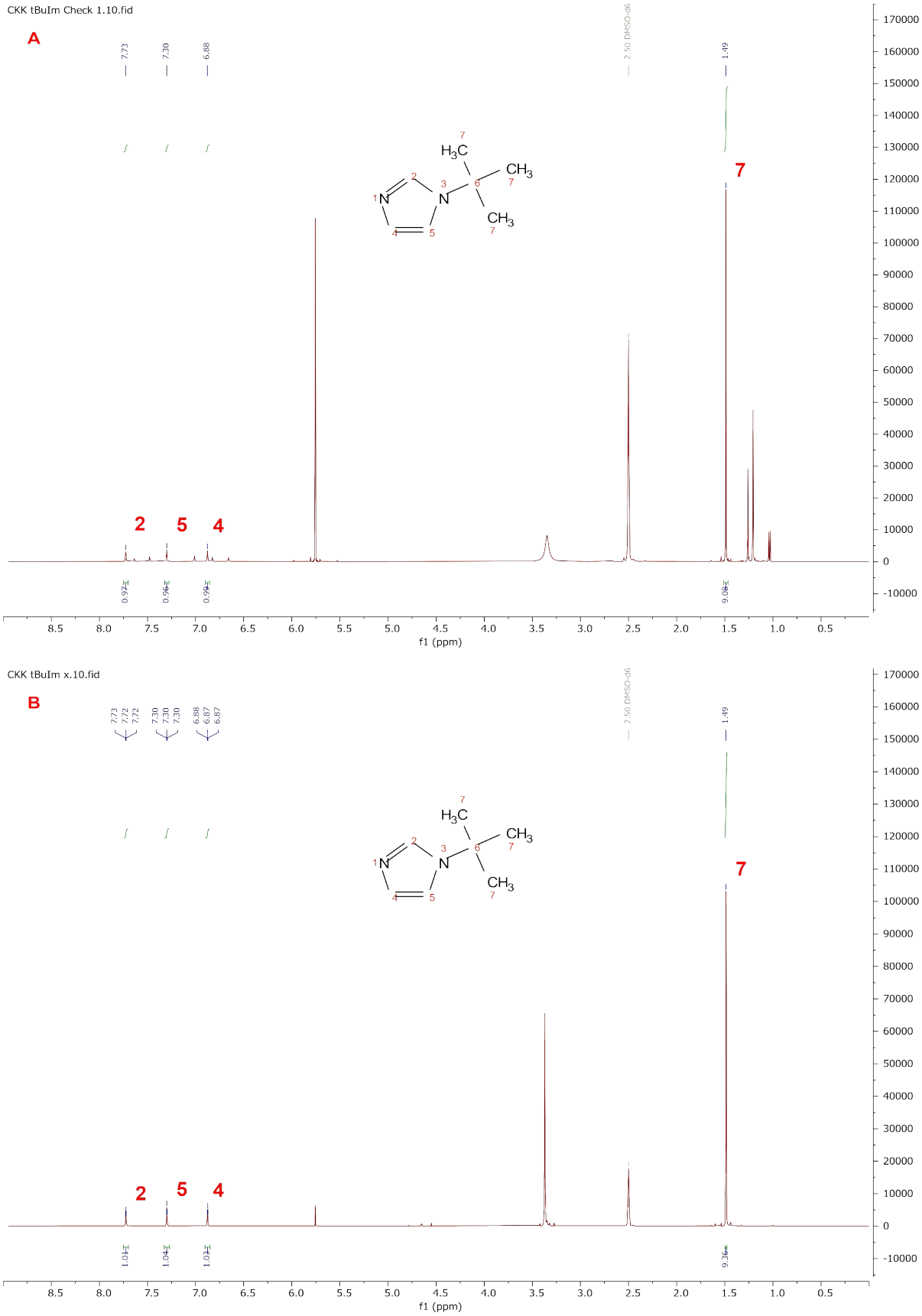


***Figure 5: Comparison of $^{1}$H NMR spectra of initial 1-tert-butylimidazole synthesis (A) and the final synthesis (B).***

A modified ring closure synthesis shown in Scheme 16 was utilized to prepare compound **6** in usable quantities. A moderate 37.5% yield was obtained using this methodology, most likely due to possible impurities formed. TLC was attempted using various combinations of eluents however no combination showed any meaningful separation. Therefore, short-path vacuum distillation was used for purification of compound **6**.

Comparison of the $^{1}$H NMR spectra for the initial trace oil produced and the product formed in the final synthesis of compound **6** is shown in Figure 5 above.

In $^{1}$H NMR spectra of compounds **1**-**6**, **H2** was the most deshielded followed by **H5** and then **H4**. These assignments were confirmed with $^{1}$H-$^{1}$H NOESY, with correlations seen between **H5** and the N-alkyl substituents.

Furthermore, the signals for **H2** and **H5** became increasingly deshielded as the size of the N-alkyl substituents increased. Stronger deshielding was observed from methyl to ethyl but plateaued for propyl and butyl groups. A significant deshielding effect (for peaks assigned to **H2** and **H5**) was observed for the isopropyl and *tert*-butyl groups, Likely because the three-dimensional structure amplifies potential electronic effects. This trend for **H2** and **H5** is shown in Figure 6. These observed trends were contrary to what was expected.

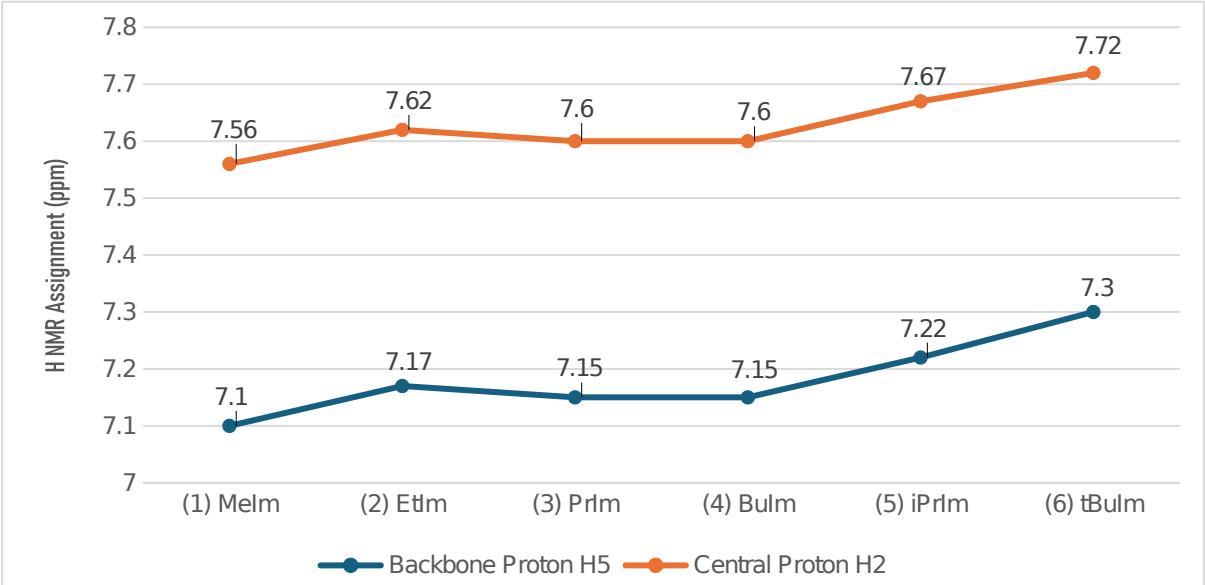


***Figure 6: Graph showing trend in $^{1}$H NMR assignments for backbone H5 and central protons H2 for compounds 1-6.***

The increase in deshielding of **H2** and **H5** suggests the alkyl groups are not donating but withdrawing electron density from the imidazole ring. This aligns with the computational work of Elliot et al., which demonstrated that alkyl groups are electron-withdrawing relative to

hydrogen.[77] The greater deshielding in compounds 5 and 6 is likely due to the size and three-dimensional structure of the isopropyl and tert-butyl groups, which further amplifies this electron-withdrawing effect.

In $^{13}C$ NMR spectra of compounds **1-6** the carbon atoms were assigned with **C2** being the most deshielded, followed by **C4** and **C5**. These assignments were supported by $^{1}H$-$^{1}H$ NOESY, $^{1}H$-$^{13}C$ HSQC and $^{1}H$-$^{13}C$ HMBC correlations. Although protons **H5** and **H4** were assigned in order of increasing deshielding, the opposite trend was observed for their corresponding carbons, with **C4** being more deshielded than **C5**.

Elemental analysis was obtained for the six liquids obtained. All elemental analysis results were within 0.5% of the calculated values shown in Table 3.

**Table 3: Elemental Analysis results for compounds 1-6**

| **Elemental analysis:** | | Carbon % | Hydrogen % | Nitrogen % |
|---|---|---|---|---|
| MeIm (1) | Calculated | 58.51 | 7.37 | 34.12 |
| | Observed | 58.55 | 7.53 | 34.06 |
| EtIm (2) | Calculated | 62.47 | 8.39 | 29.14 |
| | Observed | 62.37 | 8.58 | 29.06 |
| PrIm (3) | Calculated | 65.42 | 9.15 | 25.14 |
| | Observed | 65.32 | 9.51 | 24.93 |
| BuIm (4) | Calculated | 67.70 | 9.74 | 22.56 |
| | Observed | 67.45 | 10.01 | 22.34 |
| iPrIm (5) | Calculated | 65.42 | 9.15 | 25.14 |
| | Observed | 65.21 | 9.45 | 24.97 |
| tBuIm (6) | Calculated | 67.70 | 9.74 | 22.56 |
| | Observed | 68.03 | 9.85 | 22.12 |

### 5.1.4 1-Alkylimidazole Synthesis Conclusion

In summary, a series of 1-alkylimidazoles (alkyl = methyl, ethyl, propyl, butyl, isopropyl) were successfully produced in good to excellent yields (82.7–92.4%) via alkylation of imidazole. 1-*tert*-Butylimidazole (compound **6**) was synthesized via an alternative Debus-Radziszewski multi-component reaction, yielding a moderate 37.5% yield, due to a dominant elimination side reaction observed.

All compounds were thoroughly characterized using MS and NMR spectroscopy and correspond with known data.[37,38,83,84,85] A notable and counterintuitive trend was observed in the $^{1}$H NMR spectra. The chemical shifts of the **H2** and **H5** ring protons became progressively more deshielded with increasing size and branching of the N-alkyl substituent suggesting that the alkyl groups exert a net electron-withdrawing effect on the imidazole ring.

### 5.2.1 R,R'-Imidazolium Iodide Salt Synthesis

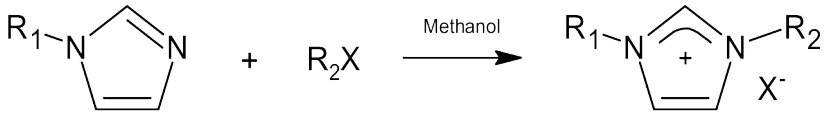


***Scheme 18: General synthesis of R, R'-Imidazolium Iodide salts, R = $CH_3$, $C_2H_5$, $C_3H_7$, $C_4H_9$ and X = I***

As shown above in Scheme 18, all the desired R,R'-imidazolium iodide salts except 1,3-di-*tert*-butylimidazolium iodide were successfully produced (which could not be synthesised by this method, see below in Section 5.2.3). The appropriate 1-alkylimidazole was reacted with the corresponding iodoalkane in methanol using a 1:1.5 molar ratio under reflux for 12 hours. Following the removal of solvent the crude products were washed with ethyl acetate and then dried under vacuum to give the desired compounds as either white / cream solids or yellow oils in good to excellent yields (68.8% - 97.2%).

All salts isolated by this method were hygroscopic, except those containing *tert*-butyl group(s).

**Table 4: Summary of MS fragments and their m/z values for compounds 7-27**

| Compound | Fragments (m/z) | | | |
|---|---|---|---|---|
| | $[M]^+$ | $[R\text{-Imidazole+H}]^+$ | $[Imidazole + H]^+$ | $[Alkyl]^+$ |
| Me2Iml (**7**) | 97 | - | - | - |
| MeEtIml (**8**) | 111 | 83 | - | - |
| MePrIml (**9**) | 125 | 83 | 69 | 43 |
| MeBuIml (**10**) | 139 | 83 | 69 | 57 |
| iPrMeIml (**11**) | 125 | 83 | 69 | 43 |
| tBuMeIml (**12**) | 139 | 83 | 69 | 57 |
| Et2Iml (**13**) | 125 | 97 | 69 | - |
| EtPrIml (**14**) | 139 | 97 | 69 | - |
| EtBuIml (**15**) | 153 | 97 | 69 | 57 |
| iPrEtIml (**16**) | 139 | 97 | 69 | 43 |
| tBuEtIml (**17**) | 153 | 97 | 69 | 57 |
| Pr2Iml (**18**) | 153 | 111 | 69 | - |
| PrBuIml (**19**) | 167 | 111 | 69 | - |
| iPrPrIml (**20**) | 153 | 111 | 69 | - |
| tBuPrIml (**21**) | 167 | 125 | 69 | 43 |
| Bu2Iml (**22**) | 181 | 125 | 69 | - |
| iPrBuIml (**23**) | 167 | 125 | 69 | 43 |

| | | | | |
|---|---|---|---|---|
| tBuBuIml (**24**) | 181 | 125 | 69 | 57 |
| iPr2Iml (**25**) | 153 | 111 | 69 | - |
| tBuiPrIml (**26**) | 167 | 125 | 69 | - |
| tBu2Iml (**27**) | 181 | 125 | 69 | 57 |

Mass spectra for compounds **7**–**26** showed molecular ion peaks consistent with their structures. The observed fragmentation patterns yielded alkyl, imidazole, and alkyl imidazole fragments as shown in Table 4.

The $^{1}$H NMR spectra of the symmetrical imidazolium salts (compounds **7, 13, 18, 22** and **25**) exhibited two characteristic signals for the imidazolium ring protons. The peaks assigned to **H2** (here and later refer to Table 4 for atom numbering scheme) appear between 9.04 – 9.29 ppm as singlets (for compounds **7**, **13**,**18** and **22**) and as an apparent triplet in compound **25**. The peaks assigned to **H3** appear between 7.67 – 8.05 ppm as apparent doublets (for compounds **13**,**18**, **22** and **27**) and as a singlet for compound **7**. The remaining signals were attributed to the alkyl substituents.

The $^{1}$H NMR spectra of the unsymmetrical imidazolium salts exhibited a similar trend to compounds **1–6**, with three distinct signals for the imidazolium ring protons. The most deshielded signal was **H2**, followed by the backbone proton adjacent to the nitrogen with the larger substituent **H5**; the least de-shielded signal corresponded to the backbone proton adjacent to the nitrogen with the smaller substituent **H4**.

When the two N-alkyl substituents on each unsymmetrical salt differed significantly e.g. methyl/ butyl and ethyl/ *iso*-propyl, the peaks for the ring protons appeared as apparent triplets. When pairing similarly sized alkyl groups (e.g., ethyl/propyl and butyl), the peaks for the ring protons appeared as singlets or poorly resolved triplets. Furthermore, the peaks for **H4** and **H5** overlapped due to the chemical shifts being closer together. Overlapping of the N-alkyl peaks was also observed for the same reason.

The $^{13}$C NMR spectra of compounds **7**–**26** were consistent with their structures, with clear differences between symmetrical and unsymmetrical salts. The symmetrical salts showed two signals in the 120–140 ppm range, assigned to **C2** (most deshielded) and **C3**. The unsymmetrical salts displayed three signals in the same region, which were assigned to **C2**, **C4**, and **C5**, with **C2** again being the most deshielded. This followed the trend seen in the $^{13}$C NMR data for compounds **1**-**6** where **C4** (backbone carbon atom adjacent to the N atom with the smaller substituent) was more desheilded. The remaining peaks were attributed to the alkyl substituents.

See Table 5 for a summary of $^{1}$H and $^{13}$C NMR data obtained for compounds **7-27**.

**Table 5: Summary of $^{1}H$ and $^{13}C$ NMR data for compounds 7-27**

| Compound & Structure | $C_{\{2\}}$-H | Backbone $C_{\{4\}}H=C_{\{5\}}H$ | R Group | R' Group |
|---|---|---|---|---|
| [**7**] Me2Iml 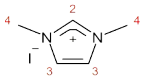 | $^{1}H$: 9.04 {s, **H2**}<br>$^{13}C$: 136.99 {**C2**} | $^{1}H$: 7.68 {s, **H3**}<br>$^{13}C$: 123.43 {**C3**} | **$CH_3$**<br>$^{1}H$: 3.84 {s, **H4**}<br>$^{13}C$: 35.74 {**C4**} | **$CH_3$**<br>$^{1}H$: 3.84 {s, **H4**}<br>$^{13}C$: 35.74 {**C4**} |
| [**8**] MeEtIml 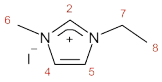 | $^{1}H$: 9.13 {s, **H2**}<br>$^{13}C$: 136.21 {**C2**} | $^{1}H$: 7.79 {app. t, J = 1.8Hz, **H5**}<br>$^{13}C$: 121.97 {**C5**}<br>$^{1}H$: 7.70 {app. t, J = 1.8Hz, **H4**}<br>$^{13}C$: 123.56 {**C4**} | **$CH_3$**<br>$^{1}H$: 3.84 {s, **H6**}<br>$^{13}C$: 35.76 {**C6**} | **$CH_2CH_3$**<br>$^{1}H$: 4.19 {q, $^{3}J$ = 7.3Hz, **H7**}, 1.42 {t, $^{3}J$ = 7.3Hz, **H8**}<br>$^{13}C$: 44.13 {**C7**}, 15.14 {**C8**} |
| [**9**] MePrIml 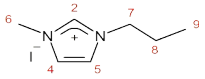 | $^{1}H$: 9.14 {app.t, J = 2.0Hz, **H2**}<br>$^{13}C$: 136.46 {**C2**} | $^{1}H$: 7.79 {app. t, J = 1.8Hz, **H5**}<br>$^{13}C$: 122.23 {**C5**}<br>$^{1}H$: 7.72 {app. t, J = 1.8Hz, **H4**}<br>$^{13}C$: 123.58 {**C4**} | **$CH_3$**<br>$^{1}H$: 3.86 {s, **H6**}<br>$^{13}C$: 35.83 {**C6**} | **$CH_2CH_2CH_3$**<br>$^{1}H$: 4.13 {t, $^{3}J$ = 7.2Hz, **H7**}, 1.80 {app. sext, $^{3}J$ = 7.4Hz, **H8**}, 0.84 {t, $^{3}J$ = 7.4Hz, **H9**}<br>$^{13}C$: 50.23 {**C7**}, 22.83 {**C8**}, 10.42 {**C9**} |
| [**10**] MeBuIml 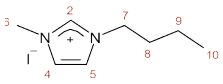 | $^{1}H$: 9.16 {app. t, J = 1.8Hz, **H2**}<br>$^{13}C$: 136.42 {**C2**} | $^{1}H$: 7.80 {app. t, J = 1.8Hz, **H5**}<br>$^{13}C$: 121.21 {**C5**}<br>$^{1}H$: 7.72 {app. t, J = 1.8Hz, **H4**}<br>$^{13}C$: 123.53 {**C4**} | **$CH_3$**<br>$^{1}H$: 3.85 {s, **H6**}<br>$^{13}C$: 35.84 {**C6**} | **$CH_2CH_2CH_2CH_3$**<br>$^{1}H$: 4.17 {t, $^{3}J$ = 7.2Hz, **H7**}, 1.76 {t, $^{3}J$ = 7.3Hz, H**8**}, 1.25 {app. sext, $^{3}J$ = 7.3Hz, **H9**}, 0.88 {t, $^{3}J$ = 7.4Hz, **H10**}<br>$^{13}C$: 48.45 {**C9**}, 31.30 {**C10**}, 18.71 {**C11**}, 13.26 {**C12**} |
| [**11**] iPrMeIml 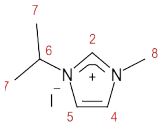 | $^{1}H$: 9.19 {app. t, J = 1.8Hz, **H2**}<br>$^{13}C$: 135.33 {**C2**} | $^{1}H$: 7.88 {app. t, J = 1.8Hz, **H5**}<br>$^{13}C$: 120.46 {**C5**}<br>$^{1}H$: 7.72 {app. t, J = 1.8Hz, **H4**}<br>$^{13}C$: 123.68 {**C4**} | **$CH_3$**<br>$^{1}H$: 3.84 {s, **H6**}<br>$^{13}C$: 35.77 {**C6**} | **$CH(CH_3)_2$**<br>$^{1}H$: 4.62 {sept, $^{3}J$ = 6.7Hz, **H6**}, 1.46 {d, $^{3}J$ = 6.6Hz, **H7**}<br>$^{13}C$: 52.12 {**C6**}, 22.36 {**C7**} |
| [**12**] tBuMeIml 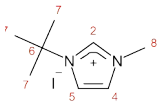 | $^{1}H$: 9.23 {app. t, J = 2.0Hz, **H2**}<br>$^{13}C$: 135.01 {**C2**} | $^{1}H$: 7.79 {app. t, J = 2.0Hz, **H5**}<br>$^{13}C$: 120.07 {**C5**}<br>$^{1}H$: 7.75 {app. t, J = 2.0Hz, **H4**}<br>$^{13}C$: 123.76 {**C4**} | **$CH_3$**<br>$^{1}H$: 3.84 {s, **H6**}<br>$^{13}C$: 35.75 {**C6**} | **$C(CH_3)_3$**<br>$^{1}H$: 1.57 {s, **H7**}<br>$^{13}C$: 59.32 {**C6**}, 29.02 {**C7**} |
| [**13**] Et2Iml 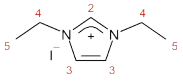 | $^{1}H$: 9.20 {s, **H2**}<br>$^{13}C$: 135.39 {**C2**} | $^{1}H$: 7.81 {app. d, J = 1.6Hz, **H3**}<br>$^{13}C$: 122.11 {**C3**} | **$CH_2CH_3$**<br>$^{1}H$: 4.19 {q, $^{3}J$ = 7.1Hz, **H4**}, 1.42 {t, $^{3}J$ = 7.3Hz, **H5**}<br>$^{13}C$: 44.19 {**C4**}, 15.06 {**C5**} | **$CH_2CH_3$**<br>$^{1}H$: 3.84 {q, $^{3}J$ = 7.1Hz, **H4**}, 1.42 {t, $^{3}J$ = 7.3Hz, **H5**}<br>$^{13}C$: 44.19 {**C4**}, 15.06 |

| | | | | |
|---|---|---|---|---|
| | | | | {**C5**} |
| [**14**] EtPrIm<br> 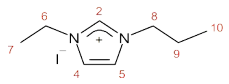 | $^{1}$H: 9.24 {s, **H2**}<br>$^{13}$C: 135.63 {**C2**} | $^{1}$H: 7.83 {s, **H5**}<br>$^{13}$C: 122.12 {**C5**}<br>$^{1}$H: 7.81 {s, **H4**}<br>$^{13}$C: 122.37 {**C4**} | **CH$_2$CH$_3$**<br>$^{1}$H: 4.20 {q, $^{3}$J = 7.3Hz, **H6**}, 1.42 {t, $^{3}$J = 7.3Hz, **H7**}<br>$^{13}$C: 44.21 {**C6**}, 15.03 {**C7**} | **CH$_2$CH$_2$CH$_3$**<br>$^{1}$H: 4.13 {t, $^{3}$J = 7.1Hz, **H8**}, 1.81 {app. sext, $^{3}$J = 7.3Hz, **H9**}, 0.85 {t, $^{3}$J = 7.3Hz, **H10**}<br>$^{13}$C: 50.29 {**C8**}, 22.78 {**C9**}, 10.44 {**C10**} |
| [**15**] EtBuIm<br> 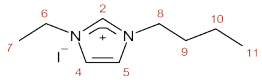 | $^{1}$H: 9.22 {s, **H2**}<br>$^{13}$C: 135.64 {**C2**} | $^{1}$H: 7.82 {s, **H5**}<br>$^{13}$C: 122.13 {**C5**}<br>$^{1}$H: 7.80 {s, **H4**}<br>$^{13}$C: 122.40 {**C4**} | **CH$_2$CH$_3$**<br>$^{1}$H: 4.18 {m, **H6**}, 1.42 {t, $^{3}$J = 7.3Hz, **H7**}<br>$^{13}$C: 48.56 {**C6**}, 15.03 {**C7**} | **CH$_2$CH$_2$CH$_2$CH$_3$**<br>$^{1}$H: 4.18 {m, **H8**}, 1.77 {quin, $^{3}$J = 7.3Hz, **H9**}, 1.26 {app. sext, $^{3}$J = 7.4Hz, **H10**}, 0.90 {t, $^{3}$J = 7.4Hz, **H11**}<br>$^{13}$C: 48.56 {**C8**}, 31.29 {**C9**}, 18.80 {**C10**}, 13.29 {**C11**} |
| [**16**] iPrEtIm<br> 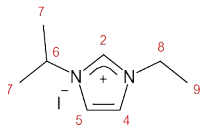 | $^{1}$H: 9.25 {s, **H2**}<br>$^{13}$C: 134.48 {**C2**} | $^{1}$H: 7.91 {app. t, J = 1.9Hz, **H5**}<br>$^{13}$C: 120.59 {**C5**}<br>$^{1}$H: 7.83 {app. t, J = 1.9Hz, **H4**}<br>$^{13}$C: 122.20 {**C4**} | **CH$_2$CH$_3$**<br>$^{1}$H: 4.18 {q, $^{3}$J = 7.3Hz, **H8**}, 1.43 {t, $^{3}$J = 7.3Hz, **H9**}<br>$^{13}$C: 44.23 {**C8**}, 15.00 {**C9**} | **CH(CH$_3$)$_2$**<br>$^{1}$H: 4.62 {sept, $^{3}$J = 6.7Hz, **H6**}, 1.47 {d, $^{3}$J = 6.7Hz, **H7**}<br>$^{13}$C: 52.19 {**C6**}, 22.34 {**C7**} |
| [**17**] tBuEtIm<br> 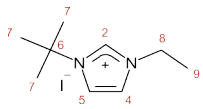 | $^{1}$H: 9.25 {app. t, J = 1.7Hz, **H2**}<br>$^{13}$C: 134.14 {**C2**} | $^{1}$H: 8.02 {app. t, J = 2.0Hz, **H5**}<br>$^{13}$C: 120.27 {**C5**}<br>$^{1}$H: 7.87 {app. t, J = 1.9Hz, **H4**}<br>$^{13}$C: 122.24 {**C4**} | **CH$_2$CH$_3$**<br>$^{1}$H: 4.18 {q, $^{3}$J = 7.3Hz, **H8**}, 1.44 {t, $^{3}$J = 7.3Hz, **H9**}<br>$^{13}$C: 44.24 {**C8**}, 15.09 {**C9**} | **C(CH$_3$)$_3$**<br>$^{1}$H: 1.58 {s, **H7**}<br>$^{13}$C: 59.37 {**C6**}, 29.02 {**C7**} |
| [**18**] Pr2Im<br> 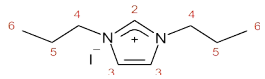 | $^{1}$H: 9.22 {s, **H2**}<br>$^{13}$C: 135.95 {**C2**} | $^{1}$H: 7.82 {app. d, J = 1.7Hz, **H3**}<br>$^{13}$C: 122.47 {**C3**} | **CH$_2$CH$_2$CH$_3$**<br>$^{1}$H: 4.14 {t, $^{3}$J = 7.1Hz, **H4**}, 1.81 {app.sext, $^{3}$J = 7.3Hz, **H5**}, 0.84 {t, $^{3}$J = 7.3Hz, **H6**}<br>$^{13}$C: 50.33 {**C4**}, 22.76 {**C5**}, 10.41 {**C6**} | **CH$_2$CH$_2$CH$_3$**<br>$^{1}$H: 4.14 {t, $^{3}$J = 7.1Hz, **H4**}, 1.81 {app.sext, $^{3}$J = 7.3Hz, **H5**}, 0.84 {t, $^{3}$J = 7.3Hz, **H6**}<br>$^{13}$C: 50.33 {**C4**}, 22.76 {**C5**}, 10.41 {**C6**} |
| [**19**] PrBuIm<br> 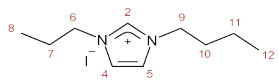 | $^{1}$H: 9.23 {s, **H2**}<br>$^{13}$C: 135.93 {**C2**} | $^{1}$H: 7.82 {m, **H5/H4**}<br>$^{13}$C: 122.46 {**C5/C4**}, 122.45 {**C5/C4**} | **CH$_2$CH$_2$CH$_3$**<br>$^{1}$H: 4.18 {t, $^{3}$J = 7.2Hz, **H6**}, 1.80 {m, **H7**}, 0.84 {t, $^{3}$J = 7.3Hz, **H9**}<br>$^{13}$C: 50.33 {**C6**}, 22.76 {**C7**}, 10.41 {**C8**} | **CH$_2$CH$_2$CH$_2$CH$_3$**<br>$^{1}$H: 4.18 {t, $^{3}$J = 7.2Hz, **H9**}, 1.80 {m, **H10**}, 1.25 {app. sext, $^{3}$J = 7.4Hz, **H11**}, 0.89 {t, $^{3}$J = 7.4Hz, **H12**}<br>$^{13}$C: 48.57 {**C9**}, 31.26 {**C10**}, 18.77 {**C11**}, 13.28 {**C12**} |
| [**20**] iPrPrIm | $^{1}$H: 9.29 {app. t, J = 1.7Hz, **H2**} | $^{1}$H: 7.93 {app. t, J = 1.9Hz, **H5**} | **CH$_2$CH$_2$CH$_3$**<br>$^{1}$H: 4.12 {t, $^{3}$J = 7.2Hz, **H9**}, 1.82 {app. sext, $^{3}$J | **CH(CH$_3$)$_2$**<br>$^{1}$H: 4.63 {sept, $^{3}$J = 6.7Hz, **H6**}, 1.48 {d, $^{3}$J |

| | | | | |
|---|---|---|---|---|
| 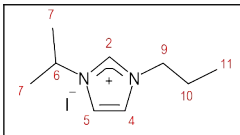 | $^{13}$C: 134.75 {**C2**} | $^{13}$C: 120.63 {**C5**}<br>$^{1}$H: 7.83 {app. t, J = 1.8Hz, **H4**}<br>$^{13}$C: 122.51 {**C4**} | = 7.4Hz, **H10**}, 0.85 {t, $^{3}$J = 7.4Hz, **H11**}<br>$^{13}$C: 50.35 {**C9**}, 22.75 {**C10**}, 10.46 {**C11**} | = 6.7Hz, **H7**}<br>$^{13}$C: 52.19 {**C6**}, 22.33 {**C7**} |
| **[21]** tBuPrIml<br> 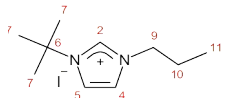 | $^{1}$H: 9.28 {app.t, J = 1.7Hz, **H2**}<br>$^{13}$C: 134.40 {**C2**} | $^{1}$H: 8.03 {app. t, J = 2.0Hz, **H5**}<br>$^{13}$C: 120.30 {**C5**}<br>$^{1}$H: 7.86 {app. t, J = 1.9Hz, **H4**}<br>$^{13}$C: 122.59 {**C4**} | **CH$_2$CH$_2$CH$_3$**<br>$^{1}$H: 4.11 {t, $^{3}$J = 7.2Hz, **H9**}, 1.83 {app. sext, $^{3}$J = 7.4Hz, **H10**}, 0.86 {t, $^{3}$J = 7.4Hz, **H11**}<br>$^{13}$C: 50.38 {**C9**}, 22.81 {**C10**}, 10.51 {**C11**} | **C(CH$_3$)$_3$**<br>$^{1}$H: 1.58 {s, **H7**}<br>$^{13}$C: 59.42 {**C6**}, 29.02 {**C7**} |
| **[22]** Bu2Iml<br> 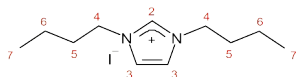 | $^{1}$H: 9.26 {s, **H2**}<br>$^{13}$C: 135.90 {**C2**} | $^{1}$H: 7.82 {app. d, J = 1.6Hz, **H3**}<br>$^{13}$C: 122.43 {**C3**} | **CH$_2$CH$_2$CH$_2$CH$_3$**<br>$^{1}$H: 4.17 {t, $^{3}$J = 7.2Hz, **H4**}, 1.77 {quin, $^{3}$J = 7.3Hz, **H5**}, 1.24 {app. sext, $^{3}$J = 7.4Hz, **H6**}, 0.89 {t, $^{3}$J = 7.4Hz, **H7**}<br>$^{13}$C: 48.56 {**C4**}, 31.24 {**C5**}, 18.76 {**C6**}, 13.26 {**C7**} | **CH$_2$CH$_2$CH$_2$CH$_3$**<br>$^{1}$H: 4.17 {t, $^{3}$J = 7.2Hz, **H4**}, 1.77 {quin, $^{3}$J = 7.3Hz, **H5**}, 1.24 {app. sext, $^{3}$J = 7.4Hz, **H6**}, 0.89 {t, $^{3}$J = 7.4Hz, **H7**}<br>$^{13}$C: 48.56 {**C4**}, 31.24 {**C5**}, 18.76 {**C6**}, 13.26 {**C7**} |
| **[23]** iPrBuIml<br> 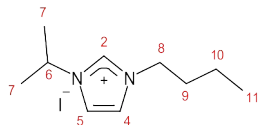 | $^{1}$H: 9.28 {s, **H2**}<br>$^{13}$C: 134.73 {**C2**} | $^{1}$H: 7.92 {app. t, J = 1.8Hz, **H5**}<br>$^{13}$C: 120.63 {**C5**}<br>$^{1}$H: 7.83 {app. t, J = 1.8Hz, **H4**}<br>$^{13}$C: 122.52 {**C4**} | **CH$_2$CH$_2$CH$_2$CH$_3$**<br>$^{1}$H: 4.15 {t, $^{3}$J = 7.3Hz, **H8**}, 1.78 {quin, $^{3}$J = 7.3Hz, **H9**}, 1.26 {app. sext, $^{3}$J = 7.4Hz, **H10**}, 0.90 {t, $^{3}$J = 7.3Hz, **H11**}<br>$^{13}$C: 48.62 {**C8**}, 31.27 {**C9**}, 18.85 {**C10**}, 13.31 {**C11**} | **CH(CH$_3$)$_2$**<br>$^{1}$H: 4.62 {sept, $^{3}$J = 6.7Hz, **H6**}, 1.48 {d, $^{3}$J = 6.7Hz, **H7**}<br>$^{13}$C: 52.20 {**C6**}, 22.33 {**C7**} |
| **[24]** tBuBuIml<br> 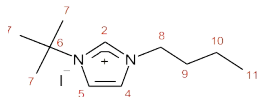 | $^{1}$H: 9.29 {app.t, J = 1.8Hz, **H2**}<br>$^{13}$C: 134.37 {**C2**} | $^{1}$H: 8.03 {app. t, J = 2.0Hz, **H5**}<br>$^{13}$C: 120.29 {**C5**}<br>$^{1}$H: 7.87 {app. t, J = 1.8Hz, **H4**}<br>$^{13}$C: 122.57 {**C4**} | **CH$_2$CH$_2$CH$_2$CH$_3$**<br>$^{1}$H: 4.15 {t, $^{3}$J = 7.3Hz, **H8**}, 1.80 {quin, $^{3}$J = 7.5Hz, **H9**}, 1.27 {app. sext, $^{3}$J = 7.3Hz, **H10**}, 0.90 {t, $^{3}$J = 7.4Hz, **H11**}<br>$^{13}$C: 48.65 {**C8**}, 31.33 {**C9**}, 18.90 {**C10**}, 13.34 {**C11**} | **C(CH$_3$)$_3$**<br>$^{1}$H: 1.58 {s, **H7**}<br>$^{13}$C: 59.42 {**C6**}, 29.02 {**C7**} |
| **[25]** iPr2Iml<br> 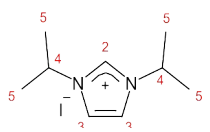 | $^{1}$H: 9.29 {app.t, J = 1.7Hz, **H2**}<br>$^{13}$C: 133.55 {**C2**} | $^{1}$H: 7.82 {app. d, J = 1.7Hz, **H3**}<br>$^{13}$C: 120.66 {**C3**} | **CH(CH$_3$)$_2$**<br>$^{1}$H: 4.62 {sept, $^{3}$J = 6.7Hz, **H4**}, 1.48 {d, $^{3}$J = 6.7Hz, **H5**}<br>$^{13}$C: 55.25 {**C4**}, 22.35 {**C5**} | **CH(CH$_3$)$_2$**<br>$^{1}$H: 4.62 {sept, $^{3}$J = 6.7Hz, **H4**}, 1.48 {d, $^{3}$J = 6.7Hz, **H5**}<br>$^{13}$C: 55.25 {**C4**}, 22.35 {**C5**} |
| **[26]** tBuiPrIml | $^{1}$H: 9.23 {app.t, J = 1.7Hz, | $^{1}$H: 8.05 {app. t, J = 2.0Hz, **H5**} | **CH(CH$_3$)$_2$**<br>$^{1}$H: 4.63 {sept, $^{3}$J = | **C(CH$_3$)$_3$**<br>$^{1}$H: 1.59 {s, **H7**} |

| | | | | |
|---|---|---|---|---|
| 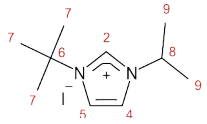 | **H2**}<br>$^{13}$C: 133.13 {**C2**} | $^{13}$C: 120.46 {**C5**}<br>$^{1}$H: 7.98 {app. t, J = 1.9Hz, **H4**}<br>$^{13}$C: 120.51 {**C4**} | 6.7Hz, **H8**}, 1.48 {d, $^{3}$J = 6.7Hz, **H9**}<br>$^{13}$C: 55.32 {**C8**}, 22.37 {**C9**} | $^{13}$C: 59.44 {**C6**}, 29.05 {**C7**} |
| [**27**] tBu2Iml<br> 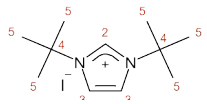 | $^{1}$H: 9.01 {app.t, J = 1.8Hz, **H2**}<br>$^{13}$C: 132.23 {**C2**} | $^{1}$H: 7.94 {app. d, J = 1.7Hz, **H3**}<br>$^{13}$C: 120.66 {**C3**} | **<u>C(CH$_3$)$_3$</u>**<br>$^{1}$H: 1.60 {s, **H5**}<br>$^{13}$C: 59.69 {**C4**}, 29.14 {**C5**} | **<u>C(CH$_3$)$_3$</u>**<br>$^{1}$H: 1.60 {s, **H5**}<br>$^{13}$C: 59.69 {**C4**}, 29.14 {**C5**} |

### 5.2.2 1,3-Di-*tert*-butylimidazolium Iodide Synthesis

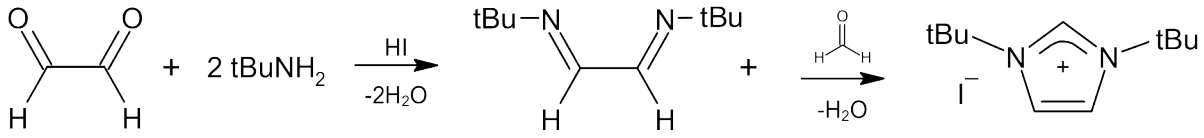


***Scheme 19: General synthesis of 1, 3-di-tert-butyl-imidazolium iodide.***

Scheme 19 shows the preparation of 1,3-di-*tert*-butylimidazolium iodide. A mixture of *tert*-butylamine and hydriodic acid was gradually added to 40% aq. glyoxal, followed by gradual addition of 37% aq. formaldehyde in a 2:1:1:1 molar ratio in methanol. The reaction mixture was then heated to reflux for 12 hours. Following the removal of the solvent, the crude product was washed with ethyl acetate and then dried under vacuum to give the desired product as a cream solid in moderate yield (54.8%).

The mass spectrum of compound **27** showed the expected molecular ion peak at m/z = 181. Fragmentation peaks were observed at m/z = 125, 69, and 57, corresponding to the 1-*tert*-butylimidazolium ($[M+H]^+$) ion, the imidazole (+H) ion, and the *tert*-butyl ion, respectively.

See Table 4 (page 93) for a summary of MS data obtained for compound **27**.

The $^1$H NMR spectrum of compound **27** displayed an apparent triplet at 9.01 ppm (1H) for the central proton **H2** and an apparent doublet at 8.06 ppm (2H) for the backbone protons **H3**. A singlet at 1.65 ppm (18H) was assigned to the methyl groups of the two *tert*-butyl substituents **H5**.

The $^{13}$C NMR spectrum was consistent with the structure of a symmetrical imidazolium salt. Two signals for the ring carbon atoms were observed at 132.23 ppm **C2** and 120.53 ppm **C3**. The remaining peaks were attributed to the quaternary carbon **C4** and the methyl groups of the *tert*-butyl substituents **C5**.

See Table 5 (page 95) for a summary of $^1$H and $^{13}$C NMR data obtained for compound **27**.

### 5.2.3 Overview of R,R'-Imidazolium Iodide Salt Syntheses

Compounds **7, 8, 9, 10, 11, 12, 13, 14, 15, 18, 19, 20, 22, 23** and **25** all previously described and characterised in literature.[86-94]

The synthesis of most of the imidazolium salts was performed without significant complications, confirming the general applicability and efficacy of the developed method. However, synthesis of the *tert*-butyl salts required some modification.

Synthesis of imidazolium salts containing *tert*-butyl functionalities was originally attempted using 2-iodo-2-methylpropane and the corresponding 1-alkylimidazole (Scheme 4), however almost no success was achieved. Only trace amounts of compound **12** (starting from 1-methylimidazole) were obtained, with none of the other products (staring from other N-alkylimidazoles) being isolated. Similar to the original attempts to synthesize compound **6** upon addition of 2-iodo-2-methylpropane and heating, evolution of white vapours was observed.

Multiple repeat attempts were made with various modifications to improve yields. The modifications made to the original methodology included dropwise addition of 2-iodo-2-methylpropane to the reaction mixture, dropwise addition of 1-alkylimidazole to a solution of 2-iodo-2-methylpropane, usage of different solvents (ethanol / propan-2-ol / toluene / ethyl acetate / acetonitrile / THF / DCM and chloroform), conduction the reaction at reflux / room temperature and at 0°C.

Unfortunately, no modifications made gave any quantifiable improvement to the yield of compounds **12**, **17**, **21**, **24, 26** and **27**.

What remained after work-up of the reaction mixture for all attempts was a viscous brown oil. Analysis of these brown oils by $^{1}$H NMR and LC-MS indicated the hydriodic acid salt of the corresponding 1-alkylimidazole used as a starting material. Addition of a base (saturated sodium carbonate solution used in this instance) to these brown oils caused vigorous evolution of gas (neutralization of the acid) and led to reforming the free-base 1-alkylimidazoles.

Like the initial synthesis attempts of compound **6** the significant steric hinderance present prevents the nucleophilic attack of the quaternary carbon atom favouring the elimination pathway (see section 5.1.3). Additional steric hinderance may come from the increasing size of the N-alkyl groups of the 1-alkylimidsazoles used. Therefore, it was necessary to use the 1-*tert*-butylimidazole previously produced as the initial building block for production of the desired imidazolium salts with the corresponding iodoalkane.

See Figure 7 for NMR data comparison of initial (A) and final (B) synthesis of compound **17**.

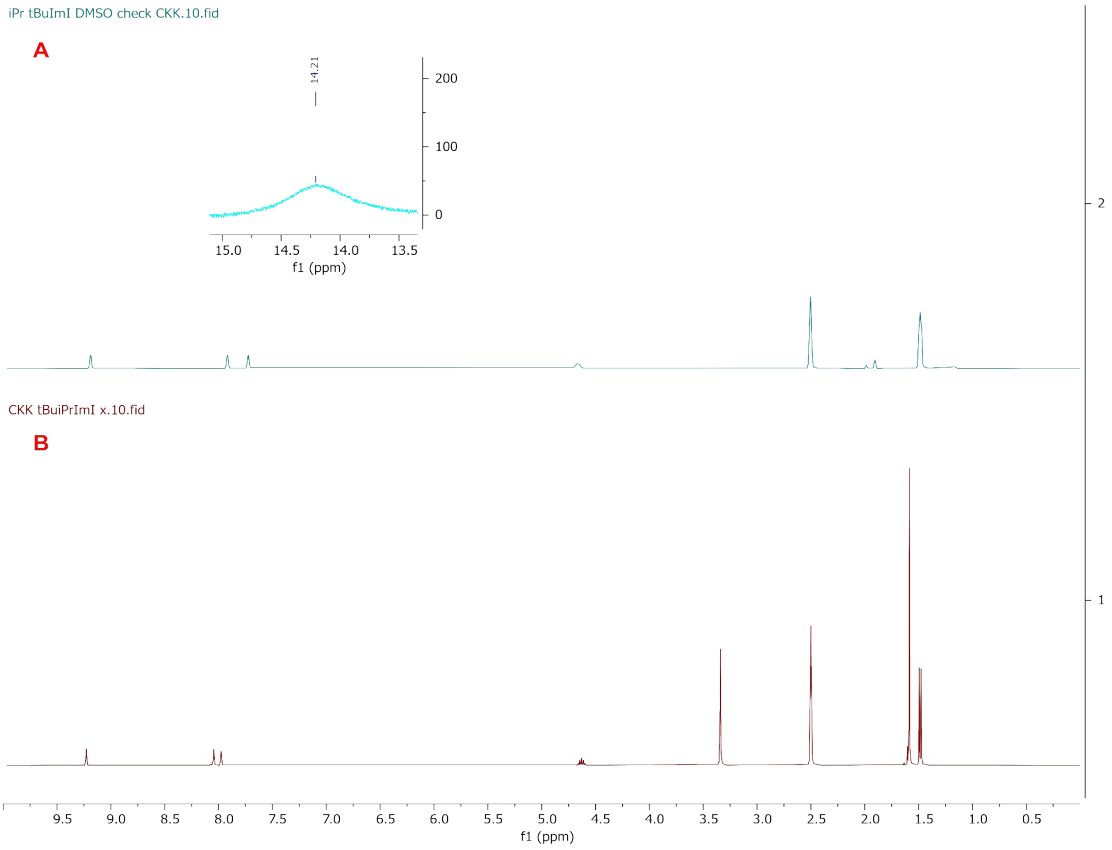


***Figure 7: Comparison of $^{1}$H NMR spectra of initial 1-ethyl-3-tert-butylimidazolium iodide synthesis (A) and the final synthesis (B).***

Successful production of compound **27** required use of the ring closure methodology where 2 equivalents of *tert*-butylamine and 1 equivalent of hydriodic acid was reacted with glyoxal followed by addition of formaldehyde and reflux. Following removal of solvent and washing with ethyl acetate compound **27** was isolated as a cream solid in moderate yield (54.8%).

The imidazolium ring protons and carbon atoms in the unsymmetrical salts were assigned based on the $^{1}$H and $^{13}$C NMR data, following the same pattern seen for compounds **1–6**.

In the $^{1}$H NMR spectra for the unsymmetrical imidazolium salts, the signals were assigned in order of increasing deshielding where **H2** is the most deshielded followed by **H5** and **H4**, where **H5** is the backbone proton adjacent to the N atom with the largest alkyl group. These assignments were confirmed $^{1}$H-$^{1}$H NOESY, with correlations seen between **H5** and largest N- alkyl substituent.

The ring protons generally became more deshielded with increasing size of the N-alkyl substituents as shown in Figures 8 and 9, with large regular increases in deshielding of **H5** when iso-propyl and tert-butyl groups were present as shown in Figure 9.

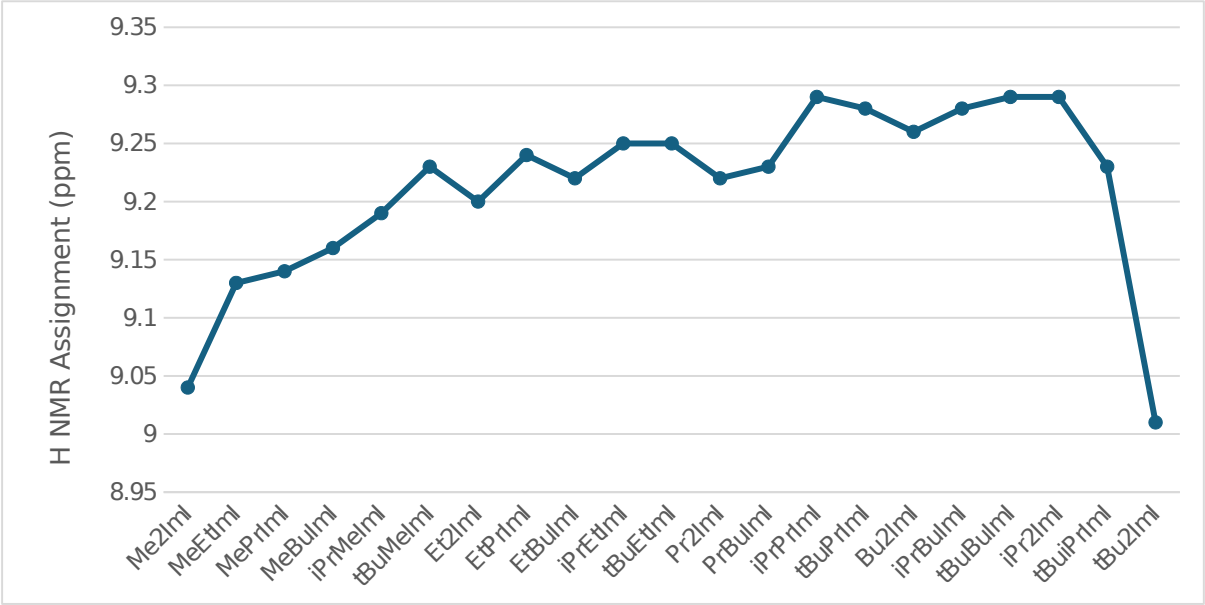


***Figure 8: Graph showing trend in $^{1}$H NMR assignments for central protons H5 for compounds 7-27.***

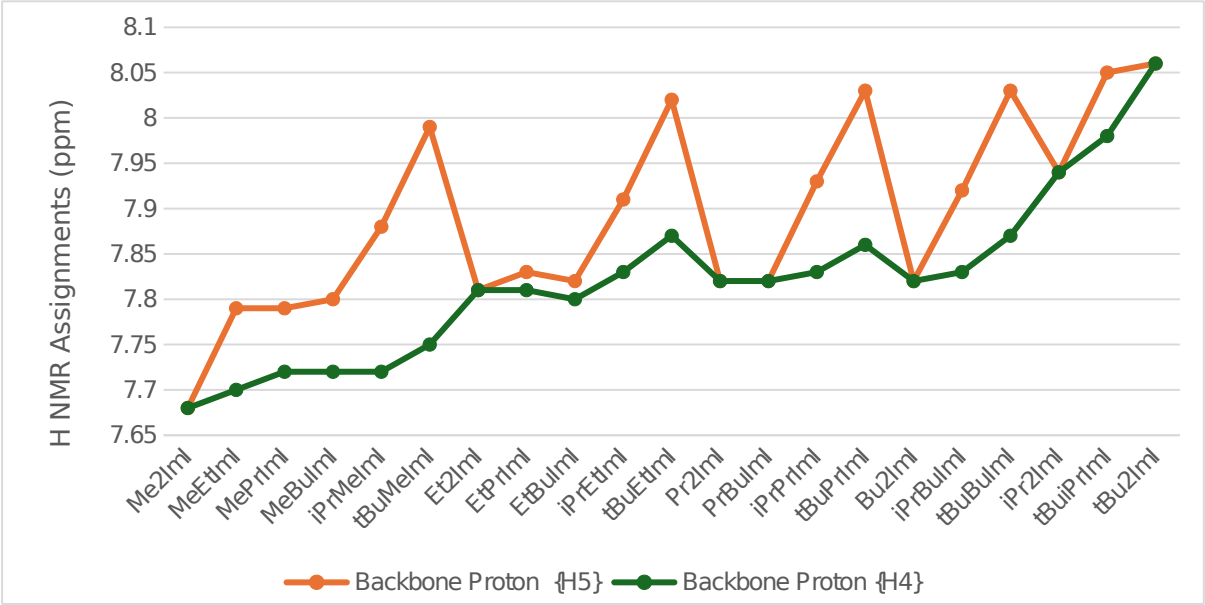


***Figure 9: Graph showing trend in $^{1}$H NMR assignments for the backbone protons H5 and H4 for compounds 7-27.***

In $^{13}$C NMR spectra, the carbon atoms were assigned with **C2** being the most deshielded, followed by **C4** and **C5**. These assignments were supported by correlations in $^{1}$H-$^{1}$H NOESY, $^{1}$H-$^{13}$C HSQC and $^{1}$H-$^{13}$C HMBC NMR spectra.

As seen for compounds **1-6** in section 5.1.3, protons **H5** and **H4** were assigned in order of increasing deshielding, the opposite trend was observed for their corresponding carbons, with **C4** being more deshielded than **C5**.

Elemental analysis was obtained for compounds **7**-**27**. All elemental analysis results were within 0.5% of the calculated values shown in Table 6.

**Table 6: Elemental analysis results for compounds 7-27**

| **Elemental Analysis** | | Carbon % | Hydrogen % | Nitrogen % |
|---|---|---|---|---|
| Me2Iml (7) | Calculated | 26.80 | 4.05 | 12.50 |
| | Observed | 26.73 | 4.18 | 12.49 |
| MeEtIml (8) | Calculated | 30.27 | 4.66 | 11.77 |
| | Observed | 30.22 | 4.66 | 11.98 |
| MePrIml (9) | Calculated | 33.35 | 5.20 | 11.11 |
| | Observed | 33.38 | 5.21 | 11.24 |
| MeBuIml (10) | Calculated | 36.11 | 5.68 | 10.53 |
| | Observed | 36.27 | 5.83 | 10.21 |
| iPrMeIml (11) | Calculated | 33.35 | 5.20 | 11.11 |
| | Observed | 32.89 | 5.24 | 11.05 |
| tBuMeIml (12) | Calculated | 36.11 | 5.68 | 10.53 |
| | Observed | 36.28 | 5.76 | 10.21 |
| Et2Iml (13) | Calculated | 33.35 | 5.20 | 11.11 |
| | Observed | 33.42 | 5.20 | 11.22 |
| EtPrIml (14) | Calculated | 36.11 | 5.68 | 10.53 |
| | Observed | 36.28 | 5.80 | 10.21 |
| EtBuIml (15) | Calculated | 38.59 | 6.12 | 10.00 |
| | Observed | 38.58 | 6.11 | 9.74 |
| iPrEtIml (16) | Calculated | 36.11 | 5.68 | 10.53 |
| | Observed | 36.52 | 5.65 | 10.27 |
| tBuEtIml (17) | Calculated | 38.59 | 6.12 | 10.00 |
| | Observed | 38.58 | 6.14 | 9.73 |
| Pr2Iml (18) | Calculated | 38.59 | 6.12 | 10.00 |
| | Observed | 38.54 | 6.13 | 9.71 |
| PrBuIml (19) | Calculated | 40.83 | 6.51 | 9.52 |
| | Observed | 40.41 | 6.46 | 9.17 |
| iPrPrIml (20) | Calculated | 38.59 | 6.12 | 10.00 |
| | Observed | 38.61 | 6.29 | 9.69 |
| tBuPrIml (21) | Calculated | 40.83 | 6.51 | 9.52 |
| | Observed | 40.35 | 6.46 | 9.07 |
| Bu2Iml (22) | Calculated | 42.87 | 6.87 | 9.09 |
| | Observed | 42.96 | 6.87 | 9.07 |
| iPrBuIml (23) | Calculated | 40.83 | 6.51 | 9.52 |

| | | | | |
|---|---|---|---|---|
| | Observed | 40.38 | 6.49 | 9.72 |
| tBuBuImI (24) | Calculated | 42.87 | 6.87 | 9.09 |
| | Observed | 43.07 | 6.89 | 9.03 |
| iPr2ImI (25) | Calculated | 38.59 | 6.12 | 10.00 |
| | Observed | 38.71 | 6.21 | 9.67 |
| tBuiPrImI (26) | Calculated | 40.83 | 6.51 | 9.52 |
| | Observed | 40.67 | 6.45 | 9.22 |
| tBu2ImI (27) | Calculated | 42.87 | 6.87 | 9.09 |
| | Observed | 42.94 | 6.90 | 9.29 |

### 5.2.4 R,R'-Imidazolium Iodide Salt Synthesis Conclusion

In summary, a large library of R,R'-imidazolium iodide salts were successfully produced in good to excellent yields (68.8–97.2%) via alkylation of the corresponding 1-alkylimidazoles with compounds **7, 8, 9, 10, 11, 12, 13, 14, 15, 18, 19, 20, 22, 23** and **25** corresponding with known data.[86-94] 1,3-Di-*tert*-butylimidazolium iodide (**27**) was synthesized via a Debus-Radziszewski multi-component reaction in a moderate 54.8% yield due to the same elimination side reaction seen previously (see section 5.1.3) being present preventing direct quaternarization.

NMR characterization revealed a consistent trend for the unsymmetrical salts where the backbone proton **H5** adjacent to the larger N-alkyl group was more deshielded than its counterpart **H4**. Furthermore, the ring protons became progressively more deshielded with increasing size of the N-alkyl groups, mirroring the trend seen in the precursor 1-alkylimidazoles (Section 5.1.3).

### 5.3.1 Potassium Tetracarbonyl Iron Hydride Synthesis K[HFe(CO)$_4$]

Synthesis of K[HFe(CO)$_4$] was adapted from previous literature where the compound was generated *in situ* for use in further reactions and no attempts were made to isolate it from the crude reaction mixtures obtained.[70,71] Therefore, the synthesis methodology was adapted in an attempt to isolate K[HFe(CO)$_4$] and obtain additional spectroscopic data.

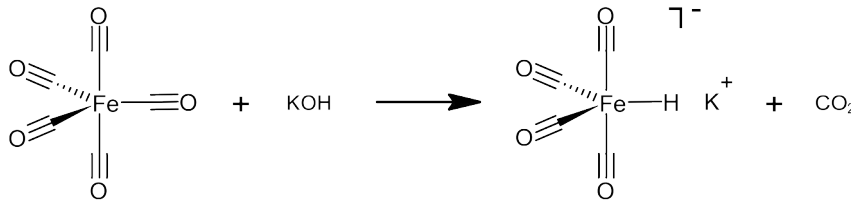


***Scheme 20: General synthesis of potassium tetracarbonyl iron hydride.***

Scheme 20 shows the preparation of potassium tetracarbonyl iron hydride K[HFe(CO)$_4$]. Under the atmosphere of dry, oxygen free argon, iron pentacarbonyl was reacted with commercial potassium hydroxide (90% purity, from Sigma-Aldrich) in a 1:1 molar ratio in dry, degassed methanol with constant stirring at room temperature for 12 hours. Following the removal of solvent and extraction of the crude product using dry, degassed acetonitrile, the acetonitrile extract was filtered *via* filter cannula and the solvent was then removed under vacuum to give the desired product as a red / maroon solid in moderate yield (51.4%).

Mass spectra of K[HFe(CO)$_4$] revealed the expected peak corresponding to the molecular ion [HFe(CO)$_4$]-, m/z = 169, in the negative mode. Additional peaks at m/z = 393, 401, 421 and 449 were also observed that may indicate the presence of polynuclear hydrides. Plausible fragments represented by these peaks include [HFe$_2$(CO)$_{10}$]-, [HFe$_3$(CO)$_8$]-, [HFe$_3$(CO)$_9$]- and [HFe$_3$(CO)$_{10}$]- respectively, however alternative fragments may be possible.

The 1H NMR spectra of as-synthesised samples of K[HFe(CO)$_4$] revealed 3 peaks at -7.61, -8.98, -15.01 ppm which have an integration ratio of 0.02 : 1 : 0.02 respectively where the peak at -8.98 ppm corresponds to the hydride proton present in [HFe(CO)$_4$]-. Like the additional peaks observed in the mass spectra obtained, the -7.61 and -15.01 ppm peaks may correspond to polynuclear iron carbonyl hydrides formed with the peak at -7.61 possibly corresponding to an impurity or another hydride and the -15.01 ppm peak corresponding to the tri-iron hydride ([HFe$_3$(CO)$_{11}$]-).[70,71]

The 13C NMR spectra of K[HFe(CO)$_4$] revealed 2 peaks at 210.15 and 219.95 ppm correspond with the axial and equatorial carbonyl ligands present. It is unknown which peak

corresponds to which position. Further $^{13}C$ NMR data for polynuclear hydrides has been previously documented where the peak(s) observed are related to the temperature. At room temperature for both $[HFe_2(CO)_8]$- and $[HFe_3(CO)_{11}]$- only one peak is observed for the bridging and terminal carbonyl ligands indicating rapid exchange of the carbonyl environments.[71,71,76] Only after being cooled below -70°C were additional peaks observed upfield of the approx. 220 ppm peak seen in the spectrum at room temperature.[70]

### 5.3.2 Overview of $K[HFe(CO)_4]$ Synthesis

The synthesis of $K[HFe(CO)_4]$was initially performed by reacting $Fe(CO)_5$ and KOH in dry/ degassed methanol for 24 hours. The resultant red/ maroon suspension was filtered leaving a pale-pink solid behind (likely potassium hydrogen carbonate/ $KHCO_3$). The solvent was removed under vacuum from the filtered solution to give a red/ brown oily solid. Even after storage in the glovebox freezer at -34°C for 18 hours it was still impossible to manipulate the solid as it was extremely sticky.

Due to the solid by-product, thought to be the result of contamination of the commercial KOH used (90%, Sigma-Aldrich), a further synthesis was attempted by first producing KOH in situ under anhydrous, $CO_2$-free conditions.

In a glovebox, remelted potassium metal was pressed against the side of a round bottom Schlenk flask, which was then taken out of the glovebox, attached to the Schlenk line and cooled in an ice bath. Dry, degassed methanol was then added dropwise *via* cannula with constant stirring whilst avoiding direct contact between the solvent and metal. The potassium was then allowed to react with the methanol vapours. Slow addition of methanol was repeated until all the potassium had reacted. Degassed water (1 equiv.) was then added. Assuming the production of KOH was quantitative, $Fe(CO)_5$ (1 equiv.) was added and left to stir for 24 hours. After 24 hours a dark red/ purple suspension with a small amount of solid was observed.

KOH was synthesized via potassium methoxide hydrolysis to avoid the dangerously exothermic direct reaction of potassium metal with water. This route provided greater control.

A sample of the reaction mixture was taken and a $^1H$ NMR spectrum was obtained to confirm if the reaction was successful when comparing against previously recorded $^1H$ NMR spectra (using a $d_6$-DMSO capillary for lock) for which this sample agreed with. Following removal of solvent under vacuum and extraction using acetonitrile, the reaction yielded 0.351g (64.4%) of a red solid that was easily manipulated.

Comparing the first synthesis (51.4% yield) to the modified route (64.4% yield) shows only a 13% yield increase, despite the *in situ* generation of pure KOH. Furthermore, a small amount of solid remained after work-up, indicating that contaminated commercial KOH was not the sole factor in its formation. This solid is likely to be $KHCO_3$, formed from the reaction of KOH with $CO_2$ generated during the synthesis shown in Scheme 21 below. Therefore, an excess of KOH is likely required to maximize yields in future attempts.

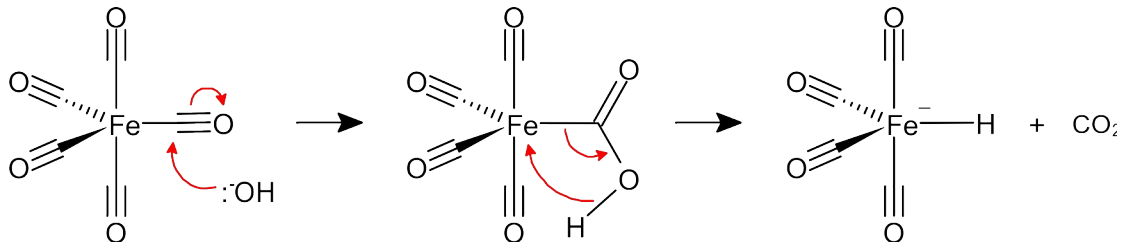


***Scheme 21: Plausible reaction mechanism leading to the formation of $[HFe(CO)_4]$- and $CO_2$.***

The $^1H$ and $^{13}C$ NMR spectra of $K[HFe(CO)_4]$ were then acquired in acetonitrile for comparison with the methanol spectra and notable differences were observed.

The $^1H$ NMR spectrum in acetonitrile displayed only two hydride signals (int ratio 1 : 0.02), compared to three in methanol (int ratio 0.02 : 1 : 0.02) shown in Figure 10. The absence of the most deshielded peak (approximately 7.4 ppm) suggests that a possible polynuclear iron hydride species may have been left behind during the extraction, decomposed, or converted into the desired product.

The $^{13}C$ NMR spectrum in acetonitrile showed only a single carbonyl peak. This contrasts with the $^{13}C$ NMR spectrum recorded in methanol, where separate signals for the axial and equatorial carbonyl ligands were observed shown in Figure 11. The single peak observed in acetonitrile solution possibly indicates the rapid exchange between axial and equatorial carbonyl ligands as seen for other hydride species.[69,78]

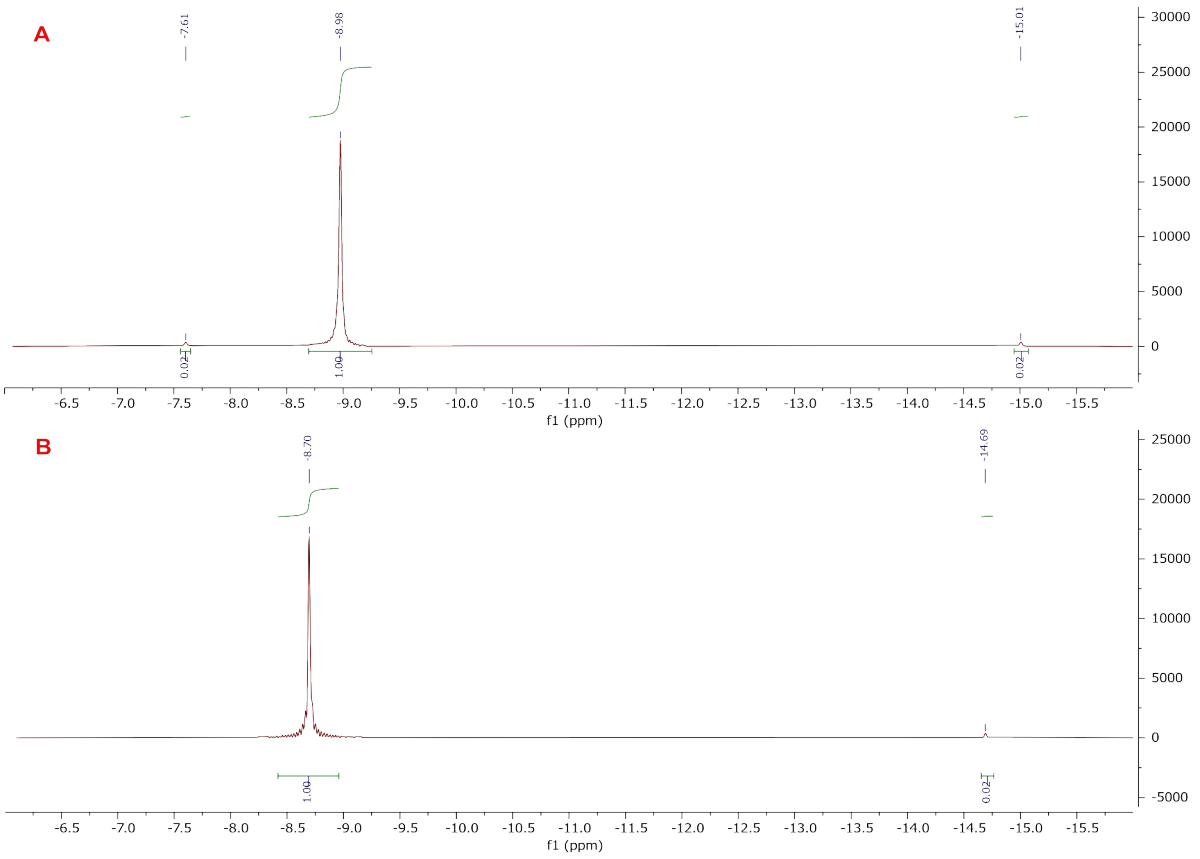


*Figure 10: Comparison of 1H NMR data for MeOH (A) and MeCN (B) solutions of K[HFe(CO)$_4$].*

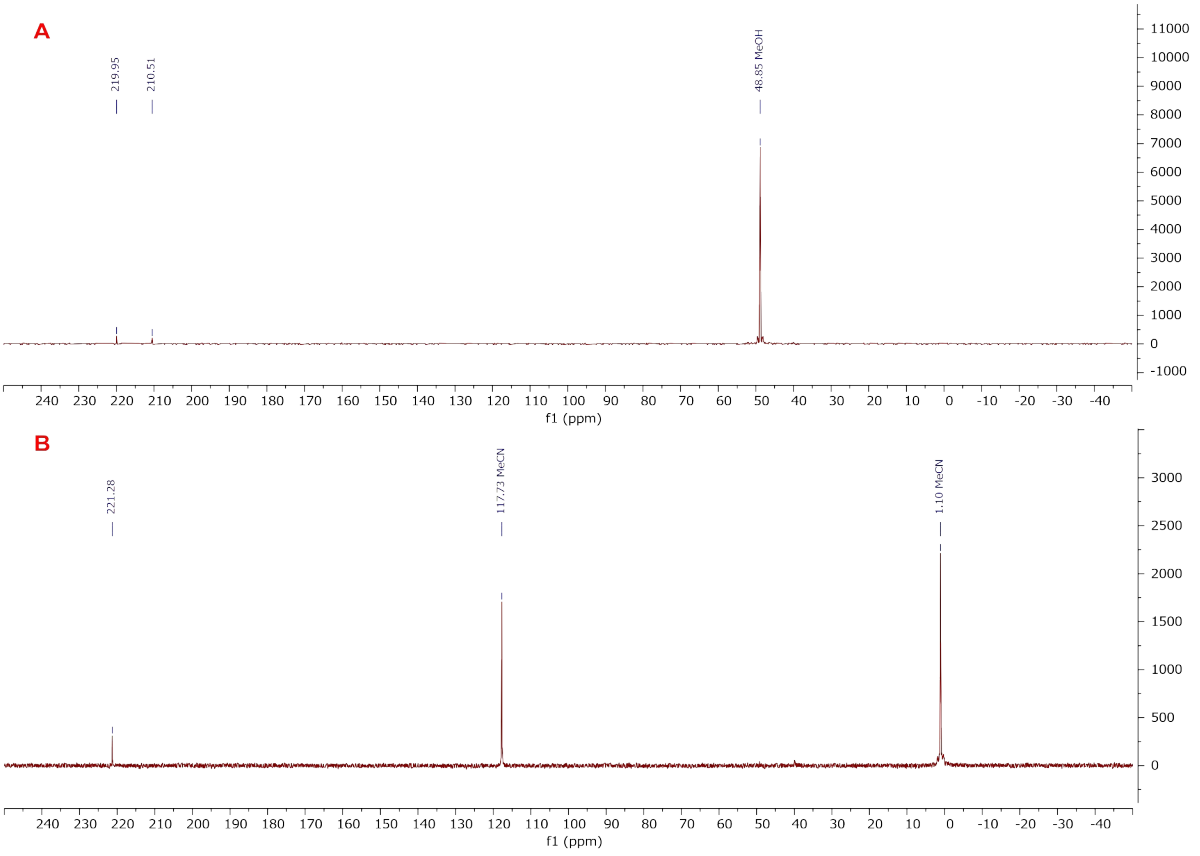


*Figure 11: Comparison of 13C NMR data for MeOH (A) and MeCN (B) solutions of K[HFe(CO)$_4$].*

The $^{1}H$ and $^{13}C$ NMR spectra of $K[HFe(CO)_4]$ were then acquired in acetonitrile for comparison with the methanol spectra and notable differences were observed.

The $^{1}H$ NMR spectrum in acetonitrile displayed only two hydride signals (int ratio 1 : 0.02), compared to three in methanol (0.02 : 1 : 0.05). The absence of the most deshielded peak (approximately 7.4 ppm) suggests that polynuclear iron hydride species may have been left behind during the extraction, decomposed, or converted into the desired product.

The $^{13}C$ NMR spectrum in acetonitrile showed only a single carbonyl peak. This contrasts with the $^{13}C$ NMR spectrum recorded in methanol, where separate signals for the axial and equatorial carbonyl ligands were observed. The single peak observed in acetonitrile solution possibly indicates the rapid exchange between axial and equatorial carbonyl ligands similar to that seen for the larger polynuclear hydrides.

Elemental analysis was performed on the solid product.

| **Elemental analysis:** | Carbon % | Hydrogen % | Nitrogen % |
|---|---|---|---|
| Calculated for $K[HFe(CO)_4]$ | 23.08 | 0.48 | 0 |
| Calculated for $K[HFe(CO)_4]$ x 0.5 MeCN | 26.28 | 1.10 | 3.06 |
| Observed | 26.41 | 0.96 | 3.48 |

The elemental analysis results showed nitrogen was present in the sample tested, alongside additional amounts of carbon and hydrogen. This indicated that there was acetonitrile still present with an approximate ratio of 1 $K[HFe(CO)_4]$: 0.5 acetonitrile.

For the first time, a stable solid, free flowing sample of $K[HFe(CO)_4]$ has been isolated, as confirmed by elemental analysis. Previous literature reports only describe this compound in solution.[70,71] The solid remained stable for at least six months when stored in a glovebox freezer, indicating that it is highly stable at low temperatures.

### 5.3.3 $K[HFe(CO)_4]$ Synthesis Conclusion

In summary, a successful method was developed for the isolation of $K[HFe(CO)_4]$ as a stable, free-flowing red solid allowing for additional characterization beyond what was previously reported [70,71] with elemental analysis confirming the solid's composition, albeit with some retained acetonitrile. Moderate yields were achieved by both methods attempted (51.4 - 64.4%) which also indicated that $KHCO_3$ formation is an inherent side reaction of the synthesis.

Comprehensive characterization, including MS and NMR spectroscopy, confirmed the identity of the product but also revealed its sensitivity to solvent. The NMR spectra obtained in different solvents showed distinct behaviour: in acetonitrile, a single $^{13}C$ NMR peak suggested rapid carbonyl ligand exchange, while in methanol, separate signals seemingly for the axial and equatorial carbonyls were observed.

### 5.4.1 Fe-NHC Complex Synthesis

The synthesis of iron carbonyl NHC complexes was first performed by Ofele et al. using $K[HFe(CO)_4]$ and 1,3-dimethylimidazolium iodide.[37] Although other methods employing $Fe_3(CO)_{12}$ or $Fe(CO)_5$ have been successful,[46,47] the $K[HFe(CO)_4]$ route has not been further explored. Therefore, Ofele's methodology was adapted to attempt the synthesis of novel complexes with different imidazolium ligands.

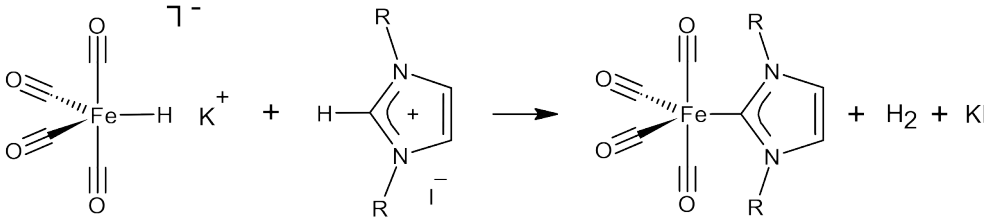


***Scheme 22: Synthesis of Fe-NHC complexes. R = $CH_3$, $C_2H_5$, $C_3H_7$, $C_4H_9$.***

As shown in Scheme 22, all the desired Fe-NHC complexes except those synthesized using *tert*-butyl group containing ligands were successfully produced. A mixture of $K[HFe(CO)_4]$ and the appropriate ligand in a 1:2 molar ratio was heated without solvent to 120°C (at which temperature all reaction mixtures were molten) under dynamic vacuum for 4 hours. Dry, degassed toluene was then used to extract the products and after the removal of solvent the desired products were isolated as yellow solids or orange oils in poor to moderate yields (17.6- 54.2%).

The solids obtained were purified *via* sublimation under vacuum onto a liquid nitrogen cooled cold finger.

The mass spectra and fragmentation patterns of the Fe-NHC complexes were influenced by the size and symmetry of the NHC ligand. Positive ion scans showed peaks corresponding to the free ligand. Negative ion scans revealed fragments including m/z = 169 and 170 (assigned to $HFe(CO)_4^-$) and m/z = 194 (tentatively assigned to $[HFe(CO)_4^- + Na]^{+/-}$), along with plausible iron-ligand fragments, complexes minus 1-3 CO ligands, complexes minus one of the N-substituents and intact complexes. Among the complexes, only $FeiPr_2$ consistently showed a significant peak for the intact complex, while $FeEt_2$ consistently produced a prominent Fe + ligand fragment.

See Table 7 for a summary of MS data obtained for complexes synthesized.

**Table 7: Summary of MS fragments and their m/z values for the complexes produced.**

| Complexes | Peaks (m/z) | |
|---|---|---|
| | Positive Mode | Negative Mode |
| FeMe2 | 97 – $[Me2Im + H]^+$<br>153 – $[Fe + Me2Im]^+$ | 169 – $[HFe(CO)_4]$- |
| FeMeEt | 111 – $[MeEtIm + H]^+$ | 169 – $[HFe(CO)_4]$- |
| FeMePr | 125 – $[MePrIm + H]^+$<br>181 – $[Fe + MePrIm]^+$ | 169 – $[HFe(CO)_4]$- |
| FeMeBu | 139 – $[MeBuIm + H]^+$ | 169 – $[HFe(CO)_4]$-<br>195 – $[Fe + MeBuIm]^-$<br>277 – $[FeMeBu – CO]^-$<br>291 – $[FeMeBu – CH_3]$-<br>305 – $[FeMeBu - H]^-$ |
| FeiPrMe | 125 – $[iPrMeIm + H]^+$<br>293 – $[FeiPrMe + H]^+$ | 169 – $[HFe(CO)_4]$-<br>291 – $[FeiPrMe – H]^-$ |
| FeEt2 | 125 – $[Et2Im + H]^+$<br>293 – $[FeEt2 + H]^+$ | 180 – $[Fe + Et2Im]^-$<br>291 – $[FeEt2 – H]^-$ |
| FeEtPr | 139 – $[EtPrIm + H]^+$ | 169 – $[HFe(CO)_4]$-<br>277 – $[FeEtPr – CO]^-$ or<br>277 – $[FeEtPr – C_2H_5]$- |
| FeEtBu | 153 – $[EtBuIm + H]^+$ | 168 – $[Fe(CO)_4]$- |
| FeiPrEt | 139 – $[iPrEtIm + H]^+$ | 169 – $[HFe(CO)_4]$-<br>277 – $[FeiPrEt – C_2H_5]$- |
| FePr2 | 153 – $[Pr2Im + H]^+$ | 319 – $[FePr2 – H]^-$ |
| FePrBu | 167 – $[PrBuIm + H]^+$ | 169 – $[HFe(CO)_4]$- |
| FeiPrPr | 153 – $[iPrPrIm + H]^+$ | 277 – $[FeiPrPr – C_3H_7]$-<br>319 – $[FeiPrPr – H]^-$ |
| FeBu2 | 181 – $[Bu2Im + H]^+$ | 169 – $[HFe(CO)_4]$- |
| FeiPrBu | 167 – $[iPrBuIm + H]^+$ | 170 – {$HFe(CO)_4$]-<br>277 – $[FeiPrBu – C_4H_9]$-<br>Or<br>277 – $[FeiPrBu – 2\ CO]^-$ |
| FeiPr2 | 153 – $[iPr2Im + H]^+$ | 319 – $[FeiPr2 - H]^-$ |

**Table 8: Summary of $^{1}H$ and $^{13}C$ NMR data for the complexes produced.**

| Complex | Carbonyl | Carbene | Backbone | R Group | R' Group |
|---|---|---|---|---|---|
| FeMe2 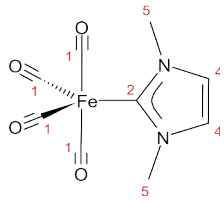 | $^{13}C$: 216.96 {**C1**} | $^{13}C$: 181.31 {**C2**} | $^{1}H$: 5.72 {s, **H4**}<br>$^{13}C$: 123.20 {**C4**} | **$CH_3$**<br>$^{1}H$: 3.03 {s, **H5**}<br>$^{13}C$: 39.13 {**C5**} | **$CH_3$**<br>$^{1}H$: 3.03 {s, **H5**}<br>$^{13}C$: 39.13 {**C5**} |
| FeMeEt 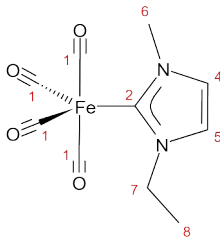 | $^{13}C$: 217.34 {**C1**} | $^{13}C$: 180.14 {**C2**} | $^{1}H$: 5.90 {s, **H5**}<br>$^{13}C$: 121.29 {**C5**}<br>$^{1}H$: 5.82 {s, **H4**}<br>$^{13}C$: 123.90 {**C4**} | **$CH_3$**<br>$^{1}H$: 3.07 {s, **H6**}<br>$^{13}C$: 39.13 {**C6**} | **$CH_2CH_3$**<br>$^{1}H$: 3.71 {q, $^{3}J$ = 7.5Hz, **H7**}, 0.88 {t, $^{3}J$ = 6.8Hz, **H8**}<br>$^{13}C$: 46.34 {**C7**}, 15.58 {**C8**} |
| FeMePr 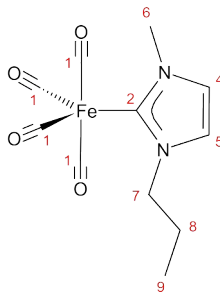 | $^{13}C$: 217.40 {**C1**} | $^{13}C$: 180.51 {**C2**} | $^{1}H$: 5.92 {d, J = 1.8Hz, **H5**}<br>$^{13}C$: 121.87 {**C5**}<br>$^{1}H$: 5.82 {d, J = 2.1Hz, **H4**}<br>$^{13}C$: 123.52 {**C4**} | **$CH_3$**<br>$^{1}H$: 3.09 {s, **H6**}<br>$^{13}C$: 39.11 {**C6**} | **$CH_2CH_2CH_3$**<br>$^{1}H$: 3.67 {t, $^{3}J$ = 7.4Hz, **H7**}, 1.40 {app. sext, $^{3}J$ = 7.3Hz, **H8**}, 0.62 {t, $^{3}J$ = 7.4Hz, **H9**}<br>$^{13}C$: 52.94 {**C7**}, 23.89 {**C8**}, 10.70 {**C9**} |
| FeMeBu 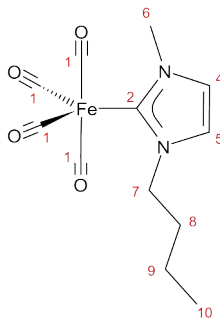 | $^{13}C$: 217.44 {**C1**} | $^{13}C$: 180.59 {**C2**} | $^{1}H$: 5.95 {d, J = 2.1Hz, **H5**}<br>$^{13}C$: 121.85 {**C5**}<br>$^{1}H$: 5.84 {d, J = 1.8Hz, **H4**}<br>$^{13}C$: 123.54 {**C4**} | **$CH_3$**<br>$^{1}H$: 3.09 {s, **H6**}<br>$^{13}C$: 39.14 {**C6**} | **$CH_2CH_2CH_2CH_3$**<br>$^{1}H$: 3.75 {t, $^{3}J$ = 7.4Hz, **H7**}, 1.39 {quin, $^{3}J$ = 7.7Hz, **H8**}, 1.04 {app. sext, $^{3}J$ = 7.4Hz, **H9**}, 0.74 {t, $^{3}J$ = 7.3Hz, **H10**}<br>$^{13}C$: 51.38 {**C7**}, 32.64 {**C8**}, 19.84 {**C9**}, 13.76 {**C10**} |
| FeiPrMe 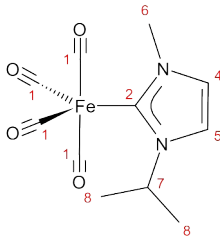 | $^{13}C$: 217.45 {**C1**} | $^{13}C$: 179.39 {**C2**} | $^{1}H$: 6.11 {d, J = 2.1Hz, **H5**}<br>$^{13}C$: 117.81 {**C5**}<br>$^{1}H$: 5.86 {d, J = 2.1Hz, **H4**}<br>$^{13}C$: 124.61 {**C4**} | **$CH_3$**<br>$^{1}H$: 3.07 {s, **H6**}<br>$^{13}C$: 39.23 {**C6**} | **$CH(CH_3)_2$**<br>$^{1}H$: 5.19 {sept, $^{3}J$ = 6.7Hz, **H7**}, 0.94 {d, $^{3}J$ = 6.7Hz, **H8**}<br>$^{13}C$: 52.70 {**C7**}, 22.68 {**C8**} |
| FeEt2 | $^{13}C$: 217.99 {**C1**} | $^{13}C$: 178.99 {**C2**} | $^{1}H$: 6.06 {s, **H4**}<br>$^{13}C$: 121.92 {**C4**} | **$CH_2CH_3$**<br>$^{1}H$: 3.77 {q, $^{3}J$ = | **$CH_2CH_3$**<br>$^{1}H$: 3.77 {q, $^{3}J$ = |

| | | | | | |
|---|---|---|---|---|---|
| 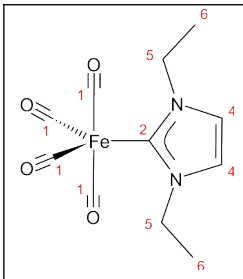 | | | | 7.4Hz, **H5**}, 0.88 {t, $^{3}$J = 7.3 Hz, **H6**} $^{13}$C: 46.29 {**C5**}, 15.57 {**C6**} | 7.4Hz, **H5**}, 0.88 {t, $^{3}$J = 7.3 Hz, **H6**} $^{13}$C: 46.29 {**C5**}, 15.57 {**C6**} |
| FeEtPr 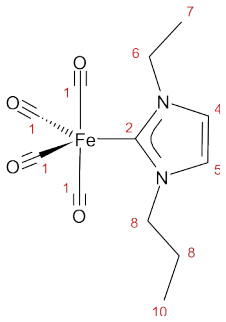 | $^{13}$C: 218.10 {**C1**} | $^{13}$C: 179.65 {**C2**} | $^{1}$H: 6.00 {s, **H4/5**} $^{13}$C: 121.40 {**C5**}, 122.52 {**C4**} | **CH$_2$CH$_3$** $^{1}$H: 3.70 {q, $^{3}$J = 7.3Hz, **H6**}, 0.88 {t, $^{3}$J = 7.4Hz, **H7**} $^{13}$C: 46.31 {**C6**}, 15.51 {**C7**} | **CH$_2$CH$_2$CH$_3$** $^{1}$H: 3.70 {t, $^{3}$J = 7.3Hz, **H8**}, 1.41 {app. sext, $^{3}$J = 7.6Hz, **H9**}, 0.63 {t, $^{3}$J = 7.4Hz, **H10**} $^{13}$C: 52.88 {**C8**}, 23.94 {**C9**}, 10.74 {**C10**} |
| FeEtBu 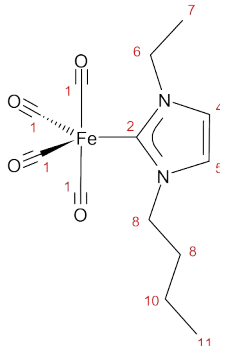 | $^{13}$C: 218.16 {**C1**} | $^{13}$C: 179.60 {**C2**} | $^{1}$H: 6.06 {d, J = 2.1Hz, **H5**} $^{13}$C: 121.47 {**C5**} $^{1}$H: 6.03 {d, J = 2.1Hz, **H4**} $^{13}$C: 122.50 {**C4**} | **CH$_2$CH$_3$** $^{1}$H: 3.77 {m, **H6**}, 0.89 {t, $^{3}$J = 7.3Hz, **H7**} $^{13}$C: 46.33 {**C6**}, 15.54 {**C7**} | **CH$_2$CH$_2$CH$_2$CH$_3$** $^{1}$H: 3.77 {m, **H8**}, 1.40 {quin, $^{3}$J = 7.7Hz, **H9**}, 1.06 {app. sext, $^{3}$J = 7.4Hz, **H10**}, 0.75 {t, $^{3}$J = 7.3Hz, **H11**} $^{13}$C: 51.31 {**C8**}, 32.69 {**C9**}, 19.85 {**C10**}, 13.76 {**C11**} |
| FeiPrEt 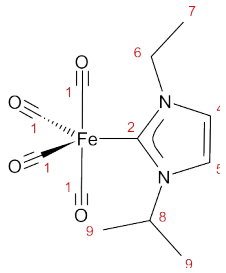 | $^{13}$C: 218.04 {**C1**} | $^{13}$C: 178.56 {**C2**} | $^{1}$H: 6.17 {d, J = 2.1Hz, **H5**} $^{13}$C: 118.40 {**C5**} $^{1}$H: 6.00 {d, J = 2.1Hz, **H4**} $^{13}$C: 122.60 {**C4**} | **CH$_2$CH$_3$** $^{1}$H: 3.70 {q, $^{3}$J = 7.3Hz, **H6**}, 0.91 {m, **H7**} $^{13}$C: 46.24 {**C6**}, 15.75 {**C7**} | **CH(CH$_3$)$_2$** $^{1}$H: 5.26 {sept, $^{3}$J = 6.7Hz, **H8**}, 0.91 {m, **H9**} $^{13}$C: 52.65 {**C8**}, 22.69 {**C9**} |
| FePr2 | $^{13}$C: 218.31 {**C1**} | $^{13}$C: 179.92 {**C2**} | $^{1}$H: 6.06 {s, **H4**} $^{13}$C: 122.18 {**C4**} | **CH$_2$CH$_2$CH$_3$** $^{1}$H: 3.74 {t, $^{3}$J = 7.4Hz, **H5**}, 1.41 {app. sext, $^{3}$J = 7.3Hz, **H6**}, 0.63 {t, $^{3}$J = 7.4Hz, **H7**} $^{13}$C: 52.92 {**C5**}, 23.87 {**C6**}, 10.77 {**C7**} | **CH$_2$CH$_2$CH$_3$** $^{1}$H: 3.74 {t, $^{3}$J = 7.4Hz, **H5**}, 1.41 {app. sext, $^{3}$J = 7.3Hz, **H6**}, 0.63 {t, $^{3}$J = 7.4Hz, **H7**} $^{13}$C: 52.92 {**C5**}, 23.87 {**C6**}, 10.77 {**C7**} |

| | | | | | |
|---|---|---|---|---|---|
| 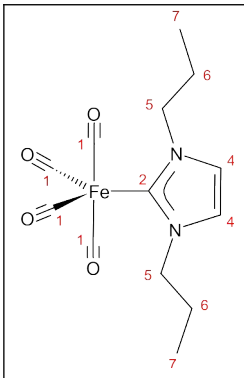 | | | | | |
| FePrBu 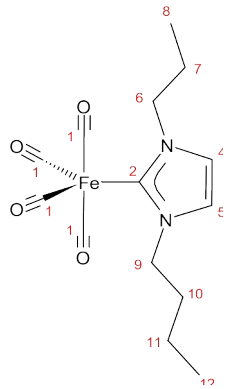 | $^{13}$C: 218.35 {**C1**} | $^{13}$C: 180.01 {**C2**} | $^{1}$H: 6.08 {d, J = 1.8Hz, **H5**} $^{13}$C: 122.12{**C5**} $^{1}$H: 6.05 {d, J = 1.8Hz, **H4**} $^{13}$C: 122.19 {**C4**} | **CH$_2$CH$_2$CH$_3$** $^{1}$H: 3.74 {t, $^{3}$J = 7.4Hz, **H6**}, 1.40 {m, **H7**}, 0.64 {t, $^{3}$J = 7.4Hz, **H8**} $^{13}$C: 52.93 {**C6**}, 23.91 {**C7**}, 10.77 {**C8**} | **CH$_2$CH$_2$CH$_2$CH$_3$** $^{1}$H: 3.82 {t, $^{3}$J = 7.3Hz, **H9**}, 1.40 {m, **H10**}, 1.06 {app. sext, $^{3}$J = 7.4Hz, **H11**}, 0.75 {t, $^{3}$J = 7.4Hz, **H12**} $^{13}$C: 51.34 {**C9**}, 32.64 {**C10**}, 19.87 {**C11**}, 13.77 {**C12**} |
| FeiPrPr 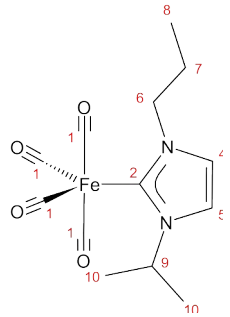 | $^{13}$C: 218.12 {**C1**} | $^{13}$C: 178.82 {**C2**} | $^{1}$H: 6.19 {d, J = 2.1Hz, **H5**} $^{13}$C: 118.18 {**C5**} $^{1}$H: 6.04 {d, J = 2.1Hz, **H4**} $^{13}$C: 123.39 {**C4**} | **CH$_2$CH$_2$CH$_3$** $^{1}$H: 3.66 {t, $^{3}$J = 7.3Hz, **H6**}, 1.44 {app. sext, $^{3}$J = 7.3Hz, **H7**}, 0.64 {t, $^{3}$J = 7.4Hz, **H8**} $^{13}$C: 52.73 {**C6**}, 24.11 {**C7**}, 10.69 {**C8**} | **CH(CH$_3$)$_2$** $^{1}$H: 5.30 {sept, $^{3}$J = 6.8Hz, **H9**}, 0.94 {d, $^{3}$J = 6.7Hz, **H10**} $^{13}$C: 52.73 {**C9**}, 22.67 {**C10**} |
| FeBu2 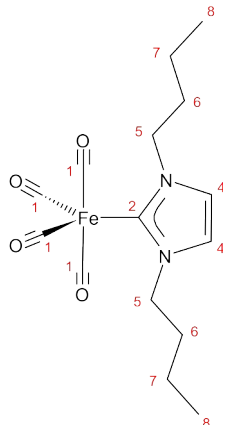 | $^{13}$C: 218.42 {**C1**} | $^{13}$C: 179.93 {**C2**} | $^{1}$H: 6.10 {s, **H4**} $^{13}$C: 122.19 {**C4**} | **CH$_2$CH$_2$CH$_2$CH$_3$** $^{1}$H: 3.82 {t, $^{3}$J = 7.4Hz, **H5**}, 1.41 {quin, $^{3}$J = 7.7Hz, **H6**}, 1.07 {app. sext, $^{3}$J = 7.4Hz, **H7**}, 0.76 {t, $^{3}$J = 7.3Hz, **H8**} $^{13}$C: 51.36 {**C5**}, 32.67 {**C6**}, 19.87 {**C7**, 13.78 {**C8**} | **CH$_2$CH$_2$CH$_2$CH$_3$** $^{1}$H: 3.82 {t, $^{3}$J = 7.4Hz, **H5**}, 1.41 {quin, $^{3}$J = 7.7Hz, **H6**}, 1.07 {app. sext, $^{3}$J = 7.4Hz, **H7**}, 0.76 {t, $^{3}$J = 7.3Hz, **H8**} $^{13}$C: 51.36 {**C5**}, 32.67 {**C6**}, 19.87 {**C7**, 13.78 {**C8**} |
| FeiPrBu | $^{13}$C: 218.18 {**C1**} | $^{13}$C: 178.90 {**C2**} | $^{1}$H: 6.21 {d, J = 2.1Hz, **H5**} $^{13}$C: 118.19 {**C5**} $^{1}$H: 6.08 {d, J = | **CH$_2$CH$_2$CH$_2$CH$_3$** $^{1}$H: 3.74 {t, $^{3}$J = 7.3Hz, **H6**}, 1.43 {quin, $^{3}$J = 7.9Hz, | **CH(CH$_3$)$_2$** $^{1}$H: 5.30 {sept, $^{3}$J = 6.8Hz, **H10**}, 0.94 {d, $^{3}$J = |

| | | | | | |
|---|---|---|---|---|---|
| 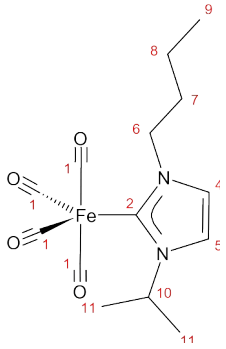 | | | 2.1Hz, **H4**}<br>$^{13}$C: 12{**C4**} | **H7**}, 1.07 {app. sext, $^{3}$J = 7.4Hz, **H8**}, 0.74 {t, $^{3}$J = 7.4Hz, **H9**}<br>$^{13}$C: 51.26 {**C6**}, 32.84 {**C7**}, 19.82 {**C8**}, 13.77 {**C9**} | 7.0Hz, **H11**}<br>$^{13}$C: 52.73 {**C10**}, 22.69 {**C11**} |
| FeiPr2<br> 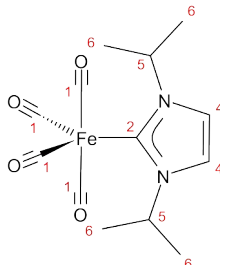 | $^{13}$C: 218.42 {**C1**} | $^{13}$C: 178.37 {**C2**} | $^{1}$H: 6.32 {s, **H4**}<br>$^{13}$C: 119.03 {**C4**} | $^{1}$H: 5.25 {sept, $^{3}$J = 6.7Hz, **H5**}, 0.93 {d, $^{3}$J = 6.7Hz, **H6**}<br>$^{13}$C: 52.46 {**C5**}, 22.74 {**C6**} | $^{1}$H: 5.25 {sept, $^{3}$J = 6.7Hz, **H5**}, 0.93 {d, $^{3}$J = 6.7Hz, **H6**}<br>$^{13}$C: 52.46 {**C5**}, 22.74 {**C6**} |

The $^{1}$H NMR spectra (in dry, degassed $C_6D_6$) of the Fe-NHC complexes resembled those of their parent ligands, with one difference: the signal for the central imidazolium proton was absent. Only signals from the backbone protons and N-substituents were observed though not as deshielded as the parent ligand however this could be due to the Fe-carbene bond or the use of a different deuterated solvent.

The $^{13}$C NMR spectra (in dry, degassed $C_6D_6$) of the Fe-NHC complexes resembled those of their parent ligands but featured two key new signals: one between 178–182 ppm, corresponding to the carbene carbon, and another between 215–220 ppm, assigned to the carbonyl ligands. The presence of a single carbonyl peak suggests rapid exchange or equivalent environments due to molecular symmetry/ geometrical distortion.

The observations made from the NMR data obtained agrees with the previously reported data for the FeMe2 and FeiPr2 complexes and the trends seen therein.[46,79]

From the NMR data obtained, all the complexes produced were observed to be diamagnetic.

See Table 8 (page 113) for a summary of $^{1}$H/ $^{13}$C NMR data obtained for complexes synthesized.

### 5.4.2 Overview of Fe-NHC Complexes Synthesis

All complexes produced are novel compounds barring **FeMe2** [39,40,48] and **FeiPr2** [48] which have both been previously described in literature.

The desired complexes were synthesized using the molten ligand as both reactant and solvent. For all reactions, a temperature of 120°C was maintained to ensure the ligand remains molten.

The yields obtained (54.2 – 17.6%) correlated with the size of the N-substituents. As the size of the N-alkyl groups increased, the yield of the desired complex decreased other than for the synthesis of FeiPr2 shown in Figure 12.

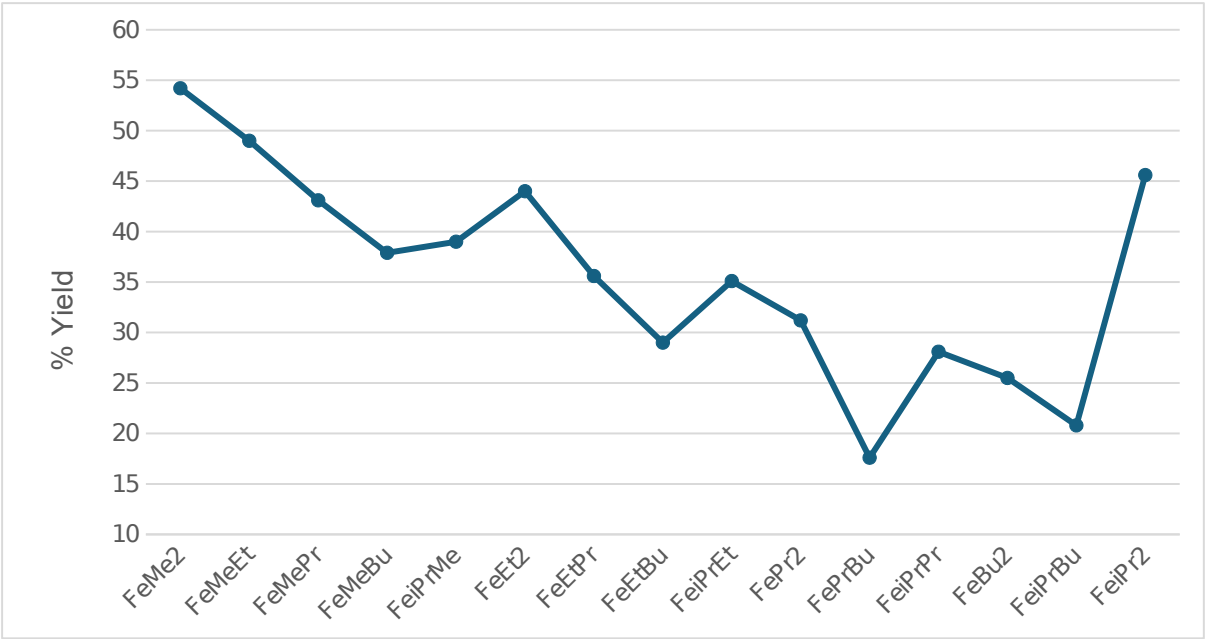


***Figure 12: Graph detailing the trend of reaction yield and size of N-substituents.***

This methodology failed for ligands bearing *tert*-butyl groups, as their higher melting points (>160°C) induced rapid decomposition of $K[HFe(CO)_4]$. Repeat synthesis were attempted using tBu2Iml via conventional reflux in toluene, acetonitrile and THF.

Initially, the toluene reaction was a pale red solution with suspended white solid, which upon being heated to reflux gradually lost its red colour, finally yielding a colourless solution and black solid. After isolation of this colourless solution by cannula filtration and removal of the solvent a very small amount of white solid formed. Toluene, deuterated benzene or acetonitrile extracts of this white solid did not show the presence of any hydrogen and/or carbon containing compounds by NMR. The black solid was extracted with acetonitrile and the presence of imidazolium ligand was observed by NMR.

Reflux in acetonitrile yielded a red solution and a white solid. After isolation of the solution and removal of the solvent, a red/ purple oil was obtained. NMR analysis of this oil confirmed this oil to be a mixture of the imidazolium ligand and $[HFe(CO)_4]$-. Presumably an ion exchange occurred, and KI precipitated out of solution due to low solubility leaving the $[(t\text{-}Bu)_2Im]$+ $[HFe(CO)_4]$- ion pair / salt in solution. Figure 13 displays the non-solvent suppressed spectrum due to removal of the singlet corresponding to the methyl groups in the solvent suppressed spectrum.

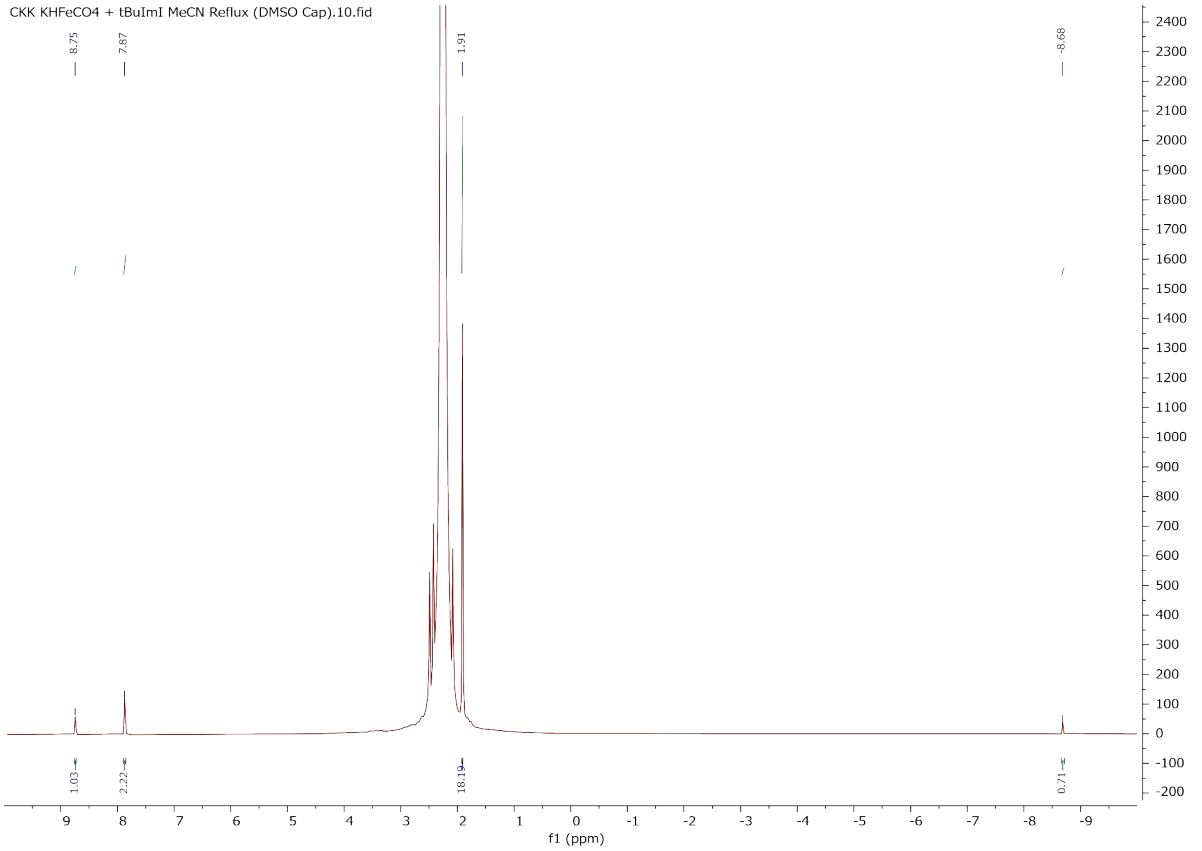


***Figure 13: $^1$H NMR spectrum of $[(t\text{-}Bu)_2Im]$+ $[HFe(CO)_4]$-.***

Initially, the THF reaction was a red solution with suspended white solid, which upon heating to reflux rapidly lost its red colour, progressing to orange and then yellow before becoming colourless. Additionally, a black solid was observed. This colourless solution was isolated *via* cannula filtration and after removal of solvent no traces of potential product were seen. Toluene, deuterated benzene nor acetonitrile extracts of anything that remained from the

colourless solution were observed in $^{1}H$ and $^{13}C$ NMR. The black solid was extracted with acetonitrile and the presence of imidazolium ligand was observed by NMR. The rapid change and then loss of colour and lack or recoverable desired product may suggest the desired complex forms transiently but rapidly decomposes.

Elemental analysis was successfully obtained for several of the complexes isolated, four of which being novel compounds (FeMeEt, FeMePr, FeMeBu, FeiPrMe). All elemental analysis results were within 0.5% of the calculated values as shown in Table 9.

**Table 9: Elemental analysis results for FeMe2, FeMeEt, FeMePr, FeMeBu, FeiPrMe and FeiPr2**

| **Elemental analysis:** | | Carbon % | Hydrogen % | Nitrogen % |
|---|---|---|---|---|
| FeMe2 | Calculated | 40.94 | 3.05 | 10.61 |
| | Observed | 40.48 | 3.16 | 10.65 |
| FeMeEt * | Calculated | 43.20 | 3.63 | 10.08 |
| | Observed | 43.31 | 3.71 | 9.81 |
| FeMePr * | Calculated | 45.24 | 4.14 | 9.59 |
| | Observed | 45.56 | 4.09 | 9.36 |
| FeMeBu * | Calculated | 47.09 | 4.61 | 9.15 |
| | Observed | 47.14 | 4.57 | 9.19 |
| FeiPrMe * | Calculated | 45.24 | 4.17 | 9.59 |
| | Observed | 45.57 | 4.23 | 9.41 |
| FeiPr2 | Calculated | 48.77 | 5.04 | 8.75 |
| | Observed | 48.85 | 5.09 | 8.70 |

### 5.4.3 Fe-NHC Complexes Synthesis Conclusion

In summary, the adaptation of Ofele's methodology successfully yielded a series of thirteen novel and two known Fe-NHC carbonyl complexes [39,40,48] from the corresponding imidazolium salts and the previously synthesized $K[HFe(CO)_4]$. The reaction proceeded effectively for ligands with methyl to isopropyl substituents, yielding products (17.6–54.2%) that were characterized by Elemental Analysis, MS and NMR spectroscopy which corresponded to previously reported data and the observations made therein.

Ligands containing *tert*-butyl groups failed to produce the desired complexes, instead leading to decomposition as the high temperatures required to melt these ligands caused the decomposition of $K[HFe(CO)_4]$, or ion exchange in more conventional reflux conditions. This underscores the critical influence of sterics on the success of this synthetic route where increasing bulk on the N-alkyl chain progressively hinders successful synthesis.

### 5.5.1 Exposure of Fe-NHC Complexes to $H_2$ Gas

The previously mentioned iron carbonyl NHC complexes were synthesized to test their ability to reversibly bind $H_2$ under milder conditions, when compared to conditions previously described in literature.[62]

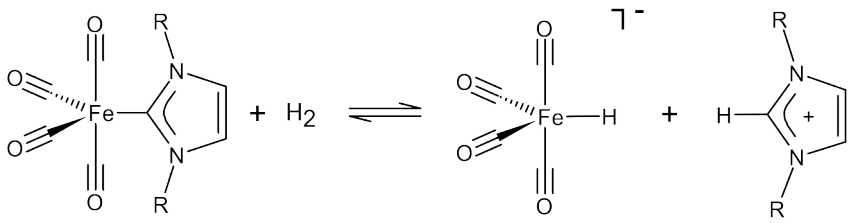

***Scheme 23: Possible reaction scheme for exposure of Fe-NHC complexes to $H_2$ gas. R = $CH_3$, $C_2H_5$, $C_3H_7$, $C_4H_9$.***

As shown in Scheme 23, all the prepared Fe-NHC complexes were exposed to hydrogen gas. A solution of the complex(s) to be tested in $d_6$-benzene in an NMR tube was degassed and exposed to an atmospheric pressure of hydrogen gas for an hour. A $^1$H NMR spectrum was recorded, and the sample(s) sealed under hydrogen atmosphere were heated at reflux overnight. An additional $^1$H NMR spectrum was recorded after the samples(s) were left to cool. After one hour of $H_2$ exposure, the $^1$H NMR spectrum of each complex showed a new signal at approximately 4.47 ppm, consistent with dissolved $H_2$ gas. No other changes were observed. Subsequent spectra taken after heating the samples overnight were identical. Comparison of this NMR data is shown in Figure 14.

Furthermore, no visible changes were observed upon $H_2$ exposure or subsequent overnight heating. The yellow solutions retained their colour, and no precipitation occurred.

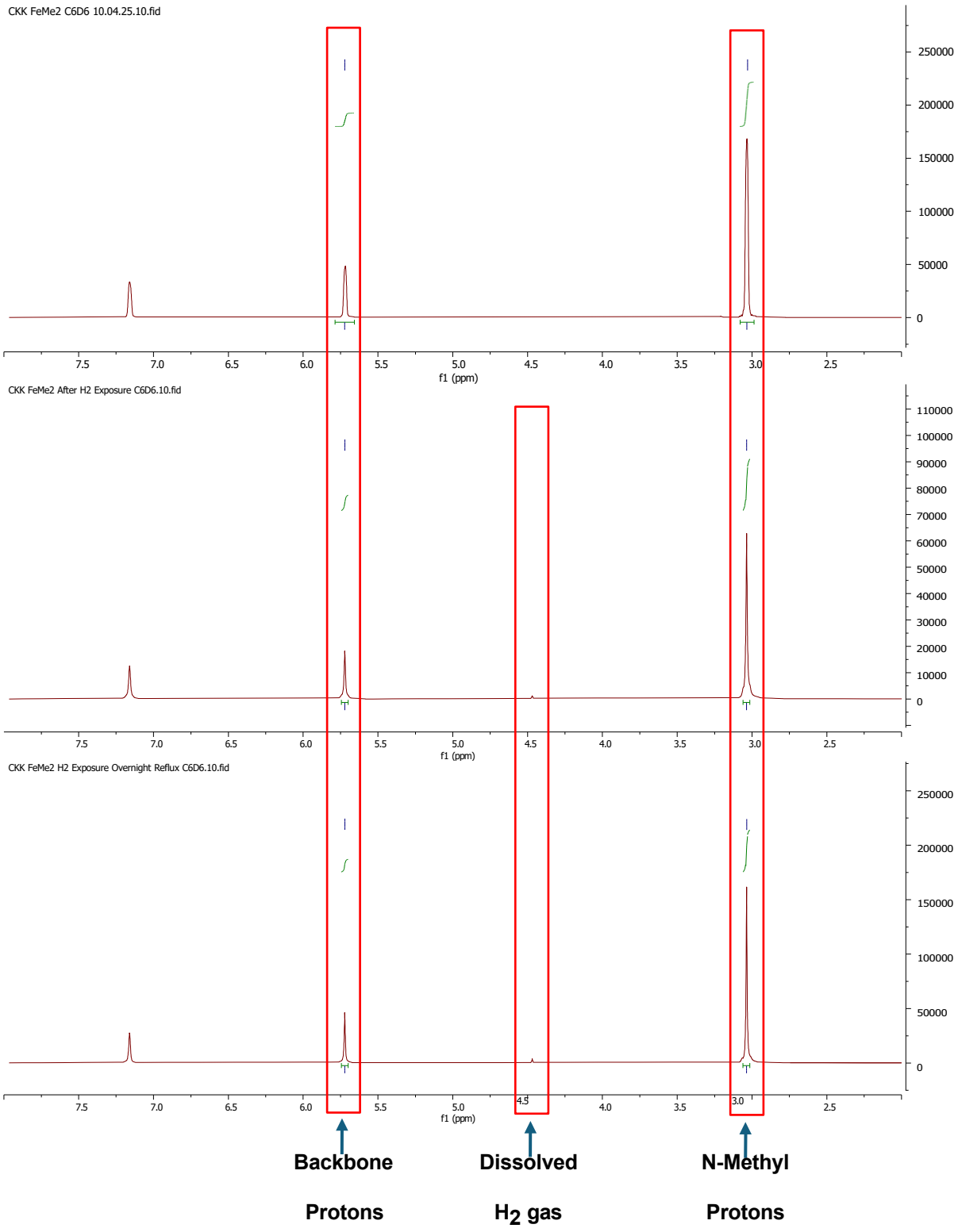


***Figure 14: Comparison of $^1$H NMR spectra of FeMe2 before, after $H_2$ exposure and after heating.***

### 5.5.2 Overview of $H_2$ testing of Fe-NHC Complexes

The lack of observed reactivity suggests the complexes did not react with hydrogen under these conditions. Future experiments should employ more rigorous degassing and significantly harsher reaction conditions, informed by previous work. Improvements would include extended heating (e.g., one week or longer) under a constant $H_2$ atmosphere at much higher pressures, such as the 1.8 MPa (18 atm) used successfully in prior literature however even then yields of the desired outcome were poor (approx. 14%) shown in Scheme 24.[62]

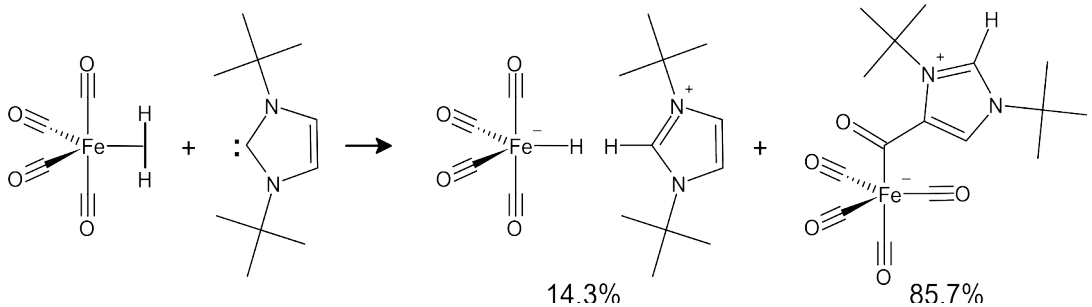


***Scheme 24: General scheme showing reaction product after $H_2$ gas exposure as described in literature where the major product is the 'abnormal' carbene complex.***

It is a possibility that the lack of successful reactions under these milder conditions may be due to the lack of strain on the Fe-C bond due to the N-alkyl substituents. The lack of 'fixed' 3D shape may be the cause of this. All the N-substituents on the Fe-NHC complexes tested would be able to rotate around the N-C and C-C bonds allowing for reduced strain on the Fe-C bond.

# Chapter 6: Conclusion and Future Work

## 6.1 Conclusion

This work successfully demonstrates the synthesis and characterization of a diverse library of 1-alkylimidazoles and their corresponding imidazolium iodide salts, alongside the preparation of potassium tetracarbonyl iron hydride K[HFe(CO)$_4$] and its subsequent use in forming Fe- NHC complexes.

The synthesis of 1-alkylimidazoles (methyl to butyl, isopropyl) *via* alkylation with iodoalkane was highly effective, giving yields of 82.7–92.4%. For the sterically hindered *tert*-butyl group, the alkylation method was unsuccessful due to an alternative elimination pathway being preferred. Instead, a modified ring closure synthesis provided 1-*tert*-butylimidazole in a 37.5% yield. Comprehensive NMR, MS and elemental analysis confirmed structures and revealed consistent trends in chemical shifts, possibly influenced by the inductive electron-donating effects of the N-alkyl substituents.

A wide range of symmetrical and unsymmetrical imidazolium iodide salts were produced in good to excellent yields (68.8–97.2%) *via* quaternization with an iodoalkane. Again, the direct method failed for salts incorporating the *tert*-butyl group due to the same steric constraints and elimination pathway. The di-*tert*-butyl salt was instead synthesized using a second ring closure reaction with hydriodic acid. NMR analysis of the salts showed characteristic deshielding of the central $C_2$-H proton (~9.0–9.3 ppm) and confirmed the electronic influence of different N- substituents on the ring protons and carbons. Additional MS and elemental analysis confirmed the structures of the imidazolium salts produced.

For the first time conclusive elemental analysis data and stable solid K[HFe(CO)$_4$] was obtained in moderate yields (~51–64%), with characterisation confirming its composition alongside minor polynuclear hydride impurities.

A library of fifteen iron carbonyl NHC complexes were synthesized from the prepared K[HFe(CO)$_4$], thirteen of which are novel, featuring a range of N-substituents. A key innovation was the use of the molten NHC ligands as both the reagent and solvent, a previously unreported method. All products were characterized by NMR and MS, with elemental analysis successfully performed on six complexes, four of them novel.

Finally, all successfully synthesized Fe-NHC complexes were tested for their ability to activate hydrogen gas. Under the conditions employed (atmospheric pressure of $H_2$, benzene, reflux), no evidence of reaction or catalytic activity was observed. This lack of reactivity is tentatively attributed to insufficient pressure of $H_2$ gas during exposure, lack of harsher reaction conditions and lack of steric strain imposed by the alkyl

substituents on the Fe-C bond, preventing the necessary activation for $H_2$ cleavage.

In conclusion, this work provides a thorough investigation into the synthesis of imidazole-based compounds, and their iron carbonyl complexes, establishing structure-property relationships and clearly defining the limitations imposed by steric hindrance. The full spectroscopic dataset provides a valuable reference for future work in this area.

### 6.2 Future Work

Immediate future work would include obtaining elemental analysis data for the other nine complexes produced and determining the crystal structures for all new complexes.

Future syntheses of iron carbonyl derivatives may take inspiration from the alternate method described in Section 5.3.2. That methodology highlights a possible synthetic route to produce iron-alkyl compounds via rection of $Fe(CO)_5$ and alkali metal alkoxides shown in Scheme 25 which could be investigated as reagents for other reactions.

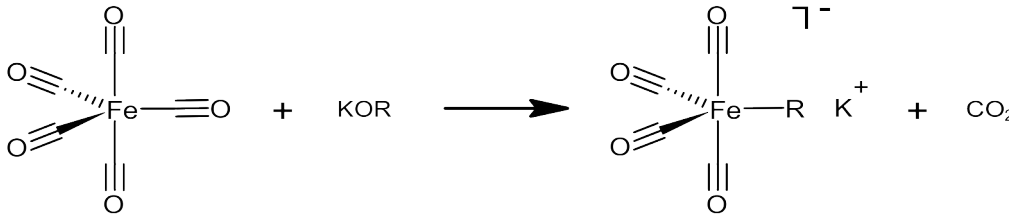


***Scheme 25: Plausible reaction scheme for the formation of K[RFe(CO)$_4$], R = Alkyl***

For future syntheses of complexes with *tert*-butyl-containing ligands, imidazolium salts with alternative counterions should be considered. The iodide salts used previously are ionic liquids, a class of compounds renowned for their tuneable physical properties (e.g., melting point, viscosity) based on N-substituents and counterions.[80] By changing the counterion and/ or N-substituent, the melting point of the ligands could be reduced so the K[$HFe(CO)_4$] used doesn't completely decompose before reacting. In addition to possibly lowering the melting points of the ligands used, lower reaction temperatures may improve yields.

Other approaches to produce Fe-NHC complexes can also be considered. Utilization of bis[bis(trimethylsilyl)amide]iron and then exposure to CO gas and a reducing agent [81] or direct reflux using $Fe_2(CO)_9$ / $Fe_3(CO)_{12}$ and the imidazolium salt 48 may allow for much larger N-substituents to be used such as phenyl, mesitylene (iMes), 2,6-diisopropylphenyl (DiPP) and adamantyl groups shown in Scheme 26. Additionally, these routes would allow for bidentate / pincer ligands to be designed for future complexes.

Additionally, these two approaches could be combined, attempting direct reactions of $Fe_2(CO)_9$ / $Fe_3(CO)_{12}$ with ligands that are liquid at room temperature or have low melting points.

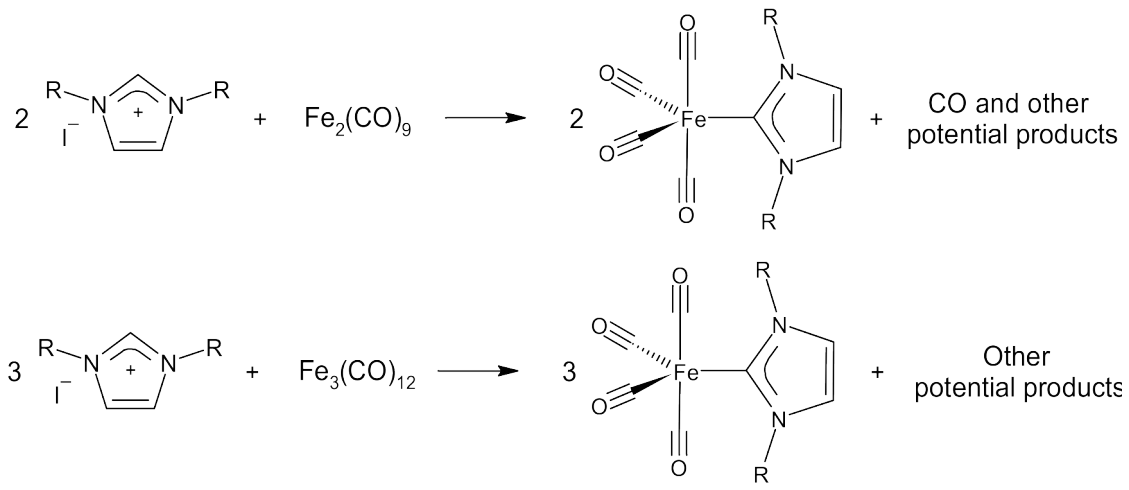


***Scheme 26: Example of possible direct reactions of 1,3-disubstituted imidazolium salts with $Fe_2(CO)_9$ and $Fe_3(CO)_{12}$.***

The synthesized Fe-NHC complexes should be screened for other catalytic reactions beyond hydrogenation, leveraging the known capabilities of iron carbonyls and NHCs. Specific examples of catalytic reactions using iron carbonyl NHC complexes include the reduction of carbonyls [48] and hydroboration of alkenes.[82]

In summary, the immediate future work should focus on overcoming synthetic challenges with bulky ligands via alternative methods, followed by a deliberate ligand design strategy to instil steric and electronic properties conducive to small molecule activation (like $H_2$), ultimately aiming to apply these new iron complexes in sustainable catalysis.

**References**

*(Plus, any additional Supplementary Information therein)*

[1] Hannah Ritchie and Pablo Rosado (2017) - “Fossil fuels” Published online at OurWorldinData.org. Retrieved from: 'https://ourworldindata.org/fossil-fuels'

[2] Zhao, Q.; Yu, P.; Mahendran, R.; Huang, W.; Gao, Y.; Yang, Z.; Ye, T.; Wen, B.; Wu, Y.; Li, S.; Guo, Y. Global Climate Change and Human Health: Pathways and Possible Solutions. *Eco-Environment & Health* **2022**, *1* (2), 53–62. https://doi.org/10.1016/j.eehl.2022.04.004.

[3] Owusu, P. A.; Asumadu-Sarkodie, S. A Review of Renewable Energy Sources, Sustainability Issues and Climate Change Mitigation. *Cogent Engineering* **2016**, *3* (1), 1167990. https://doi.org/10.1080/23311916.2016.1167990.

[4] Ellabban, O.; Abu-Rub, H.; Blaabjerg, F. Renewable Energy Resources: Current Status, Future Prospects and Their Enabling Technology. *Renewable and Sustainable Energy Reviews* **2014**, *39*, 748–764. https://doi.org/10.1016/j.rser.2014.07.113.

[5] Acar, C.; Dincer, I. The Potential Role of Hydrogen as a Sustainable Transportation Fuel to Combat Global Warming. *International Journal of Hydrogen Energy* **2020**, *45* (5), 3396–3406. https://doi.org/10.1016/j.ijhydene.2018.10.149.

[6] Singla, M. K.; Nijhawan, P.; Oberoi, A. S. Hydrogen Fuel and Fuel Cell Technology for Cleaner Future: A Review. *Environ Sci Pollut Res* **2021**, *28* (13), 15607–15626. https://doi.org/10.1007/s11356-020-12231-8.

[7] El-Shafie, M.; Kambara, S.; Hayakawa, Y. Hydrogen Production Technologies Overview. *JPEE* **2019**, *07* (01), 107–154. https://doi.org/10.4236/jpee.2019.71007.

[8] Hosseini, S. E.; Wahid, M. A. Hydrogen from Solar Energy, a Clean Energy Carrier from a Sustainable Source of Energy. *Int J Energy Res* **2020**, *44* (6), 4110–4131. https://doi.org/10.1002/er.4930.

[9] Maeda, K.; Domen, K. Photocatalytic Water Splitting: Recent Progress and Future Challenges. *J. Phys. Chem. Lett.* **2010**, *1* (18), 2655–2661. https://doi.org/10.1021/jz1007966.

[10] Abe, J. O.; Popoola, A. P. I.; Ajenifuja, E.; Popoola, O. M. Hydrogen Energy, Economy and Storage: Review and Recommendation. *International Journal of Hydrogen Energy* **2019**, *44* (29), 15072–15086. https://doi.org/10.1016/j.ijhydene.2019.04.068.

[11] Sikiru, S.; Oladosu, T. L.; Amosa, T. I.; Olutoki, J. O.; Ansari, M. N. M.; Abioye, K. J.; Rehman, Z. U.; Soleimani, H. Hydrogen-Powered Horizons: Transformative Technologies in Clean Energy Generation, Distribution, and Storage for Sustainable Innovation. *InternationalJournal of Hydrogen Energy* **2024**, *56*, 1152–1182. https://doi.org/10.1016/j.ijhydene.2023.12.186.

[12] Eberle, U.; Felderhoff, M.; Schüth, F. Chemical and Physical Solutions for Hydrogen Storage. *Angew Chem Int Ed* **2009**, *48* (36), 6608–6630. https://doi.org/10.1002/anie.200806293.

[13] Murata, K.; Kaneko, K.; Kanoh, H.; Kasuya, D.; Takahashi, K.; Kokai, F.; Yudasaka, M.; Iijima, S. Adsorption Mechanism of Supercritical Hydrogen in Internal and Interstitial Nanospaces of Single-Wall Carbon Nanohorn Assembly. *J. Phys. Chem. B* **2002**, *106* (43), 11132–11138. https://doi.org/10.1021/jp020583u.

[14] Liu, C.; Chen, Y.; Wu, C.-Z.; Xu, S.-T.; Cheng, H.-M. Hydrogen Storage in Carbon Nanotubes Revisited. *Carbon* **2010**, *48* (2), 452–455. https://doi.org/10.1016/j.carbon.2009.09.060.

[15] Yang, R. T. Hydrogen Storage by Alkali-Doped Carbon Nanotubes–Revisited. *Carbon* **2000**, *38* (4), 623–626. https://doi.org/10.1016/S0008-6223(99)00273-0.

[16] Barghi, S. H.; Tsotsis, T. T.; Sahimi, M. Chemisorption, Physisorption and Hysteresis during Hydrogen Storage in Carbon Nanotubes. *International Journal of Hydrogen Energy* **2014**, *39* (3), 1390–1397. https://doi.org/10.1016/j.ijhydene.2013.10.163.

[17] Furukawa, H.; Cordova, K. E.; O'Keeffe, M.; Yaghi, O. M. The Chemistry and Applications of Metal-Organic Frameworks. *Science* **2013**, *341* (6149), 1230444. https://doi.org/10.1126/science.1230444.

[18] Furukawa, H.; Ko, N.; Go, Y. B.; Aratani, N.; Choi, S. B.; Choi, E.; Yazaydin, A. Ö.; Snurr, R. Q.; O'Keeffe, M.; Kim, J.; Yaghi, O. M. Ultrahigh Porosity in Metal-Organic Frameworks. *Science* **2010**, *329* (5990), 424–428. https://doi.org/10.1126/science.1192160.

[19] Alabdulhadi, R. A.; Khan, S.; Khan, A.; Alfuhaid, L. T.; Khan, M. Y.; Usman, M.; Maity, N.; Helal, A. Potential Use of Reticular Materials (MOFs, ZIFs, and COFs) for Hydrogen Storage. *ACS Appl. Energy Mater.* **2025**, *8* (3), 1397–1413. https://doi.org/10.1021/acsaem.4c02317.

[20] Suh, M. P.; Park, H. J.; Prasad, T. K.; Lim, D.-W. Hydrogen Storage in Metal–Organic Frameworks. *Chem. Rev.* **2012**, *112* (2), 782–835. https://doi.org/10.1021/cr200274s.

[21] Modi, P.; Aguey-Zinsou, K.-F. Room Temperature Metal Hydrides for Stationary and

Heat Storage Applications: A Review. *Front. Energy Res.* **2021**, *9*, 616115. https://doi.org/10.3389/fenrg.2021.616115.

[22] Sakintuna, B.; Lamaridarkrim, F.; Hirscher, M. Metal Hydride Materials for Solid Hydrogen Storage: A Review☆. *International Journal of Hydrogen Energy* **2007**, *32* (9), 1121–1140. https://doi.org/10.1016/j.ijhydene.2006.11.022.

[23] Züttel, A.; Wenger, P.; Rentsch, S.; Sudan, P.; Mauron, Ph.; Emmenegger, Ch. LiBH4 a New Hydrogen Storage Material. *Journal of Power Sources* **2003**, *118* (1–2), 1–7. https://doi.org/10.1016/S0378-7753(03)00054-5.

[24] Orimo, S.; Nakamori, Y.; Eliseo, J. R.; Züttel, A.; Jensen, C. M. Complex Hydrides for Hydrogen Storage. *Chem. Rev.* **2007**, *107* (10), 4111–4132. https://doi.org/10.1021/cr0501846.

[25] De Frémont, P.; Marion, N.; Nolan, S. P. Carbenes: Synthesis, Properties, and Organometallic Chemistry. *Coordination Chemistry Reviews* **2009**, *253* (7–8), 862–892. https://doi.org/10.1016/j.ccr.2008.05.018.

[26] Bourissou, D.; Guerret, O.; Gabbaï, F. P.; Bertrand, G. Stable Carbenes. *Chem. Rev.* **2000**, *100* (1), 39–92. https://doi.org/10.1021/cr940472u.

[27] Arduengo, A. J.; Dias, H. V. R.; Harlow, R. L.; Kline, M. Electronic Stabilization of Nucleophilic Carbenes. *J. Am. Chem. Soc.* **1992**, *114* (14), 5530–5534. https://doi.org/10.1021/ja00040a007.

[28] Hoffmann, R.; Zeiss, G. D.; Van Dine, G. W. The Electronic Structure of Methylenes. *J. Am. Chem. Soc.* **1968**, *90* (6), 1485–1499. https://doi.org/10.1021/ja01008a017.

[29] Taylor, T. E.; Hall, M. B. Theoretical Comparison between Nucleophilic and Electrophilic Transition Metal Carbenes Using Generalized Molecular Orbital and Configuration Interaction Methods. *J. Am. Chem. Soc.* **1984**, *106* (6), 1576–1584. https://doi.org/10.1021/ja00318a007.

[30] Frenking, G.; Solà, M.; Vyboishchikov, S. F. Chemical Bonding in Transition Metal Carbene Complexes. *Journal of Organometallic Chemistry* **2005**, *690* (24–25), 6178–6204. https://doi.org/10.1016/j.jorganchem.2005.08.054.

[31] Khramov, D. M.; Lynch, V. M.; Bielawski, C. W. N-Heterocyclic Carbene−Transition Metal Complexes: Spectroscopic and Crystallographic Analyses of π-Back-Bonding Interactions. *Organometallics* **2007**, *26* (24), 6042–6049. https://doi.org/10.1021/om700591z.

[32] Hopkinson, M. N.; Richter, C.; Schedler, M.; Glorius, F. An Overview of N-Heterocyclic Carbenes. *Nature* **2014**, *510* (7506), 485–496. https://doi.org/10.1038/nature13384.

[33] Nelson, D. J.; Nolan, S. P. Quantifying and Understanding the Electronic Properties of N- Heterocyclic Carbenes. *Chem. Soc. Rev.* **2013**, *42* (16), 6723. https://doi.org/10.1039/c3cs60146c.

[34] Wang, N.; Xu, J.; Lee, J. K. The Importance of N-Heterocyclic Carbene Basicity in Organocatalysis. *Org. Biomol. Chem.* **2018**, *16* (37), 8230–8244. https://doi.org/10.1039/C8OB01667D.

[35] Cowley, A. H. Some Aspects of the Lewis Base and Ligand Behavior of N-Heterocyclic Carbenes. *Journal of Organometallic Chemistry* **2001**, *617–618*, 105–109. https://doi.org/10.1016/S0022-328X(00)00649-5.

[36] Arduengo, A. J.; Krafczyk, R.; Schmutzler, R.; Craig, H. A.; Goerlich, J. R.; Marshall, W. J.; Unverzagt, M. Imidazolylidenes, Imidazolinylidenes and Imidazolidines. *Tetrahedron* **1999**, *55* (51), 14523–14534. https://doi.org/10.1016/S0040-4020(99)00927-8.

[37] Serpell, C. J.; Cookson, J.; Thompson, A. L.; Brown, C. M.; Beer, P. D. Haloaurate and Halopalladate Imidazolium Salts: Structures, Properties, and Use as Precursors for Catalytic Metal Nanoparticles. *Dalton Trans.* **2013**, *42* (5), 1385–1393. https://doi.org/10.1039/C2DT31984E.

[38] Kumar, N.; Jain, R. Convenient Syntheses of Bulky Group Containing Imidazolium Ionic Liquids. *Journal of Heterocyclic Chem* **2012**, *49* (2), 370–374. https://doi.org/10.1002/jhet.751.

[39] Öfele, K.; Kreiter, C. G. (1.4-Dimethyl-tetrazolium)-carbonylferrate, Ausgangsprodukte für (1.4-Dimethyl-tetrazolinyliden)- und Bis(methylamino)carben-Komplexe. *Chem. Ber.* **1972**, *105* (2), 529–540. https://doi.org/10.1002/cber.19721050218.

[40] K. Öfele, J. organometallic Chem. 12, P42 (1968)

[41] Wilson, D. J. D.; Couchman, S. A.; Dutton, J. L. Are N-Heterocyclic Carbenes “Better” Ligands than Phosphines in Main Group Chemistry? A Theoretical Case Study of Ligand-Stabilized $E_2$ Molecules, L-E-E-L (L = NHC, Phosphine; E = C, Si, Ge, Sn, Pb, N, P, As, Sb, Bi). *Inorg. Chem.* **2012**, *51* (14), 7657–7668. https://doi.org/10.1021/ic300686n.

[42] Duda, D. P.; Edwards, K. C.; Dixon, D. A. Phosphine versus Carbene Metal Interactions: Bond Energies. *Inorg. Chem.* **2024**, *63* (31), 14525–14538. https://doi.org/10.1021/acs.inorgchem.4c01796.

[43] Herrmann, W. A.; Elison, M.; Fischer, J.; Köcher, C.; Artus, G. R. J. N-Heterocyclic Carbenes: Generation under Mild Conditions and Formation of Group 8–10 Transition Metal

Complexes Relevant to Catalysis. *Chemistry A European J* **1996**, *2* (7), 772–780. https://doi.org/10.1002/chem.19960020708.

[44] Arnold, P. L.; Pearson, S. Abnormal N-Heterocyclic Carbenes. *Coordination Chemistry Reviews* **2007**, *251* (5–6), 596–609. https://doi.org/10.1016/j.ccr.2006.08.006.

[45] Schuster, O.; Yang, L.; Raubenheimer, H. G.; Albrecht, M. Beyond Conventional *N* -Heterocyclic Carbenes: Abnormal, Remote, and Other Classes of NHC Ligands with Reduced Heteroatom Stabilization. *Chem. Rev.* **2009**, *109* (8), 3445–3478. https://doi.org/10.1021/cr8005087.

[46] Riener, K.; Haslinger, S.; Raba, A.; Högerl, M. P.; Cokoja, M.; Herrmann, W. A.; Kühn, F. E. Chemistry of Iron *N* -Heterocyclic Carbene Complexes: Syntheses, Structures, Reactivities, and Catalytic Applications. *Chem. Rev.* **2014**, *114* (10), 5215–5272. https://doi.org/10.1021/cr4006439.

[47] Liang, Q.; Song, D. Iron N-Heterocyclic Carbene Complexes in Homogeneous Catalysis. *Chem. Soc. Rev.* **2020**, *49* (4), 1209–1232. https://doi.org/10.1039/C9CS00508K.

[48] Warratz, S.; Postigo, L.; Royo, B. Direct Synthesis of Iron(0) N-Heterocyclic Carbene Complexes by Using $Fe_3(CO)_{12}$ and Their Application in Reduction of Carbonyl Groups. *Organometallics* **2013**, *32* (3), 893–897. https://doi.org/10.1021/om3012085.

[49] Kernbach, U., Ramm, M., Luger, P. and Fehlhammer, W.P. (1996), A Chelating Triscarbene Ligand and Its Hexacarbene Iron Complex. Angew. Chem. Int. Ed. Engl., 35: 310-312. https://doi.org/10.1002/anie.199603101

[50] Andersen, R. A.; Faegri, K.; Green, J. C.; Haaland, A.; Lappert, M. F.; Leung, W. P.; Rypdal, K. Synthesis of Bis[Bis(Trimethylsilyl)Amido]Iron(II). Structure and Bonding in M[N(SiMe3)2]2 (M = Manganese, Iron, Cobalt): Two-Coordinate Transition-Metal Amides. *Inorg. Chem.* **1988**, *27* (10), 1782–1786. https://doi.org/10.1021/ic00283a022.

[51] Gardiner, M. G.; Ho, C. C. Recent Advances in Bidentate Bis(N-Heterocyclic Carbene) Transition Metal Complexes and Their Applications in Metal-Mediated Reactions. *Coordination Chemistry Reviews* **2018**, *375*, 373–388. https://doi.org/10.1016/j.ccr.2018.02.003.

[52] Stephan, D. W. Frustrated Lewis Pairs: A New Strategy to Small Molecule Activation and Hydrogenation Catalysis. *Dalton Trans.* **2009**, No. 17, 3129. https://doi.org/10.1039/b819621d.

[53] Stephan, D. W. Frustrated Lewis Pairs: From Concept to Catalysis. *Acc. Chem. Res.* **2015**, *48* (2), 306–316. https://doi.org/10.1021/ar500375j.

[54] Welch, G. C.; Stephan, D. W. Facile Heterolytic Cleavage of Dihydrogen by Phosphines and Boranes. *J. Am. Chem. Soc.* **2007**, *129* (7), 1880–1881. https://doi.org/10.1021/ja067961j.

[55] Ullrich, M.; Lough, A. J.; Stephan, D. W. Reversible, Metal-Free, Heterolytic Activation of $H_2$ at Room Temperature. *J. Am. Chem. Soc.* **2009**, *131* (1), 52–53. https://doi.org/10.1021/ja808506t.

[56] Heshmat, M.; Ensing, B. Optimizing the Energetics of FLP-Type $H_2$ Activation by Modulating the Electronic and Structural Properties of the Lewis Acids: A DFT Study. *J. Phys. Chem. A* **2020**, *124* (32), 6399–6410. https://doi.org/10.1021/acs.jpca.0c03108.

[57] Stephan, D. W. A Tale of Two Elements: The Lewis Acidity/Basicity Umpolung of Boron and Phosphorus. *Angew Chem Int Ed* **2017**, *56* (22), 5984–5992. https://doi.org/10.1002/anie.201700721.

[58] Holschumacher, D.; Bannenberg, T.; Hrib, C. G.; Jones, P. G.; Tamm, M. Heterolytic Dihydrogen Activation by a Frustrated Carbene–Borane Lewis Pair. *Angew Chem Int Ed* **2008**, *47* (39), 7428–7432. https://doi.org/10.1002/anie.200802705.

[59] Chase, P. A.; Stephan, D. W. Hydrogen and Amine Activation by a Frustrated Lewis Pair of a Bulky N-Heterocyclic Carbene and $B(C_6F_5)_3$. *Angew Chem Int Ed* **2008**, *47* (39), 7433–7437. https://doi.org/10.1002/anie.200802596.

[60] Stephan, D. W. The Broadening Reach of Frustrated Lewis Pair Chemistry. *Science* **2016**, *354* (6317), aaf7229. https://doi.org/10.1126/science.aaf7229.

[61] Flynn, S. R.; Wass, D. F. Transition Metal Frustrated Lewis Pairs. *ACS Catal.* **2013**, *3* (11), 2574–2581. https://doi.org/10.1021/cs400754w.

[62] Ivanov, D. M.; Bokach, N. A.; Kukushkin, V. Y.; Frontera, A. Metal Centers as Nucleophiles: Oxymoron of Halogen Bond-Involving Crystal Engineering.

[63] Runyon, J. W.; Steinhof, O.; Dias, H. V. R.; Calabrese, J. C.; Marshall, W. J.; Arduengo, A. J. Carbene-Based Lewis Pairs for Hydrogen Activation. *Aust. J. Chem.* **2011**, *64* (8), 1165. https://doi.org/10.1071/CH11246.

[64] Brunet, J.-J.; Chauvin, R.; Diallo, O.; Kindela, F.; Leglaye, P.; Neibecker, D. Coordination Chemistry of Mononuclear Iron Carbonyl Complexes. *Coordination Chemistry*

*Reviews* **1998**, *178–180*, 331–351. https://doi.org/10.1016/S0010-8545(98)00075-7.

[65] Schroeder, M. A.; Wrighton, M. S. Pentacarbonyliron(0) Photocatalyzed Hydrogenation and Isomerization of Olefins. *J. Am. Chem. Soc.* **1976**, *98* (2), 551–558. https://doi.org/10.1021/ja00418a039.

[66] Wrighton, M. Photochemistry of Metal Carbonyls.

[67] Collman, J. P. Disodium Tetracarbonylferrate, a Transition Metal Analog of a Grignard Reagent. *Acc. Chem. Res.* **1975**, *8* (10), 342–347. https://doi.org/10.1021/ar50094a004.

[68] Collman, J. P. Disodium Tetracarbonylferrate, a Transition Metal Analog of a Grignard Reagent. *Acc. Chem. Res.* **1975**, *8* (10), 342–347. https://doi.org/10.1021/ar50094a004.

[69] Collman, J. P.; Finke, R. G.; Cawse, J. N.; Brauman, J. I. Oxidative-Addition Reactions of the Na2Fe(CO)$_4$, Supernucleophile. *Journal of the American Chemical Society* **1977**.

[70] Wilkinson, J. R.; Todd, L. J. Solution Properties of the HFe3(CO)11−ion. *Journal of Organometallic Chemistry* **1976**, *118* (2), 199–204. https://doi.org/10.1016/S0022-328X(00)92154-5.

[71] Keiter, R. L.; Keiter, E. A.; Hecker, K. H.; Boecker, C. A. A Facile, High-Yield Synthesis of Trans-Fe(CO)3(PR3)2 from Fe(CO)5, Fe(CO)4CHO-, HFe(CO)4-, or HFe(CO)3PR3-. *Organometallics* **1988**, *7* (12), 2466–2469. https://doi.org/10.1021/om00102a006.

[72] Noyori, R.; Umeda, I.; Ishigami, T. Selective Hydrogenation of .Alpha.,.Beta.-Unsaturated Carbonyl Compounds via Hydridoiron Complexes. *J. Org. Chem.* **1972**, *37* (10), 1542–1545. https://doi.org/10.1021/jo00975a017.

[73] Cainelli, G. F.; Panunzio, M.; Umani-Ronchi, A. Chemistry of Alkali Metal Tetracarbonylferrates. A Simple Method for Alkylating and Arylating Carbonyl Compounds and Active Methylene Compounds. *J. Chem. Soc., Perkin Trans. 1* **1975**, No. 13, 1273. https://doi.org/10.1039/p19750001273.

[74] Noyori, R.; Umeda, I.; Ishigami, T. Selective Hydrogenation of .Alpha.,.Beta.-Unsaturated Carbonyl Compounds via Hydridoiron Complexes. *J. Org. Chem.* **1972**, *37* (10), 1542–1545. https://doi.org/10.1021/jo00975a017.

[75] Cainelli, G. F.; Panunzio, M.; Umani-Ronchi, A. Chemistry of Alkali Metal Tetracarbonylferrates. A Simple Method for Alkylating and Arylating Carbonyl Compounds and Active Methylene Compounds. *J. Chem. Soc., Perkin Trans. 1* **1975**, No. 13, 1273. https://doi.org/10.1039/p19750001273.

[76] Collman, J. P.; Matlock, P. L.; Wahren, R.; Komoto, R. G.; Brauman, J. I. Synthetic and Mechanistic Studies of the Reduction of ,ß-Unsaturated Carbonyl Compounds by the Binuclear Cluster, NaHFe2(CO)s.

[77] Brunet, J. J. Tetracarbonylhydridoferrates, MHFe(CO)4: Versatile Tools in Organic Synthesis and Catalysis. *Chem. Rev.* **1990**, *90* (6), 1041–1059. https://doi.org/10.1021/cr00104a006.

[78] Elliott, M. C.; Hughes, C. E.; Knowles, P. J.; Ward, B. D. Alkyl Groups in Organic Molecules Are NOT Inductively Electron-Releasing. *Org. Biomol. Chem.* **2025**, *23* (2), 352–359. https://doi.org/10.1039/D4OB01572J.

[79] Öfele, K.; Kreiter, C. G. (1.4-Dimethyl-tetrazolium)-carbonylferrate, Ausgangsprodukte für (1.4-Dimethyl-tetrazolinyliden)- und Bis(methylamino)carben-Komplexe. *Chem. Ber.* **1972**, *105* (2), 529–540. https://doi.org/10.1002/cber.19721050218.

[80] Noorhisham, N. A.; Amri, D.; Mohamed, A. H.; Yahaya, N.; Ahmad, N. M.; Mohamad, S.; Kamaruzaman, S.; Osman, H. Characterisation Techniques for Analysis of Imidazolium-Based Ionic Liquids and Application in Polymer Preparation: A Review. *Journal of Molecular Liquids* **2021**, *326*, 115340. https://doi.org/10.1016/j.molliq.2021.115340.

[81] Danopoulos, A. A.; Pugh, D.; Smith, H.; Saßmannshausen, J. Structural and Reactivity Studies of “Pincer” Pyridine Dicarbene Complexes of Fe $^{0}$ : Experimental and Computational Comparison of the Phosphine and NHC Donors. *Chemistry A European J* **2009**, *15* (22), 5491–5502. https://doi.org/10.1002/chem.200900027.

[82] Zheng, J.; Sortais, J.; Darcel, C. [(NHC)Fe(CO)$_4$ ] Efficient Pre-catalyst for Selective Hydroboration of Alkenes. *ChemCatChem* **2014**, *6* (3), 763–766. https://doi.org/10.1002/cctc.201301062.

[83] Ouk, S.; Thiébaud, S.; Borredon, E.; Chabaud, B. N-Methylation of Nitrogen-Containing Heterocycles with Dimethyl Carbonate. *Synthetic Communications* **2005**, *35* (23), 3021–3026. https://doi.org/10.1080/00397910500278578.

[84] Clarke, C. J.; Morgan, P. J.; Hallett, J. P.; Licence, P. Linking the Thermal and Electronic Properties of Functional Dicationic Salts with Their Molecular Structures. *ACS Sustainable Chem. Eng.* **2021**, *9* (18), 6224–6234. https://doi.org/10.1021/acssuschemeng.0c08564.

[85] Sauerbrey, S.; Majhi, P. K.; Daniels, J.; Schnakenburg, G.; Brändle, G. M.; Scherer, K.; Streubel, R. Synthesis, Structure, and Reactions of 1-Tert-Butyl-2-Diphenylphosphino-

Imidazole. *Inorganic Chemistry* **2011**, *50* (3), 793–799. https://doi.org/10.1021/ic101122n.

[86] Mandal, T.; Yadav, S.; Choudhury, J. Steric Effect of NHC Ligands in Pd(II)–NHC-Catalyzed Non-Directed C–H Acetoxylation of Simple Arenes. *Journal of Organometallic Chemistry* **2021**, *953*, 122047. https://doi.org/10.1016/j.jorganchem.2021.122047.

[87] Gardner, S.; Kawamoto, T.; Curran, D. P. Synthesis of 1,3-Dialkylimidazol-2-Ylidene Boranes from 1,3-Dialkylimidazolium Iodides and Sodium Borohydride. *J. Org. Chem.* **2015**, *80* (19), 9794–9797. https://doi.org/10.1021/acs.joc.5b01682.

[88] Turner, E. A.; Pye, C. C.; Singer, R. D. Use of Ab Initio Calculations toward the Rational Design of Room Temperature Ionic Liquids. *J. Phys. Chem. A* **2003**, *107* (13), 2277–2288. https://doi.org/10.1021/jp021694w.

[89] Archer, R. H.; Zones, S. I.; Davis, M. E. Imidazolium Structure Directing Agents in Zeolite Synthesis: Exploring Guest/Host Relationships in the Synthesis of SSZ-70. *Microporous and Mesoporous Materials* **2010**, *130* (1–3), 255–265. https://doi.org/10.1016/j.micromeso.2009.11.018.

[90] Wang, S.; Liu, M.; Yue, Y.; Hu, X.; Zhang, Y.; Shen, G.; Dong, R.; Shi, L.; Yu, B.; Huang, X. Sustainable Preparation of 2-Acylbenzothiazoles under the Cooperation of Ionic Liquids and Microwave Irradiation. *Org. Biomol. Chem.* **2024**, *22* (18), 3732–3739. https://doi.org/10.1039/D4OB00315B.

[91] Jiao, N.; Zhang, Y.; Liu, L.; Shreeve, J. M.; Zhang, S. IL-Oxidizer/IL-Fuel Combinations as Greener Hypergols. *New J. Chem.* **2019**, *43* (3), 1127–1129. https://doi.org/10.1039/C8NJ04676J.

[92] Wang, Z. G.; Guo, Y.; Liao, A. H.; Zhang, H. M. Synthesis, Crystal Structure of Poly-Catena-[(1-Ethyl-3-Isopropyl-Imidozolium) Hexa-Iodo-Tetra Silver(I)]. *Asian J. Chem.* **2014**, *26* (22), 7677–7679. https://doi.org/10.14233/ajchem.2014.17580.

[93] Bouhrara, M.; Jeanneau, E.; Veyre, L.; Copéret, C.; Thieuleux, C. Dissymmetric Gold(I) N-Heterocyclic Carbene Complexes: A Key Unexpected Structural Parameter for Highly Efficient Catalysts in the Addition of Alcohols to Internal Alkynes. *Dalton Trans.* **2011**, *40* (12), 2995. https://doi.org/10.1039/c0dt00932f.

[94] Chan, B.; Chang, N.; Grimmett, M. The Synthesis and Thermolysis of Imidazole Quaternary Salts. *Australian Journal of Chemistry* **1977**, *30* (9), 2005–2013. https://doi.org/10.1071/CH9772005.